ABSTRACT

Title of Dissertation: HARMFUL ALGAE IN CHESAPEAKE BAY: A STUDY FOCUSED ON *KARLODINIUM VENEFICUM* APPLYING TIME SERIES, PHYSIOLOGICAL, AND MODELING APPROACHES

Chih-Hsien (Michelle) Lin,
Doctor of Philosophy, 2018

Dissertation directed by: Professor Patricia M. Glibert,
Marine Estuarine Environmental Sciences

Harmful algal blooms (HABs) are expanding worldwide. The harmful dinoflagellate *Karlodinium veneficum* is of concern because its toxigenic properties cause fish kills. Despite considerable study on nutrient-HAB relationships, there is a lack of data on HAB nutrient physiology because of the complexity of HAB nutrition. Many bloom-forming harmful algae consume particulate prey when nutrients are not available in the dissolved form. The goal of this dissertation was to apply statistical time series analysis, together with a series of laboratory experiments, and multi-nutrient quota models to improve our understanding and predictive capability of this important HAB species. Statistical time series analysis of *K. veneficum* abundance in Chesapeake Bay showed the predictive power of multiplicative factors (i.e., physical factors, nutrients, and prey) and the importance of temporal lags in some of these factors in bloom promotion.

In laboratory experiments, feeding rates were determined for *K. veneficum* on

prey when both were in varying nutritional conditions. Highest feeding rates were found for *K. veneficum* initially under low nitrogen:phosphorus condition and fed nitrogen-rich prey. Based on these data, a conceptual model was developed of mid-Bay summer *K. veneficum* blooms that incorporates the role of prey with a high nitrogen:phosphorus ratio originating from river inputs and a source inocula of *K. veneficum* from southern Bay waters with a lower nitrogen:phosphorus content. Further laboratory experiments were conducted using multi-wavelength fluorometry to measure growth, grazing and photo-physiology of *K. veneficum* with single and multiple prey species. Growth of *K. veneficum* increased with increasing prey concentrations of the cryptophyte *Rhodomonas salina*, but declined with *Synechococcus* as the prey.

Subsequent multi-nutrient mechanistic modeling was undertaken, simulating the growth of dinoflagellate *K. veneficum* and its common prey, *Rhodomonas*. The model was run varying nutrient ratios (molar nitrogen:phosphorus of 4, 16 and 32) and temperatures. The modeled biomass of *K. veneficum* was highest when they consumed prey under high nitrogen:phosphorus conditions. When nutrients were in balanced proportions, lower biomass of the dinoflagellate was attained at all temperatures in the model. This study underscores the importance of considering prey and their nutritional quality, as well as dissolved nutrients, in modeling HAB dynamics.

HARMFUL ALGAE IN CHESAPEAKE BAY: A STUDY FOCUSED ON *KARLODINIUM VENEFICUM* APPLYING TIME SERIES, PHYSIOLOGICAL, AND MODELING APPROACHES

by

Chih-Hsien (Michelle) Lin

Dissertation submitted to the Faculties of the Graduate School of the
University of Maryland, College Park, and the University of Maryland
Center for Environmental Science, in partial fulfillment
of the requirements for the degree of
Doctor of Philosophy
2018

Advisory Committee:
Professor Patricia M. Glibert, Chair
Dr. Ming Li
Dr. Vyacheslav Lyubchich
Dr. Diane Stoecker
Dr. Kevin Sellner
Dean's Representative: Amir Sapkota

Dedication

I dedicate this to my grandma and parents,

for their love, support and endless encouragement.

Acknowledgements

After 5 years full of scientific training, reading and writing, I finally arrived at my final lines of the dissertation. I appreciate all those many people, who challenged, supported and stuck with me along the way. Without their help and counsel, this work would have been immeasurably more difficult.

I would first like to thank my advisor, Patricia Glibert, who helped mold me into a strong, confident and hard-working ecologist. Pat, your door was always open. I greatly appreciate your endless patience for my Chinglish writing and your guides through this challenging PhD path. I was very lucky to work with you and learn the insights and rigorous research experiences from you. Choosing to study abroad would be the best experience and memory of my life, and doing science with you would be the most valuable lesson I have ever had. My thanks also go to my major committee members, Diane Stoecker, Kevin Sellner, Ming Li, Slava Lyubchich, and a previously committee member, Alyson Santoro, who provided me valuable comments and feedback during my comprehensive exam, student seminars and various stages of graduate studies. Amir Sapkota, thank you for being my Dean's representative.

Furthermore, I want to thank all my co-authors who helped shape the manuscripts resulting from this work. My co-authors on the laboratory studies (Chapter 3, 4) were Pat Glibert and Stefano Accoroni, Thank you, Pat, again for providing guidance on experimental design, data analysis and interpretation of results. Stefano Accoroni, big "thank you" for the help in grazing and bioassay experiments as well as manuscript revisions of Chapter 3. Without you as a team member, I could not complete all the microscopic slides within 4 months and this dissertation

definitely would be much thinner. Discussing science and all the non-scientific issues with you was always a pleasure. Slava Lyubchich, thank you for providing statistical guidance and constructive suggestions for Chapter 2. Kevin Flynn and Aditee Mitra, thank you for squeezing me into your crazy busy teaching schedule during my short visit to Swansea, UK. I truly appreciate and value everything about models of plankton mixotrophy you have taught me. Your contribution greatly improved the modeling in Chapter 5. Many thanks also go to Todd Kana who provided his instrument and advice on the use of Phyto-PAM fluorometry and constructive feedback on the data interpretation for the study in Chapter 4.

Thanks also go to funding sources from Taiwanese Government and the Bay and Rivers Fellowship from the Horn Point Laboratory for supporting my research and graduate education. I am also grateful for the travel support to the UK from the Ryan Saba Memorial Fellowship, the Croucher Foundation of Hong Kong for the summer course at the Hong Kong University of Science and Technology, as well as the additional support for laboratory studies and modeling from the National Oceanic and Atmospheric Administration National Center for Coastal Ocean Science Competitive Research program under award no. NA17NOS4780180 to Ming Li and Patricia Glibert. The Maryland Department of Natural Resources and the United States Geological Survey collected and made the environmental data publically available that played an important role in the statistical analyses and modeling works.

I thank Jeff Alexander, Bob Carey, and the staff of the Oyster Hatchery for assistance and for supplying cultures and larvae for experimentation. I greatly appreciate Zhonghua Zhao for her comments on my proposal writing and several

scientific talks in US and China during her visits. Thanks to current and previous members of Glibert lab, Yini Shangguan, Melanie Jackson, Katie Bentley, Linwei Lin, Junxiang Lai and Samantha Gleich for all the mental support in the form of discussion and those encouraging words that were sources of energy to recover from the frustrations in the life of a PhD-student. Thank you Katherine Liu Slater, Serena Lee, Jacqueline Tay, Catherine Fitzgerald, Hannah Morrissette, for your time and help on my English writing and speaking. I will remember your company on the many trips we did together. Many thanks go to faculty, staff and all the international students in the Horn Point community for always being supportive.

Finally, I acknowledge all my friends and family from Taiwan for providing inspiration and encouragement throughout studying overseas. I gratefully thank you, my partner in life, Hugo Kang, for everything.

Table of Contents

List of Tables

List of Figures

Chapter 1: Introduction and Overview

Harmful algae are growing phenomena, which are coupled with the increasing nutrient enrichment of many coastal waters worldwide from diverse anthropogenic activities and with the changing climate (e.g., rainfall patterns; Anderson et al., 2002; Glibert et al., 2005; Heisler et al., 2008; Hallegraeff, 2010; Wells et al., 2015). For example, increased nutrient loading to Chesapeake Bay from fertilizer use in agriculture, sewage, and atmospheric deposition has been recognized and linked closely to outbreaks of harmful algal blooms (HABs) over the past decades (Boesch et al., 2001; Glibert et al., 2004; Kemp et al., 2005; Anderson et al., 2008; Li et al., 2015). Climate-related changes in the amount and timing of nutrient runoff may have also promoted the occurrences of HABs and added complexity in nutrient-HAB relationships (Glibert et al., 2001; Burkholder et al., 2006). Although it is now widely accepted that diversity of nutrient sources and forms, relative proportions of nutrient pools, physiological responses within algal species, and interactive effects among those factors are all important in determining whether HABs proliferate (Glibert and Burkholder, 2011; Glibert and Burford, 2017), the appropriate data for developing predictive models of HABs based on nutrient physiology are insufficient (Flynn, 2005, 2010; Glibert et al., 2010). Therefore, this dissertation aims to 1) synthesize critical environmental parameters underlying the population dynamics of an important harmful algal species for Chesapeake Bay, *Karlodinium veneficum*, 2) characterize the nutrient physiology of this species in laboratory experiments, and 3) develop a model of this HAB based on its physiological responses to better inform its behavior under climate change conditions.

Karlodinium veneficum (formerly *Gyrodinium galatheanum, Gymnodinium galatheanum* and *Karlodinium micrum*) is a common ichthyotoxic dinoflagellate that is globally distributed in a wide range of estuarine systems (Li et al., 2000a; Adolf et al., 2008; Place et al., 2012; Dai et al., 2013; Adolf et al., 2015). Wherever it has been previously reported, a series of recurrent blooms of *K. veneficum* is evident during summer months. In Chesapeake Bay, the blooms of *K. veneficum* have been reported to be the cause of fish kills (Adolf et al., 2006, 2008; Deeds, 2009) and implicated in the failure of oyster spawning (Glibert et al., 2007; Stoecker et al., 2008). Such monospecific algal blooms of *K. veneficum* appear to be increasing in magnitude and frequency, and the potential threats to ecosystem have suggested this species is of central importance in the study of harmful algae (Li et al., 2015).

The Chesapeake Bay has been negatively affected by nutrient over-enrichment, as evidenced by recurrent low dissolved oxygen (DO) conditions, losses of submersed aquatic vegetation, and frequent HABs events (Boynton et al., 1995; Glibert et al., 2001; Gurbisz and Kemp, 2014; Li et al., 2015). Nitrogen (N) concentrations of 1990 were 2.5 times more than those in 1945 due to the increases in human densities and fertilizer use, but there has been a modest decrease in N loading from 1990 to 2012 following implementation of nutrient reduction efforts in the Bay (Kemp et al., 2005; Gurbisz and Kemp, 2014). Peaks in *K. veneficum* abundance are often observed throughout upper and middle Chesapeake Bay, where nutrients from Susquehanna and/or Potomac River discharge mostly in spring and where strong benthic ammonium and phosphate (P) fluxes occur in summer (Malone et al., 1988; Kemp et al., 2005). Because cultural eutrophication and biogeochemical processes

affect the nutrient dynamics of the Bay, N:P ratios show regional and seasonal variability (Fisher, 1992; Kemp et al., 2005). Thus, balanced Redfield ratios (N:P stoichiometry of 16:1 by atom) are not often attained during summer dinoflagellate blooms (Li et al., 2015).

Many dinoflagellates in eutrophic estuaries are known to use mixotrophy (i.e., the combinations of phototrophy and phagotrophy) under varying environmental conditions when light or nutrients can be limiting and/or when nutrients are sufficiently available but not in balanced Redfield proportions (Burkholder et al., 2008; Glibert and Burford, 2017; Millette et al., 2017). Such phagotrophic nutrition appears to be a significant physiological adaptation for the growth of *K. veneficum* (Li et al., 1999; Adolf et al., 2006; Calbet et al., 2011). As cellular photosynthetic efficiency under mixotrophic nutrition can be reduced by 24-52% compared to autotrophic growth, the contribution of heterotrophic metabolism to the mixotrophic growth of this species can be dominant (Adolf et al., 2006). Although the understanding that *K. veneficum* can benefit from prey ingestion (Li et al., 2000b; Adolf et al., 2008) and knowledge of associated metabolic pathways is rapidly advancing (Mitra et al., 2014; 2016; Stoecker et al., 2017), the questions of how feeding in *K. veneficum* may be affected by nutritional quality of prey, and its physiological states, and how mixotrophic metabolism can be advantageous to the organisms living under varying environmental conditions, remain unanswered.

The genus of *Karlodinium* (synonym of *Gymnodinium*) is found to be omnivorous, feeding on a wide range of phytoplankton species (Berge et al., 2008a,b). However, feeding mechanisms have generally been examined

experimentally with the addition of single prey species and mainly with prey cryptophytes as they have been shown to be important food sources for *K. veneficum* (Adolf et al., 2008). Single prey are used experimentally largely due to the difficulty of distinguishing feeding experimentally with multiple prey species that blur the relationships between losses of prey and total gains of mixotroph. There is much to be explored about the grazing capability of *K. veneficum* on different taxa under a range of conditions. This study applied a new multiwavelength fluorescent approach to assess grazing by *K. veneficum* on cryptophytes alone and in combination with the picocyanobacterium, *Synechococcus*. The latter has been found to be readily grazed by other gymnodinoid dinoflagellates (Jeong et al., 2005a; Glibert et al., 2009).

As the variety of nutrient sources is involved in the ecology of *K. veneficum*, applying simplistic dose-response and classic kinetic relationship to understand bloom response to nutrients in a eutrophic system is not sufficient (Glibert et al., 2013; Kana and Glibert, 2017; Glibert et al., 2018). Classic kinetic models often assume fixed nutrient stoichiometry but they are deficient in consideration of nutrient uptake and growth under variable nutrient conditions (Flynn, 2005, 2009, 2010; Glibert et al., 2010). More importantly, modeling mixotrophy in HAB species is not a simple additive process but rather a mechanistic adaptive relationship that integrates physiological interactions between autotrophy and heterotrophy (Flynn and Mitra, 2009; Mitra and Flynn, 2010). Only a few model constructs have considered the feedback function of rates of change during mixotrophic feeding, the nutritional status of both predator and prey, and linkages to cellular stoichiometric balancing between

physiological interactions (Mitra and Flynn, 2006, 2010). This study advances these model constructs for *K. veneficum*.

This dissertation research herein tested the following overarching hypothesis: phagotrophy is an adaptive strategy that may aid dinoflagellates in compensating for nutritional imbalances. As a result, increasing nutrient and prey availability associated with nutrient-enriched conditions will favor HABs that are comprised of mixotrophic species. More specifically, the dinoflagellate *K. veneficum* is prevalent in varying environmental conditions because it can use mixotrophy to adjust to the variations in nutrient availability. When nutrient supply ratio is imbalanced, the cellular nutrient stoichiometry of this dinoflagellate will change accordingly. Quantifying the interactive effects of nutrient supply and prey availability on mixotrophy will improve the ability to predict mixotrophic growth responses to nutrient over-enrichment. In order to understand the effects of various sources of nutrient on mixotrophic growth of *K. veneficum* in the Chesapeake Bay, the following specific questions were addressed:

- What combinations of environmental factors including climate-related variables (e.g., temperature, salinity, and flow), nutrient and prey concentrations best predict the occurrence of *K. veneficum* in different regions of Chesapeake Bay?
- How does the nutrient condition of the mixotroph and/or the prey affect the rates of feeding and putative toxicity of *K. veneficum*?
- How does feeding and growth by *K. veneficum* change in response to multiple prey species and their concentrations?

- How does prey availability under different temperature regimes influence the growth response of *K. veneficum* in modeled simulations?

To answer these questions, first, long-term time series data from Chesapeake Bay were analyzed to statistically model relationships among the abundance of *K. veneficum*, flow, temperature, salinity, nutrient forms and ratios, and potential prey (Chapter 2). Then, feeding mechanisms and responses under nutrient conditions of mixotroph and prey, as well as toxicity that are associated with physiological conditions of the mixotroph itself, were examined experimentally (Chapter 3). The species-specific biological factors that influence the feeding capability of this dinoflagellate with multiple prey species were explored using a multiwavelength-excitation pulse-amplitude-modulated (PAM) fluorometer (Chapter 4). A mechanistic model for mixotrophic *K. veneficum* was developed based on the framework of an existing quota-based CNP model of Flynn and Mitra (2009) with predator stoichiometry, prey stoichiometry (i.e., food quality) and its feedback interactions. Climate change scenarios in prey availability and bloom formation were also simulated (Chapter 5). Finally, overall conclusions and synthesis is presented (Chapter 6).

The main chapters of the thesis were prepared as the following manuscripts.

I. Lin, C.-H., V. Lyubchich, and P. M. Glibert (2018). Time series models of decadal trends in the harmful algal species *Karlodinium veneficum* in Chesapeake Bay. Harmful Algae **73**: 110-118.

II. Lin, C.-H., S. Accoroni, and P. M. Glibert (2017). *Karlodinium veneficum* feeding responses and effects on larvae of the eastern oyster *Crassostrea virginica* under variable nitrogen: phosphorus stoichiometry. Aquat. Micro. Ecol. **79:** 101-114.

III. Lin, C.-H. and P. M. Glibert. Mixotrophy with multiple prey species measured with a multiwavelength-excitation AM fluorometer: case study of *Karlodinium veneficum*. J. Plankt. Res. Submitted.

IV. Lin, C.-H., K. J. Flynn, M. Aditee and P. M. Glibert. Modeling effects of variable nutrient stoichiometry and temperature on mixotrophy in the harmful dinoflagellate *Karlodinium veneficum*. Front. Mar. Sci. Submitted.

References

Adolf, J.E., Bachvaroff, T., Place, A.R., 2008. Can cryptophyte abundance trigger toxic *Karlodinium veneficum* blooms in eutrophic estuaries? Harmful Algae 8(1), 119-128.

Adolf, J.E., Bachvaroff, T.R., Deeds, J.R., Place, A.R., 2015. Ichthyotoxic *Karlodinium veneficum* (Ballantine) J Larsen in the Upper Swan River Estuary (Western Australia): Ecological conditions leading to a fish kill. Harmful Algae 48, 83-93.

Adolf, J.E., Stoecker, D.K., Harding, L.W., 2006. The balance of autotrophy and heterotrophy during mixotrophic growth of *Karlodinium micrum* (Dinophyceae). J. Plankt. Res. 28(8), 737-751.

Anderson, D.M., Burkholder, J.M., Cochlan, W.P., Glibert, P.M., Gobler, C.J., Heil, C.A., Kudela, R.M., Parsons, M.L., Rensel, J.E.J., Townsend, D.W., 2008. Harmful algal blooms and eutrophication: examining linkages from selected coastal regions of the United States. Harmful Algae 8(1), 39-53.

Anderson, D.M., Glibert, P.M., Burkholder, J.M., 2002. Harmful algal blooms and eutrophication: nutrient sources, composition, and consequences. Estuaries 25(4), 704-726.

Berge, T., Hansen, P.J., Moestrup, O., 2008a. Prey size spectrum and bioenergetics of the mixotrophic dinoflagellate *Karlodinium armiger*. Aquat. Microb. Ecol. 50(3), 289.

Berge, T., Hansen, P.J., Moestrup, Ø., 2008b. Feeding mechanism, prey specificity and growth in light and dark of the plastidic dinoflagellate *Karlodinium armiger*. Aquat. Microb. Ecol. 50(3), 279-288.

Boesch, D.F., Brinsfield, R.B., Magnien, R.E., 2001. Chesapeake Bay Eutrophication. J. Environ. Qual. 30(2), 303-320.

Boynton, W.R., Garber, J.H., Summers, R., Kemp, W.M., 1995. Inputs, transformations, and transport of nitrogen and phosphorus in Chesapeake Bay and selected tributaries. Estuar. Coast. 18(1), 285-314.

Burkholder, J.M., Dickey, D.A., Kinder, C.A., Reed, R.E., Mallin, M.A., McIver, M.R., Cahoon, L.B., Melia, G., Brownie, C., Smith, J., 2006. Comprehensive

trend analysis of nutrients and related variables in a large eutrophic estuary: a decadal study of anthropogenic and climatic influences. Limnol. Oceanogr. 51(1part2), 463-487.

Burkholder, J.M., Glibert, P.M., Skelton, H.M., 2008. Mixotrophy, a major mode of nutrition for harmful algal species in eutrophic waters. Harmful Algae 8(1), 77-93.

Calbet, A., Bertos, M., Fuentes-Grünewald, C., Alacid, E., Figueroa, R., Renom, B., Garcés, E., 2011. Intraspecific variability in *Karlodinium veneficum*: Growth rates, mixotrophy, and lipid composition. Harmful Algae 10(6), 654-667.

Dai, X., Lu, D., Guan, W., Wang, H., He, P., Xia, P., Yang, H., 2013. Newly recorded *Karlodinium veneficum* dinoflagellate blooms in stratified water of the East China Sea. Deep Sea Res. II 101, 237-243.

Deeds, J., 2009. The evolving story of *Gymnodinium galatheanum= Karlodinium micrum= Karlodinium veneficum*. A ten year perspective. J. Phycol. 45, 1-2.

Fisher, T.R., 1992. Nutrient limitation of phytoplankton in Chesapeake Bay. Mar. Ecol. Prog. Ser. 82, 51-63.

Flynn, K.J., 2005. Castles built on sand: dysfunctionality in plankton models and the inadequacy of dialogue between biologists and modellers. J. Plankt. Res. 27(12), 1205-1210.

Flynn, K.J., 2010. Do external resource ratios matter?: Implications for modelling eutrophication events and controlling harmful algal blooms. J. Mar. Syst. 83(3), 170-180.

Flynn, K.J., 2009. Going for the slow burn: why should possession of a low maximum growth rate be advantageous for microalgae? Plant Ecol. Divers. 2(2), 179-189.

Flynn, K.J., Mitra, A., 2009. Building the "perfect beast": modelling mixotrophic plankton. J. Plankt. Res. 31(9), 965-992.

Glibert, P.M., Alexander, J., Meritt, D.W., North, E.W., Stoecker, D.K., 2007. Harmful algae pose additional challenges for oyster restoration: Impacts of the harmful algae *Karlodinium veneficum* and *Prorocentrum minimum* on early life stages of the oysters *Crassostrea virginica* and *Crassostrea ariakensis*. J. Shellfish Res. 26(4), 919-925.

Glibert, P.M., Allen, J.I., Bouwman, A.F., Brown, C.W., Flynn, K.J., Lewitus, A.J., Madden, C.J., 2010. Modeling of HABs and eutrophication: status, advances, challenges. J. Mar. Syst. 83(3), 262-275.

Glibert, P.M., Burford, M.A., 2017. Globally changing nutrient loads and harmful algal blooms: Recent advances, new paradigms, and continuing challenges. Oceanogr. 30(1), 58-69.

Glibert, P.M., Burkholder, J.M., 2011. Harmful algal blooms and eutrophication:"strategies" for nutrient uptake and growth outside the Redfield comfort zone. Chin. J. Oceanol. Limnol. 29(4), 724-738.

Glibert, P.M., Burkholder, J.M., Kana, T.M., Alexander, J., Skelton, H., Shilling, C., 2009. Grazing by *Karenia brevis* on *Synechococcus* enhances its growth rate and may help to sustain blooms. Aquat. Microb. Ecol. 55(1), 17-30.

Glibert, P.M., Heil, C.A., F., W., C, D.R., 2018. Nutrient and HABs: dynamics kinetics and flexible nutrition, In: Glibert, P.M., Berdalet, E., Burford, M.A., Pitcher, G.C., Zhou, M. (Eds.), Global Ecology and Oceanography of Harmful Algal Blooms. Springer, In press, USA.

Glibert, P.M., Kana, T.M., Brown, K., 2013. From limitation to excess: the consequences of substrate excess and stoichiometry for phytoplankton physiology, trophodynamics and biogeochemistry, and the implications for modeling. J. Mar. Syst. 125, 14-28

Glibert, P.M., Magnien, R., Lomas, M.W., Alexander, J., Tan, C., Haramoto, E., Trice, M., Kana, T.M., 2001. Harmful algal blooms in the Chesapeake and coastal bays of Maryland, USA: Comparison of 1997, 1998, and 1999 events. Estuaries 24(6), 875-883.

Glibert, P.M., Magnien, R.E., Hall, S., Anderson, D., Kleindinst, J., Zhu, M., Zou, Y., 2004. Harmful algal blooms in the Chesapeake Bay, USA: common species, relationships to nutrient loading, management approaches, successes, and challenges. Harmful algae management and mitigation. Asia-Pacific Economic Cooperation Publications (204-MR-04.2), Singapore, pp. 48-55.

Glibert, P.M., Seitzinger, S., Heil, C.A., Burkholder, J.M., Parrow, M.W., Codispoti, L.A., Kelly, V., 2005. The role of eutrophication in the global proliferation of harmful algal blooms. Oceanogr. 18(2), 198-209.

Gurbisz, C., Kemp, W.M., 2014. Unexpected resurgence of a large submersed plant bed in Chesapeake Bay: Analysis of time series data. Limnol. Oceanogr. 59(2), 482-494.

Hallegraeff, G.M., 2010. Ocean climate change, phytoplankton community responses, and harmful algal blooms: a formidable predictive challenge[1]. J. Phycol. 46(2), 220-235.

Heisler, J., Glibert, P.M., Burkholder, J.M., Anderson, D.M., Cochlan, W., Dennison, W.C., Dortch, Q., Gobler, C.J., Heil, C.A., Humphries, E., 2008. Eutrophication and harmful algal blooms: a scientific consensus. Harmful algae 8(1), 3-13.

Jeong, H.J., Park, J.Y., Nho, J.H., Park, M.O., Ha, J.H., Seong, K.A., Jeng, C., Seong, C.N., Lee, K.Y., Yih, W.H., 2005. Feeding by red-tide dinoflagellates on the cyanobacterium *Synechococcus*. Aquat. Microb. Ecol. 41(2), 131-143.

Kana, T.M., Glibert, P.M., 2017. On saturating response curves from the dual perspectives of photosynthesis and nitrogen metabolism, In: Glibert, P.M., Kana, T.M. (Eds.), Aquatic Microbiology and Biogeochemistry – A Dual Perspective. Springer Internatioanl Pub., Switzerland, pp. 93-102.

Kemp, W., Boynton, W., Adolf, J., Boesch, D., Boicourt, W., Brush, G., Cornwell, J., Fisher, T., Glibert, P., Hagy, J., 2005. Eutrophication of Chesapeake Bay: historical trends and ecological interactions. Mar. Ecol. Prog. Ser. 303(21), 1-29.

Li, A., Stoecker, D.K., Adolf, J.E., 1999. Feeding, pigmentation, photosynthesis and growth of the mixotrophic dinoflagellate *Gyrodinium galatheanum*. Aquat. Microb. Ecol. 19, 163-176.

Li, A., Stoecker, D.K., Coats, D.W., 2000a. Spatial and temporal aspects of *Gyrodinium galatheanum* in Chesapeake Bay: distribution and mixotrophy. J. Plankt. Res. 22(11), 2105-2124.

Li, A., Stoecker, D.K., Coats, D.W., 2000b. Mixotrophy in *Gyrodinium galatheanum* (Dinophyceae): grazing responses to light intensity and inorganic nutrients. J. Phycol. 36(1), 33-45.

Li, J., Glibert, P.M., Gao, Y., 2015. Temporal and spatial changes in Chesapeake Bay water quality and relationships to *Prorocentrum minimum*, *Karlodinium veneficum*, and CyanoHAB events, 1991–2008. Harmful Algae 42, 1-14.

Malone, T.C., Crocker, L.H., Pike, S.E., Wendler, B.W., 1988. Influences of river flow on the dynamics of phytoplankton production in a partially stratified estuary. Mar. Ecol. Prog. Ser. 48(3), 235-249.

Millette, N.C., Pierson, J.J., Aceves, A., Stoecker, D.K., 2017. Mixotrophy in *Heterocapsa rotundata*: A mechanism for dominating the winter phytoplankton. Limnol. Oceanogr. 62(2), 836-845.

Mitra, A., Flynn, K.J., 2010. Modelling mixotrophy in harmful algal blooms: More or less the sum of the parts? J. Mar. Syst. 83(3), 158-169.

Mitra, A., Flynn, K.J., 2006. Accounting for variation in prey selectivity by zooplankton. Ecol. Modell. 199(1), 82-92.

Mitra, A., Flynn, K.J., Burkholder, J., Berge, T., Calbet, A., Raven, J.A., Granéli, E., Glibert, P.M., Hansen, P.J., Stoecker, D.K., 2014. The role of mixotrophic protists in the biological carbon pump. Biogeosciences 10(8), 13535-13562.

Mitra, A., Flynn, K.J., Tillmann, U., Raven, J.A., Caron, D., Stoecker, D.K., Not, F., Hansen, P.J., Hallegraeff, G., Sanders, R., 2016. Defining planktonic protist functional groups on mechanisms for energy and nutrient acquisition: incorporation of diverse mixotrophic strategies. Protist 167(2), 106-120.

Place, A.R., Bowers, H.A., Bachvaroff, T.R., Adolf, J.E., Deeds, J.R., Sheng, J., 2012. *Karlodinium veneficum* —The little dinoflagellate with a big bite. Harmful Algae 14, 179-195.

Stoecker, D.K., Adolf, J.E., Place, A.R., Glibert, P.M., Meritt, D.W., 2008. Effects of the dinoflagellates *Karlodinium veneficum* and *Prorocentrum minimum* on early life history stages of the eastern oyster (*Crassostrea virginica*). Mar. Biol. 154(1), 81-90.

Stoecker, D.K., Hansen, P.J., Caron, D.A., Mitra, A., 2017. Mixotrophy in the marine plankton. Annu. Rev. Mar. Sci. 9, 311-335.

Wells, M.L., Trainer, V.L., Smayda, T.J., Karlson, B.S.O., Trick, C.G., Kudela, R.M., Ishikawa, A., Bernard, S., Wulff, A., Anderson, D.M., 2015. Harmful algal blooms and climate change: Learning from the past and present to forecast the future. Harmful Algae 49, 68-93.

Chapter 2: Time series models of decadal trends in the harmful algal species *Karlodinium veneficum* in Chesapeake Bay[1]

Abstract

The harmful dinoflagellate, *Karlodnium veneficum*, has been implicated in fish-kill and other toxic, harmful algal bloom (HAB) events in waters worldwide. Blooms of *K. veneficum* are known to be related to coastal nutrient enrichment but the relationship is complex because this HAB taxon relies not only on dissolved nutrients but also particulate prey, both of which have also changed over time. Here, applying cross-correlations of climate-related physical factors, nutrients and prey, with abundance of *K. veneficum* over a 10-year (2002 – 2011) period, a synthesis of the interactive effects of multiple factors on this species was developed for Chesapeake Bay, where blooms of the HAB have been increasing. Significant upward trends in the time series of *K. veneficum* were observed in the mesohaline stations of the Bay, but not in oligohaline tributary stations. For the mesohaline regions, riverine sources of nutrients with seasonal lags, together with particulate prey with zero lag, explained 15 % – 46 % of the variation in the *K. veneficum* time series. For the oligohaline regions, nutrients and particulate prey generally showed significant decreasing trends with time, likely a reflection of nutrient reduction efforts. A conceptual model of mid-Bay blooms is presented, in which *K. veneficum*, derived from the oceanic end member of the Bay, may experience enhanced growth if it encounters prey

[1] Published as Lin et al. (2018). *Harmful Algae* 73(C)**,** 110-118. doi: 10.1016/j.hal.2018.02.002.

originating from the tributaries with different patterns of nutrient loading and which are enriched in nitrogen. For all correlation models developed herein, prey abundance was a primary factor in predicting of *K. veneficum* abundance.

Introduction

Harmful algal blooms (HABs) are escalating worldwide, recognized to be significantly associated with human-induced nutrient pollution as well as global climate change (Anderson et al., 2002; Glibert et al., 2005; Heisler et al., 2008; Hallegraeff, 2010; Wells et al., 2015; Glibert and Burford, 2017). There is a need to quantify these relationships but there is inherent inconsistency and variability in and/or between time-series data of algal taxa and of the associated environmental factors (Cloern and Jassby, 2010). New quantitative tools that can integrate multifactorial data are needed to unambiguously parameterize HAB species responses to dynamics environmental conditions, while accounting for natural variability and confounding factors.

Of the many HAB taxa, the toxic dinoflagellate *Karlodinium veneficum* is of particular concern worldwide due to its ichthyotoxic properties (Deeds et al., 2002; 2006; Place et al., 2012). Blooms of *K. veneficum* (formerly *Gyrodinium galatheanum, Gymnodinium galatheanum* and *K. micrum*) have been reported in a wide range of estuarine systems, including the South Africa, Europe, Western Australia and the eastern United States seaboard (Adolf et al., 2009; Place et al., 2012, and reference therein). In Chesapeake Bay, toxicity of *K. veneficum* has been implicated in fish kills (Deeds et al., 2002; 2006) and in the failure of oyster spawning and in the growth of early life stages of oysters (Glibert et al., 2007;

Stoecker et al., 2008). The Chesapeake Bay has been negatively impacted by anthropogenic nutrient enrichment over the past several decades, as evidenced by recurrent low dissolved oxygen (DO) conditions, losses of submersed aquatic vegetation (SAV; Cooper and Brush, 1991; Boynton et al., 1995; Hagy et al., 2004; Kemp et al., 2005; Gurbisz and Kemp, 2014) and increasing observations of *K. veneficum* as well as other HAB taxa are a manifestation of these nutrient effects (HABs; e.g. Glibert et al., 2001; Marshall et al., 2005; Li et al., 2015). As a well-monitored estuary, Chesapeake Bay provides an excellent model system with which to explore how dynamic environmental conditions affect this HAB species.

A number of previous studies have examined the factors that can influence *K. veneficum* occurrence, but these have yet to be collectively quantified in such a way as to allow predictive power for this dinoflagellate in a dynamic system such as Chesapeake Bay. The abundance of *K. veneficum* is positively associated with temperature, and negatively with depth and salinity, based on field observations (Li et al., 2000a); it commonly occurs over a broad salinity range (7 – 17) in the mid and upper Bay regions during late summer when temperatures are high (Li et al., 2000a; Li et al., 2015). High ambient dissolved inorganic phosphate (DIP), and resultant low N:P ratios in summer, also show some correspondence with bloom occurrence (Li et al., 2015; Lundgren et al., 2016). These trends are supported by laboratory studies showing a high P demand by these cells (Nielsen, 1996; Li et al., 2000b). It has also been noted that *K. veneficum* blooms are favored when there is a predominance of NH_4^+ or other reduced forms of nitrogen (N, e.g., urea, dissolved organic N) over NO_3^- and NO_2^- concentrations (Glibert and Terlizzi, 1999; Kempton et al., 2002).

Furthermore, because *K. veneficum* is a mixotroph (Place et al., 2012), prey availability and prey quality also affect its abundance and its rate of growth (Li et al., 2000b; Adolf et al., 2008). Moreover, recent laboratory experiments have shown that the physiological or nutritional conditions of both predator and prey affect the feeding behavior and growth rate of *K. veneficum* (Lin et al., 2017).

Adding further complexity, it is conceivable that HABs such as *K. veneficum* may have increased in frequency in Chesapeake Bay due to climate-induced changes in hydrology and nutrient loading. Future climate scenarios project increases in spring river flows to Chesapeake Bay, a trajectory that may undermine efforts for eutrophication recovery and that may strengthen nonlinear interactions among biogeochemical processes (Najjar et al., 2010). Such changes may alter competitive outcomes that are favorable for initiation and development of HAB species (Wells et al., 2015).

Here, using the extensive time series data from Chesapeake Bay, this study extends the previously documented trends in *K. veneficum* and quantifies the relationships between abundance of this HAB taxon in time and space in relation to physical factors, nutrient concentrations, forms and ratios, as well as prey availability. Advanced time-series models with multiplicative and lagged terms were used to address the hypothesis that a combination of increasing N, altered nutrient ratios, and concentrations and nutritional quality of prey have contributed significantly to increased *K. veneficum* abundance in mid-Chesapeake Bay. These quantitative tools may help to guide managers in predicting how these blooms may change as they can be applied in future scenarios of climate change and nutrient management actions.

Materials and Methods

Overview of dataset and study stations

Data from 2002 to 2011 on phytoplankton abundance and water quality were acquired from the Chesapeake Bay Program (link: http://www.chesapeakebay.net) and flow data were acquired from USGS (http://md.water.usgs.gov). Phytoplankton and water quality data acquisition was restricted to near-surface samples at seven stations in mid-Chesapeake Bay and tributaries that were selected because they experienced a reoccurrence of *K. veneficum* for more than five years and thus represent the broad spatial distribution of this species in the estuary (Fig. 2.1). The oligohaline and mesohaline salinity zone was defined based on Harding and Perry (1997). The stations analyzed included the main-channel stations of CB3.3C, CB4.3C and CB5.2 and the tributary stations of the Patapsco River (WT5.1), Choptank River (ET5.2), Patuxent River (LE1.1) and Potomac River (LE2.2).

Routine sampling by the Chesapeake Bay Program was conducted on a biweekly to monthly basis. Phytoplankton abundance in the Chesapeake Bay Program is enumerated with conventional light microscopy. Phytoplankton data were mainly available from biweekly sampling in April, May, July and August, and monthly sampling in March, June, September, October, and December for each station, each year. The data analyzed here encompassed only the period from 2002 to 2011 because prior to 2002 the presence of *K. veneficum* was variably reported with different names, including *Gyrodinium estuarali*, *Gymnodinium galatheanum* or *Gymnodinium veneficum* and thus its presence, while documented, is difficult to unravel with certainty in the database. Since 2002, this species was reported as *Karlodinium*

micrum, or more recently as *K. veneficum* (Bergholtz et al., 2006). Frequency of sampling and enumeration has declined since 2011, thus making the window from 2002-2011 the most complete data set. Data on the common prey for *K. veneficum*, *Cryptomonas* spp. and unidentified microphytoflagellates (< 10 μm), were also retrieved from the database. Nutrient data in the Chesapeake Bay Program database were available from biweekly sampling in April, May, July and August, and monthly sampling for the other months. Variables included dissolved inorganic nitrogen (DIN: sum of NO_3^-, NO_2^- and NH_4^+), DIP, total N, total P, dissolved organic N and P (DON, DOP). Physical and climate-related variables included temperature, salinity and flow (the sum of measures for Susquehanna and Potomac River).

Statistical analyses

Several approaches were taken for data analysis, and all data processing was conducted using the R language (R Core Team, 2016). Where data availability was more frequent than monthly, averages were calculated so that all datasets and variables from different sources were comparable for any month during the 10-year studying period.

First, in order to determine the relationship between river flow and nutrient concentrations, linear correlations between flow and nutrient variables were calculated and significance was estimated using Pearson's product moment coefficients. Second, the nonparametric seasonal Mann-Kendall (SMK) test was applied to detect monotonic trends in time series of *K. veneficum* and other variables. This test, somewhat analogous to regression analysis, is better suited for water-quality data sets with irregular sampling intervals, non-normality and missing data and it is

less affected by extreme values because it is based on sign differences, not actual values.

Next, Fourier sine and cosine series were used to remove the seasonal components from the time series data. Then, the Wang-Akritas-Van Keilegom (WAVK) test was further applied to assess potentially non-monotonic parametric trends in weakly stationary time-series (Lyubchich et al., 2013). Thus, the time series were detrended, deseasonalized and statistically tested to obtain stationary residuals. After such decomposition, autocorrelation and partial autocorrelation functions were used to examine the temporal persistence of all variables at each station.

The detrended time series of *K. veneficum* were then modeled using transfer functions to relate the change in abundance with the other detrended, environmental, nutrient and biological variables. Relationships were compared contemporaneously and with time lags. To explore both non-lagged and lagged relations between variables, cross-correlation functions (CCF) were applied to the stationarized time-series of the abundance of *K. veneficum* and 1) nutrient concentrations, including DIP, different N forms (e.g. NO_3^-, NH_4^+ and DON) and nutrient ratios (DIN:DIP, DON:DOP, and TN:TP) and 2) the abundance of prey, the cryptophyte *Cryptomonas* spp. and unidentified microphytoflagellates. Overall, 13 cross-correlations, with lags from 0 to 12 months, were calculated for each comparison. A total of 14 environmental, nutrient and biological variables, showing significant lagged correlation with the dependent variable (*K. veneficum*) individually were pre-selected for further regression modeling. Leading factors for nutrient variables are defined

based on a greater correlation coefficient and/or lag with a lower value, while secondary factors are comparably less well correlated and/or have longer lag time.

Finally, regression models of the time series between *K. veneficum* abundance and the various physical, nutrient and biological factors were developed using two approaches, one based on nutrient concentrations as well as other factors (Model I) and one based on nutrient ratios and the other factors (Model II). Models I and II were built separately to avoid multi-collinearity between nutrient concentrations and ratios. Multi-collinearity was considered as $|r| > 0.8$ and was assessed before estimating a regression function with a combination of predictors. The models (with all possible variables) were then each re-specified using backward stepwise elimination based on Akaike's information criterion (AIC) in order to reduce the variables to the minimum necessary for a good fit. The AIC approach simultaneously quantifies goodness-of-fit and complexity of a model (lower AIC is better). In the stepwise procedure, one variable at a time was removed from the regression if it did not lead to an increase in AIC, until no further variables could be deleted. This provided the reduced models with the minimum number of significant variables. Uncorrelatedness, normality, and variance homogeneity of model residuals were assessed using residual time series and Q-Q plots, Shapiro−Wilk normality tests and plots of autocorrelation and partial autocorrelation functions (Shapiro and Wilk, 1965; Kendall and Ord, 1990).

Results

Trends and seasonal patterns of hydrology

Stream flow did not display any significant trend in 2002 – 2011 ($p_{SMK} = 0.97$; Fig. 2.2A). Water temperature showed a positive significant trend only at station ET5.2 (Choptank River; Table 2.1). Salinity showed no significant trends, except a barely significant decrease at ET5.2 ($p_{SMK} = 0.05$; Table 2.1).

Seasonal patterns of flows of both the Susquehanna and Potomac Rivers were similar, with highest flows in March (Fig. 2.2B,C). The seasonal patterns in flow of these rivers (Fig. 2.2B,C) paralleled those of N concentrations at the stations nearest to their respective river mouths (Fig. 2.2 D,E), and relationships between flow and TN at CB4.3C ($r^2 = 0.33$, $p < 0.001$) and with DIN at LE2.2 ($r^2 = 0.46$, $p < 0.001$) were the strongest among them. No significant correlations were found between flow and DON at either CB4.3C or LE2.2.

Trends in nutrient and nutrient ratio

Most nutrient concentrations showed decreasing trends over the time period examined. Significant decreasing trends were detected for both TN and DON for the main-stem stations of CB4.3C and CB5.2, and TN, DIN, and NO_3^- decreased significantly in the tributary sites of WT5.1 (Patapsco River) and LE2.2 (Potomac River; Fig. AI.1, Table 2.1). Concentrations of DIN, including NO_3^- and NH_4^+, also decreased at stations CB3.3C (Fig. AI.1, Table 2.1), as did those of DIP. Concentrations of NH_4^+ and DIP also decreased significantly at station WT5.1 (Fig. AI.1, Table 2.1). Moreover, both TN:TP ratio and DON:DOP ratio showed significant

decreasing trends at the main-stem station CB4.3C (Table 2.1). In contrast, concentrations of TP and DOP, as well as the DIN:DIP ratio, showed no significant change in the study area during the studied time period (Fig. AI.1, Table 2.1).

Decadal trends and seasonal patterns in phytoplankton abundance

Trends in abundance of *K. veneficum* over the studied period showed, in general, irregular variation (Fig. AI.2). The highest concentrations (~16×10^6 cells L^{-1}) were observed at the western-shore stations of WT5.1 (Patapsco River), while medium abundance levels (~8×10^6 cells L^{-1}) were observed in the main-stem stations (e.g. CB3.3C and CB4.3C) and lowest cell concentrations (~1×10^6 cells L^{-1}) were found at CB5.2 and the eastern-shore station of ET5.2 (Choptank River). Trend analysis indicated that monthly *K. veneficum* abundance increased significantly for all stations in the mesohaline zone but not in the oligohaline zone (Fig. AI.2, Table 2.1).

Among potential prey species, significant decreasing trends were recorded for *Cryptomonas* spp. and the unidentified microphytoflagellates at all stations located in the mesohaline zone, except station CB5.2. In the oligohaline zone, there was a downward trend for *Cryptomonas* spp. in Patapsco River and for both prey types at station CB3.3C (Fig. AI.2, Table 2.1).

With regards to the seasonality of *K. veneficum* and its prey in the main-channel (station CB5.2), median average values of *K. veneficum* were highest in May (Fig. 2.3A). *Cryptomonas* spp. was highest in July (Fig. 2.3B), while microphytoflagellates had a similar pattern as that of *K. veneficum*, reaching their greatest density in May (Fig. 2.3C). The relationship between *K. veneficum* and microphytoflagellates was significant at $p < 0.01$ (Table 2.2).

Cross-correlation and transfer function models

Cross-correlations between *K. veneficum* and other variables were examined with time lags at each station (Table 2.2). Positive relationships between temperature and *K. veneficum* were observed with zero lags in the tributary stations, but these relationships showed longer lag periods (5 months) at the main-stem stations (Table 2.2). Negative correlations between *K. veneficum* abundance and salinity, and positive correlation with flow were observed with sequential lags (1-3 months) at stations LE2.2 (Potomac River), CB4.3C, and CB5.2 in the mesohaline zone (Table 2.2).

In general, cross-correlation relationships between *K. veneficum* and each nutrient concentration and/or ratios were contemporaneous or had a single lag association within the same stations, but the significance of the correlations and lag responses varied among stations (Table 2.2). Positive correlations with DIN, but negative correlations with DIP, were observed (Table 2.2). *Cryptomonas* spp. and microphytoflagellates were positively cross-correlated with *K. veneficum* at all stations except the main-stem station CB3.3C (Table 2.2). Correlations with *Cryptomonas* spp. generally showed no lagged response, but one seasonal lag at station ET5.2 (Choptank River) was observed. Relationships between *K. veneficum* and microphytoflagellates at most stations were most significant with 1-2 months lag, but at station CB5.2 in the mesohaline bay, no lagged responses were seen.

Using variables with significant cross-correlations, full transfer function models were developed for each station and minimum numbers of significant variables were determined using AIC to get the best-fitting model. The transfer functions models for the mesohaline zone of CB described between 15 % and 46 % of

the variance in *K. veneficum* based on Model I (using nutrient concentrations), while Model II (using nutrient ratios) appeared to explain less variability of *K. veneficum* abundance (Table 2.3). The leading variables differed between stations, but for most stations included the concentration of one of the prey species. Forms of N (e.g. DIN, TN or DON) were consistently the secondary factors in the models, with short-term (2-month lag) correlations with DIN and TN, and long-term (8-month lag) correlations with DON. Environmental variables described approximately 4 % – 10 % of the variance for stations in the mesohaline zone (calculated from the square of the correlation coefficient in Table 2.2). For the stations in the oligohaline zone, forms of P were the main predicators of *K. veneficum* based on the lowest AIC for station WT5.1 (Patapsco River), while a combination of salinity at lag 2 and DIN at lag 0 were the best indicators for the main-stem station of CB3.3C (Table 2.3).

Discussion

The statistical modeling approach applied here has shown that complex lag-response associations between flow-regulated nutrients and the abundance of *Karlodinium veneficum* can be effectively disentangled from strong seasonal trends. These analyses showed that nutrients and prey availability, along with physical-chemical factors, explained up to 46 % of the variation in the dynamics of this HABs species. These results further underscore that the classic eutrophication paradigm based on dose-effect relationships (e.g. the 'Phase I' model of Cloern, 2001) does not hold in understanding biodiversity changes and that there is a need for more complex,

multi-scale relationships between specific HAB species, hydrology and nutrient supplies (Smayda, 2008; Glibert, 2017).

There were spatial and temporal differences in the relationships that emerged. The abundance of *K. veneficum* had significant upward trends for the stations located in the mesohaline zone, but not in the oligohaline zone where nutrients and prey time series indicated decreasing trends. Such patterns might reflect successful nutrient reduction efforts in the oligohaline zone but associated time-lagged effects leading to upward trends in *K. veneficum* abundance in the mesohaline zone. Yet, the abundance of *K. veneficum* in the oligohaline western tributaries was also highly associated with prey *Cryptomonas* spp. with no time lag and with microphytoflagellates at zero and/or one-month lag, suggesting that ambient nutrients were incorporated into prey biomass especially in the tributaries. Climate-related variables (e.g. salinity and flow), nutrient forms (e.g. DIN, TN and DOP) and nutrient ratios were correlated with *K. veneficum* abundance with lag-patterns at seasonal scale (1-3 months) in at least the Potomac River station, and in the mesohaline zone.

This analysis, together with previous studies on *K. veneficum* in Chesapekae Bay, suggest a conceptual model of summer blooms that incorporate the role of prey with a high N:P ratio originating from river inputs and their flow-regulated changes in N loading with a southern Bay source of the mixotrophs (Fig. 2.4). Nutrient inputs through tributaries are greatest during the high-flow period, typically starting through March to May. During this period, prey species can accumulate in the tributaries, and are typically characterized by high N:P ratios due to disproportionate high N loading (Fisher, 1992; Kemp et al., 2005). The peak in summer *K. veneficum* blooms

generally occurs 1-3 months later relative to these freshet inputs, in June through September (Li et al., 2015). From the perspective of the mixotroph, it has been suggested that inocula of *K. veneficum* to the upper Bay are delivered via subsurface transport from the southern Chesapeake Bay and grow and accumulate when exposed to favorable environmental conditions including prey (Li et al., 2000a). This suggests that enhanced growth of *K. veneficum* derived from the oceanic end member of the Bay may be enhanced if it encounters prey originating from the tributaries with different patterns of nutrient loading. Both Li et al. (2000b) and Lin et al. (2017) have shown that feeding increases at higher N:P conditions of prey, especially when the mixotroph is in a condition of comparatively low N:P (which would be more typical of the southern Bay inocula). Therefore, prey that is N-rich likely play an important role in determining *K. veneficum* abundance at stations located in the mesohaline zone (e.g. CB 5.2).

While this analysis has highlighted the importance of prey quantity and quality, as well as time-lagged effects on the abundance of *K. veneficum*, the most powerful models still only explained about half of the variability observed. Although analysis of stream flow in this study did not display a significant trend in the 2002–2011 time frame studied, climate-driven changes in hydrology and stream flow are known to have strong effects on trend analyses of nutrient loading (Burkholder et al., 2006; Glibert et al., 2014; Harding et al., 2016). Such flow-regulated changes in nutrient loading alter the dynamics of other species, including competing algal taxa and those that graze on *K. veneficum*. As more knowledge emerges about these dynamics, the models presented here can be reassessed. Nevertheless, this approach

has shown the importance of nutrients, in quantity and quality, as dissolved or as particulate prey, in determining the distribution of this important mixotroph.

References

Adolf, J.E., Bachvaroff, T., Place, A.R., 2008. Can cryptophyte abundance trigger toxic *Karlodinium veneficum* blooms in eutrophic estuaries? Harmful Algae 8(1), 119-128.

Adolf, J.E., Bachvaroff, T.R., Place, A.R., 2009. Environmental modulation of karlotoxin levels in strains of the cosmopolitan dinoflagellate, *Karlodinium veneficum*. J. Phycol. 45(1), 176-192.

Anderson, D.M., Glibert, P.M., Burkholder, J.M., 2002. Harmful algal blooms and eutrophication: nutrient sources, composition, and consequences. Estuaries 25(4), 704-726.

Bergholtz, T., Daugbjerg, N., Moestrup, Ø., Fernández-Tejedor, M., 2006. On the identity of *Karlodinium veneficum* and description of *Karlodinium armiger* sp. *nov.* (Dinophyceae), based on light and electron microscopy, nuclear-encoded LSU rDNA, and pigment composition. J. Phycol. 42(1), 170-193.

Boynton, W.R., Garber, J.H., Summers, R., Kemp, W.M., 1995. Inputs, transformations, and transport of nitrogen and phosphorus in Chesapeake Bay and selected tributaries. Estuar. Coast. 18(1), 285-314.

Burkholder, J.M., Dickey, D.A., Kinder, C.A., Reed, R.E., Mallin, M.A., McIver, M.R., Cahoon, L.B., Melia, G., Brownie, C., Smith, J., 2006. Comprehensive trend analysis of nutrients and related variables in a large eutrophic estuary: a

decadal study of anthropogenic and climatic influences. Limnol. Oceanogr. 51(1part2), 463-487.

Cloern, J.E., 2001. Our evolving conceptual model of the coastal eutrophication problem. Mar. Ecol. Prog. Ser. 210(2001), 223-253.

Cloern, J.E., Jassby, A.D., 2010. Patterns and scales of phytoplankton variability in estuarine–coastal ecosystems. Estuar. Coast. 33(2), 230-241.

Cooper, S.R., Brush, G.S., 1991. Long-term history of Chespeake Bay anoxia. Science 254(5034), 992.

Deeds, J.R., Reimschuessel, R., Place, A.R., 2006. Histopathological effects in fish exposed to the toxins from *Karlodinium micrum*. J. aquat. animal health 18(2), 136-148.

Deeds, J.R., Terlizzi, D.E., Adolf, J.E., Stoecker, D.K., Place, A.R., 2002. Toxic activity from cultures of *Karlodinium micrum* (= *Gyrodinium galatheanum*)(Dinophyceae)—a dinoflagellate associated with fish mortalities in an estuarine aquaculture facility. Harmful Algae 1(2), 169-189.

Fisher, T.R., 1992. Nutrient limitation of phytoplankton in Chesapeake Bay. Mar. Ecol. Prog. Ser. 82, 51-63.

Glibert, P.M., 2017. Eutrophication, harmful algae and biodiversity—Challenging paradigms in a world of complex nutrient changes. Marine Poll. Bull. 124(2), 591-606.

Glibert, P.M., Alexander, J., Meritt, D.W., North, E.W., Stoecker, D.K., 2007. Harmful algae pose additional challenges for oyster restoration: Impacts of the harmful algae *Karlodinium veneficum* and *Prorocentrum minimum* on early

life stages of the oysters *Crassostrea virginica* and *Crassostrea ariakensis*. J. Shellfish Res. 26(4), 919-925.

Glibert, P.M., Burford, M.A., 2017. Globally changing nutrient loads and harmful algal blooms: Recent advances, new paradigms, and continuing challenges. Oceanogr. 30(1), 58-69.

Glibert, P.M., Hinkle, D.C., Sturgis, B., Jesien, R.V., 2014. Eutrophication of a Maryland/Virginia coastal lagoon: a tipping point, ecosystem changes, and potential causes. Estuar. Coast. 37(1), 128-146.

Glibert, P.M., Magnien, R., Lomas, M.W., Alexander, J., Tan, C., Haramoto, E., Trice, M., Kana, T.M., 2001. Harmful algal blooms in the Chesapeake and coastal bays of Maryland, USA: Comparison of 1997, 1998, and 1999 events. Estuaries 24(6), 875-883.

Glibert, P.M., Seitzinger, S., Heil, C.A., Burkholder, J.M., Parrow, M.W., Codispoti, L.A., Kelly, V., 2005. The role of eutrophication in the global proliferation of harmful algal blooms. Oceanogr. 18(2), 198-209.

Glibert, P.M., Terlizzi, D.E., 1999. Cooccurrence of elevated urea levels and dinoflagellate blooms in temperate estuarine aquaculture ponds. Appl. Environ. Microbiol. 65(12), 5594-5596.

Gurbisz, C., Kemp, W.M., 2014. Unexpected resurgence of a large submersed plant bed in Chesapeake Bay: Analysis of time series data. Limnol. Oceanogr. 59(2), 482-494.

Hagy, J.D., Boynton, W.R., Keefe, C.W., Wood, K.V., 2004. Hypoxia in Chesapeake Bay, 1950–2001: long-term change in relation to nutrient loading and river flow. Estuaries 27(4), 634-658.

Hallegraeff, G.M., 2010. Ocean climate change, phytoplankton community responses, and harmful algal blooms: a formidable predictive challenge[1]. J. Phycol. 46(2), 220-235.

Harding, L.W., Gallegos, C.L., Perry, E.S., Miller, W.D., Adolf, J.E., Mallonee, M.E., Paerl, H.W., 2016. Long-term trends of nutrients and phytoplankton in Chesapeake Bay. Estuar. Coast. 39(3), 664-681.

Harding, L.W., Perry, E.S., 1997. Long-term increase of phytoplankton biomass in Chesapeake Bay, 1950–1994. Mar. Ecol. Prog. Ser., 39-52.

Heisler, J., Glibert, P.M., Burkholder, J.M., Anderson, D.M., Cochlan, W., Dennison, W.C., Dortch, Q., Gobler, C.J., Heil, C.A., Humphries, E., 2008. Eutrophication and harmful algal blooms: a scientific consensus. Harmful algae 8(1), 3-13.

Kemp, W., Boynton, W., Adolf, J., Boesch, D., Boicourt, W., Brush, G., Cornwell, J., Fisher, T., Glibert, P., Hagy, J., 2005. Eutrophication of Chesapeake Bay: historical trends and ecological interactions. Mar. Ecol. Prog. Ser. 303(21), 1-29.

Kempton, J.W., Lewitus, A.J., Deeds, J.R., Law, J.M., Place, A.R., 2002. Toxicity of *Karlodinium micrum* (Dinophyceae) associated with a fish kill in a South Carolina brackish retention pond. Harmful Algae 1(2), 233-241.

Kendall, M.G., Ord, J.K., 1990. Time-series. Edward Arnold London.

Li, A., Stoecker, D.K., Coats, D.W., 2000a. Spatial and temporal aspects of *Gyrodinium galatheanum* in Chesapeake Bay: distribution and mixotrophy. J. Plankt. Res. 22(11), 2105-2124.

Li, A., Stoecker, D.K., Coats, D.W., 2000b. Mixotrophy in *Gyrodinium galatheanum* (Dinophyceae): grazing responses to light intensity and inorganic nutrients. J. Phycol. 36(1), 33-45.

Li, J., Glibert, P.M., Gao, Y., 2015. Temporal and spatial changes in Chesapeake Bay water quality and relationships to *Prorocentrum minimum*, *Karlodinium veneficum*, and CyanoHAB events, 1991–2008. Harmful Algae 42, 1-14.

Lin, C.-H., Accoroni, S., Glibert, P.M., 2017. *Karlodinium veneficum* feeding responses and effects on larvae of the eastern oyster *Crassostrea virginica* under variable nitrogen: phosphorus stoichiometry. Aquat. Microb. Ecol. 79(2), 101-114.

Lundgren, V.M., Glibert, P.M., Granéli, E., Vidyarathna, N.K., Fiori, E., Ou, L., Flynn, K.J., Mitra, A., Stoecker, D.K., Hansen, P.J., 2016. Metabolic and physiological changes in *Prymnesium parvum* when grown under, and grazing on prey of, variable nitrogen: phosphorus stoichiometry. Harmful Algae 55, 1-12.

Lyubchich, V., Gel, Y.R., El-Shaarawi, A., 2013. On detecting non-monotonic trends in environmental time series: a fusion of local regression and bootstrap. Environmetrics 24(4), 209-226.

Marshall, H.G., Burchardt, L., Lacouture, R., 2005. A review of phytoplankton composition within Chesapeake Bay and its tidal estuaries. J. Plankt. Res. 27(11), 1083-1102.

Najjar, R.G., Pyke, C.R., Adams, M.B., Breitburg, D., Hershner, C., Kemp, M., Howarth, R., Mulholland, M.R., Paolisso, M., Secor, D., 2010. Potential climate-change impacts on the Chesapeake Bay. Estuar. Coast. Shelf. Sci. 86(1), 1-20.

Nielsen, M.V., 1996. Growth and chemical composition of the toxic dinoflagellate *Gymnodinium galatheanum* in relation to irradiance, temperature and salinity. Mar. Ecol. Prog. Ser. 136, 205-211.

Place, A.R., Bowers, H.A., Bachvaroff, T.R., Adolf, J.E., Deeds, J.R., Sheng, J., 2012. *Karlodinium veneficum* —The little dinoflagellate with a big bite. Harmful Algae 14, 179-195.

R Core Team, 2016. R: A Language and Environment for Statistical Computing. Vienna, Austria: R Foundation for Statistical Computing; 2014. R Foundation for Statistical Computing, http://www.R-project.org.

Shapiro, S.S., Wilk, M.B., 1965. An analysis of variance test for normality (complete samples). Biometrika 52(3/4), 591-611.

Smayda, T.J., 2008. Complexity in the eutrophication–harmful algal bloom relationship, with comment on the importance of grazing. Harmful Algae 8(1), 140-151.

Stoecker, D.K., Adolf, J.E., Place, A.R., Glibert, P.M., Meritt, D.W., 2008. Effects of the dinoflagellates *Karlodinium veneficum* and *Prorocentrum minimum* on

early life history stages of the eastern oyster (*Crassostrea virginica*). Mar. Biol. 154(1), 81-90.

Wells, M.L., Trainer, V.L., Smayda, T.J., Karlson, B.S.O., Trick, C.G., Kudela, R.M., Ishikawa, A., Bernard, S., Wulff, A., Anderson, D.M., 2015. Harmful algal blooms and climate change: Learning from the past and present to forecast the future. Harmful Algae 49, 68-93.

Tables

Table 2. 1. Results of the seasonal Mann−Kendall trend test for various abiotic and biotic parameters presumed to be associated with *Karlodinium veneficum* abundance in Chesapeake Bay. Bold indicates significance.

Variables		Oligohaline zone		Mesohaline zone				
		Patapsco R. WT5.1	Main-stem CB3.3C	Choptank R. ET5.2	Patuxent R. LE1.1	Potomac R. LE2.2	Main-stem CB4.3C	Main-stem CB5.2
Water temperature	Tau	0.11	0.07	**0.17**	0.12	0.02	0.02	0.04
	p-value	0.11	0.30	**0.03**	0.09	0.81	0.79	0.57
Salinity	Tau	-0.09	-0.07	-0.15	0.01	-0.04	-0.05	-0.08
	p-value	0.22	0.33	0.05	0.92	0.58	0.47	0.25
Ammonium (NH_4^+)	Tau	**-0.28**	**-0.15**	-0.12	-0.04	-0.10	-0.08	-0.12
	p-value	**<0.001**	**0.034**	0.12	0.51	0.18	0.28	0.08
Nitrate (NO_3^-)	Tau	**-0.23**	**-0.17**	-0.08	-0.14	**-0.18**	**-0.14**	-0.12
	p-value	**0.001**	**0.020**	0.26	0.05	**0.011**	**0.049**	0.11
Dissolved inorganic nitrogen (DIN)	Tau	**-0.29**	**-0.16**	-0.08	-0.08	**-0.21**	-0.11	**-0.15**
	p-value	**<0.001**	**0.023**	0.32	0.24	**0.004**	0.09	**0.039**
Dissolved inorganic phosphate (DIP)	Tau	**-0.20**	-0.11	-0.12	0.05	0.03	0.02	0.05
	p-value	**0.005**	0.16	0.13	0.49	0.71	0.76	0.50
DIN: DIP ratio	Tau	0.04	0.01	0.03	-0.07	-0.13	-0.10	-0.03
	p-value	0.51	0.84	0.68	0.31	0.07	0.14	0.64
Total nitrogen (TN)	Tau	**-0.19**	-0.13	-0.05	-0.05	**-0.24**	**-0.22**	**-0.15**
	p-value	**0.008**	0.06	0.52	0.52	**0.001**	**0.003**	**0.034**
Total phosphate (TP)	Tau	-0.12	0.03	-0.11	0.13	-0.01	-0.02	0.03
	p-value	0.09	0.70	0.18	0.06	0.95	0.82	0.68
TN:TP ratio	Tau	0.03	-0.04	0.03	**-0.16**	-0.13	**-0.20**	-0.13
	p-value	0.66	0.54	0.75	**0.023**	0.06	**0.006**	0.08
Dissolved organic nitrogen (DON)	Tau	0.09	0.07	0.03	0.04	-0.10	**-0.29**	**-0.32**
	p-value	0.20	0.32	0.72	0.58	0.15	**<0.001**	**<0.001**
Dissolved organic phosphate (DOP)	Tau	-0.01	0.05	-0.03	0.07	0.01	0.03	-0.02
	p-value	0.91	0.49	0.70	0.30	0.97	0.68	0.77
DON:DOP ratio	Tau	0.03	-0.04	0.07	-0.06	-0.04	**-0.21**	-0.09
	p-value	0.66	0.54	0.40	0.41	0.49	**0.003**	0.23
Karlodinium veneficum	Tau	0.17	0.13	**0.41**	**0.20**	**0.42**	**0.21**	**0.36**
	p-value	0.09	0.17	**<0.001**	**0.035**	**<0.001**	**0.017**	**<0.001**
Cryptomonas spp.	Tau	**-0.23**	**-0.19**	**-0.20**	-0.17	**-0.24**	**-0.34**	-0.16
	p-value	**0.011**	**0.032**	**0.020**	0.05	**0.007**	**<0.001**	0.07
Microphytoflagellate	Tau	-0.13	**-0.20**	**-0.22**	**-0.25**	-0.17	**-0.26**	-0.14
	p-value	0.13	**0.023**	**0.011**	**0.004**	0.07	**<0.001**	0.13

Table 2. 2. Cross-correlation between time series of physical factors or different nutrients forms and ratios and of two potential prey and *Karlodinium veneficum* for seven stations in Chesapeake Bay with lags ranging from 0 to 12 months. Asterisks denote correlation significant (*$p < 0.05$, **$p < 0.01$) greater than zero. Leading factors for nutrient variables are defined based on a stronger relationship and/or lag with a lower value, while secondary factors are comparably less well correlated and/or have a longer lag time response.

Variables	Oligohaline zone				Mesohaline zone									
	Patapsco R. WT5.1		Main-stem CB3.3C		Choptank R. ET5.2		Patuxent R. LE1.1		Potomac R. LE2.2		Main-stem CB4.3C		Main-stem CB5.2	
	Lag	Corr	Lag	Corr	Lag	Corr	Lag	Corr	Lag	Corr	Lag	Corr	Lag	Corr
Water temperature	0	0.24*		ns	0	0.23*	0	0.21*		ns	5	0.25*	5	0.33*
Salinity		ns	2	-0.20*		ns	2	-0.24*	2	-0.25*	2	-0.23*	1	-0.23*
													5	0.36*
Flow	0	-0.25*		ns		ns		ns	3	0.22*	3	0.32*	2	0.23*
									7	-0.22*			6	-0.30*
Dissolved inorganic nitrogen (DIN)	0	-0.31*	7	-0.22*	3	0.26*	4	0.21*	2	0.21*	2	0.33*	1	0.22*
Dissolved inorganic phosphate (DIP)	8	0.40**	7	0.26*	0	-0.28*	10	-0.28*	0	-0.21*	9	-0.30*	9	-0.29*
Total nitrogen (TN)		ns	7	-0.20*		ns	1	0.25*	2	0.24*	2	0.37*	4	-0.26*
							2	0.31*						
Total phosphate (TP)	8	0.23*	7	0.21*	1	-0.23*	1	0.38*	4	0.23*	9	-0.23*		ns
Dissolved organic nitrogen (DON)	0	0.22*		ns		ns	8	0.31*		ns	6	0.30*		ns
Dissolved organic phosphate (DOP)	0	0.45**		ns	6	0.23*		ns		ns		ns	4	0.22*
DIN:DIP ratio	4	0.26*	2	0.27*	2	0.29*	4	0.28*	2	0.33*	2	0.47*	1	0.30*
			3	0.36*										
DON:DOP ratio	0	0.24*		ns		ns		ns	2	0.28*		ns	1	0.24*
TN:TP ratio	4	0.25*	3	0.24*	3	0.31*	3	0.24*	2	0.32*	2	0.36*	1	0.38*
Cryptomonoas spp.		ns		ns	5	0.28*	0	0.36*	0	0.27*	0	0.27*	0	0.37*
Microphytoflagellate	1	0.25*		ns		ns	1	0.30*	1	0.73**	2	0.24*	0	0.66**

Table 2. 3. Best transfer function models for *Karlodinium veneficum* time series from 2002-2011 across seven stations in the Chesapeake Bay based on Akaike's information criterion (AIC). Superscripts denote model scenarios; Model I equations were based on nutrient concentrations and Model II equation were based on the ratios. Stations in the oligohaline zone are WT5.1 and CB3.3C; the rest of the stations are in the mesohaline zone.

Latitude	Stations	Best models for *Karlodinium* time series	n	R^2	F	*p*-value
39.21	Patapsco R. WT5.1	*K. veneficum*^{I} = DOP + DIP	78	0.24	20.28	<0.001
38.99	Main-stem CB3.3C	*K. veneficum*^{I} = Salinity lag2 + DIN	82	0.10	3.67	<0.05
38.58	Choptank R. ET5.2	*K. veneficum*^{I} = Temperature + DIP	84	0.15	5.724	<0.01
38.42	Patuxent R. LE1.1	*K. veneficum*^{I} = *Cryptomonas* + Temperature + DON lag8	81	0.21	7.18	<0.001
		K. veneficum^{II} = *Cryptomonas* + Temperature	81	0.15	7.848	<0.001
38.16	Potomac R. LE2.2	*K. veneficum*^{I} = *Cryptomonas* + Salinity lag2 + DIN lag2	90	0.18	5.58	<0.001
		K. veneficum^{II} = *Cryptomonas* + Salinity lag2 + Flow lag2	90	0.15	4.29	<0.01
38.55	Main-stem CB4.3C	*K. veneficum*^{I} = *Cryptomonas* + TN lag2 + flow lag3	82	0.15	3.87	<0.01
		K. veneficum^{II} = *Cryptomonas* + Temperature lag3	82	0.10	4.58	<0.05
38.13	Main-stem CB5.2	*K. veneficum*^{I} = Microphytoflagellate + *Cryptomonas*	82	0.46	33.24	<0.001
		K. veneficum^{II} = Microphytoflagellate	82	0.44	62.07	<0.001

Figures

Fig. 2. 1. Map of the Chesapeake Bay showing the sampling stations from the Chesapeake Bay Program that were analyzed for trends in *Karlodinium veneficum*. Stations were selected based on 10-year averaged cell counts L^{-1}. The salinity zones are defined as oligohaline (Salinity < 10) and mesohaline (10 < Salinity < 20).

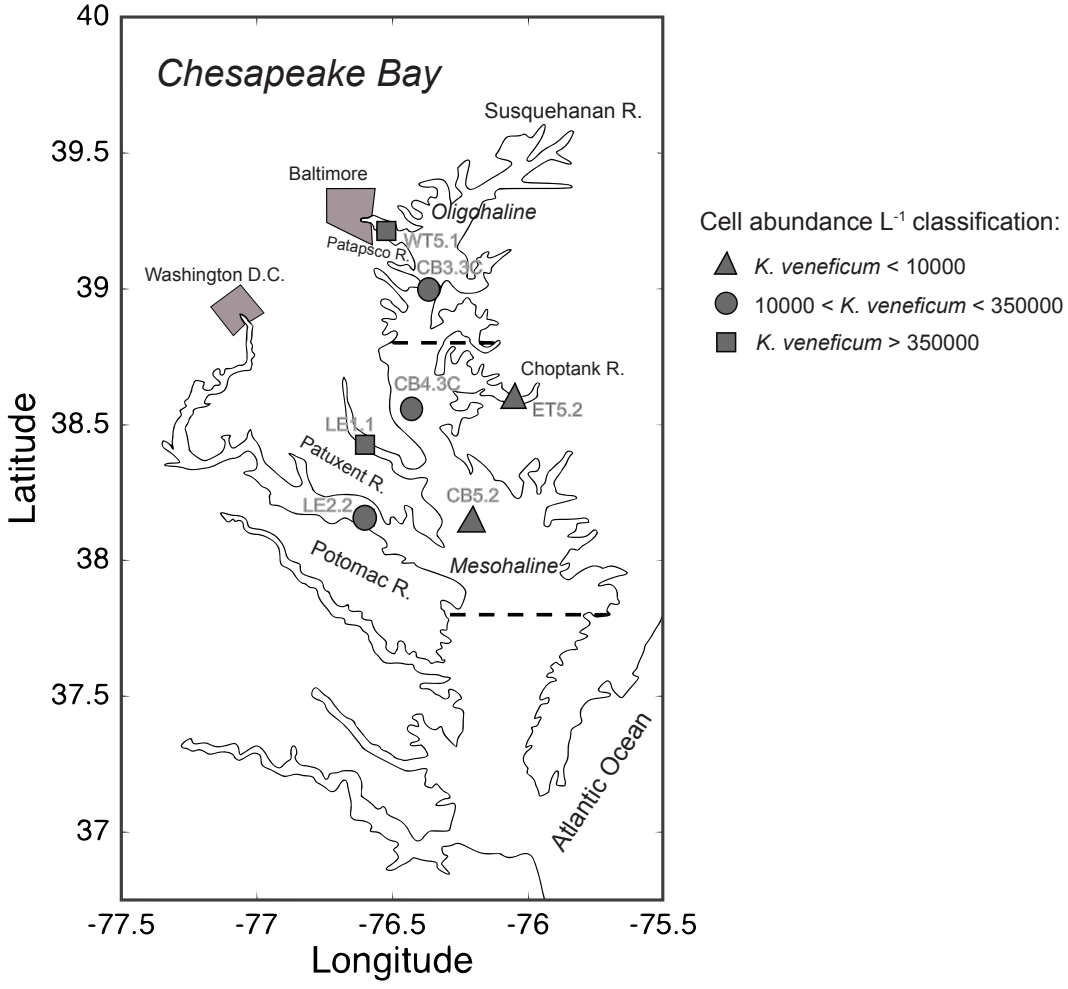

Fig. 2. 2. Panel A: Change in flow rate of the Susquehanna and Potomac Rivers over a decadal time scale. Panels B,C,D,E: Average monthly flow of the Susquehanna River, the Potomac River, total nitrogen (TN) at the mid Bay station CB4.3, and dissolved inorganic nitrogen (DIN) at LE2.2 in the mesohaline zone, respectively. Flow and water quality data were acquired from the USGS and Chesapeake Bay Program as described in text.

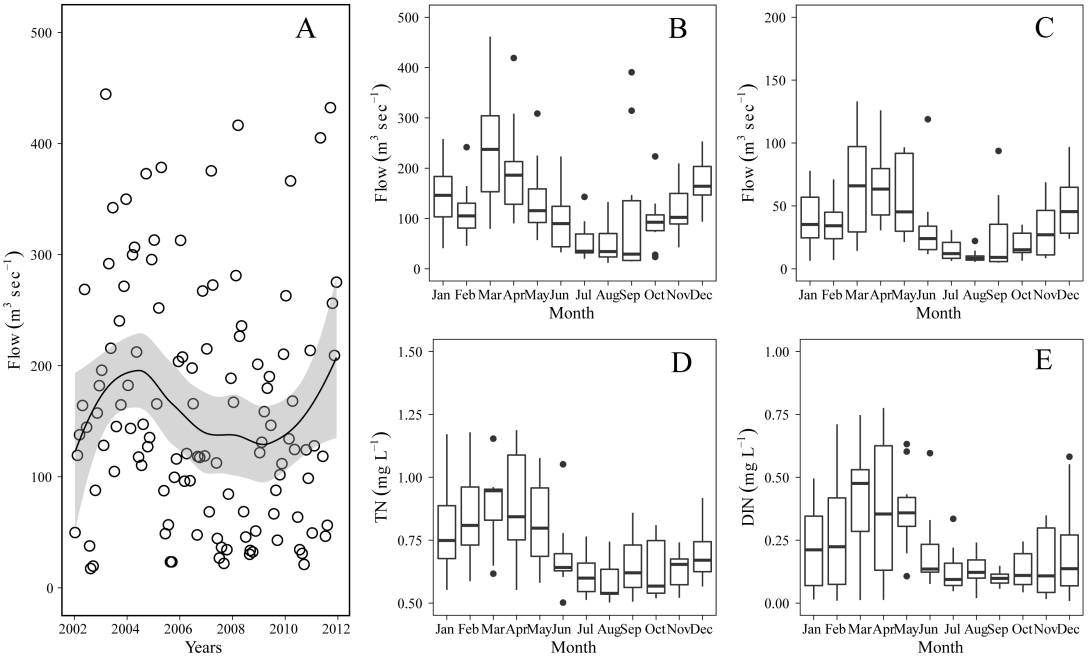

Fig. 2. 3. Average monthly change in abundance of *Karlodinium veneficum* (Panel A) *Cryptomonas* spp. (Panel B), and microphytoflagellates (Panel C) at CB5.2 in the mesohaline zone.

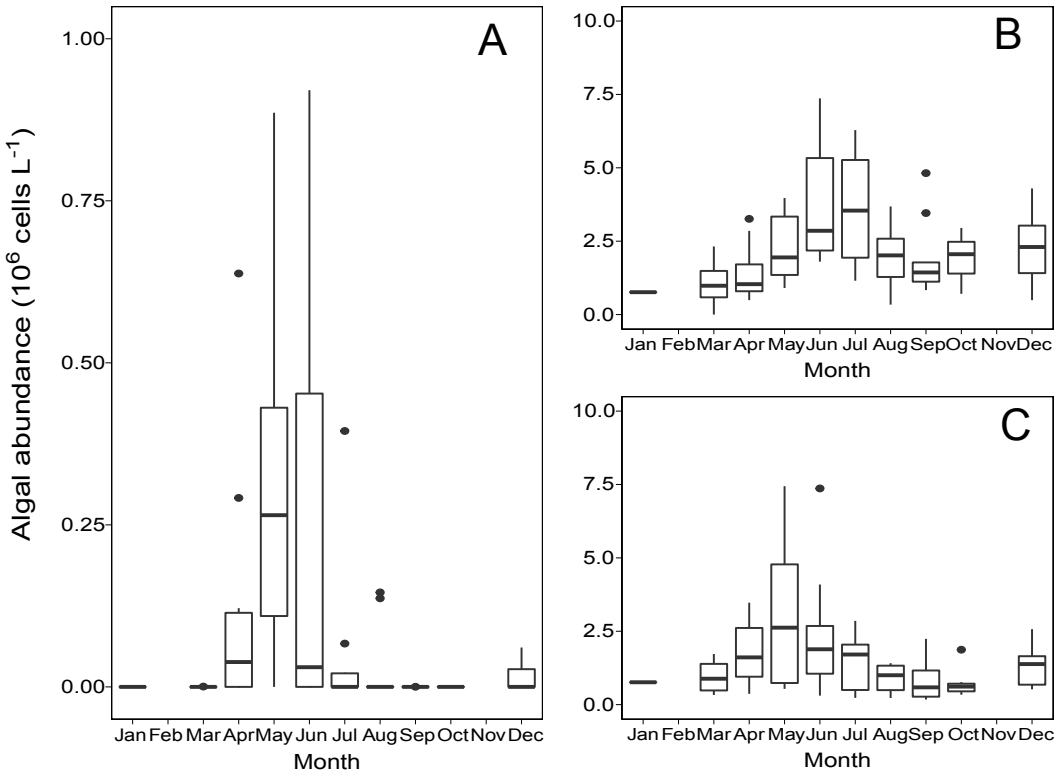

Fig. 2. 4. Conceptual diagram of links between flow, dissolved N and P availability and nutritional condition of prey and of *Karlodinium veneficum* in summer in the mesohaline zone of Chesapeake Bay. These conditions are suggested to lead to late-summer blooms of *K. veneficum*.

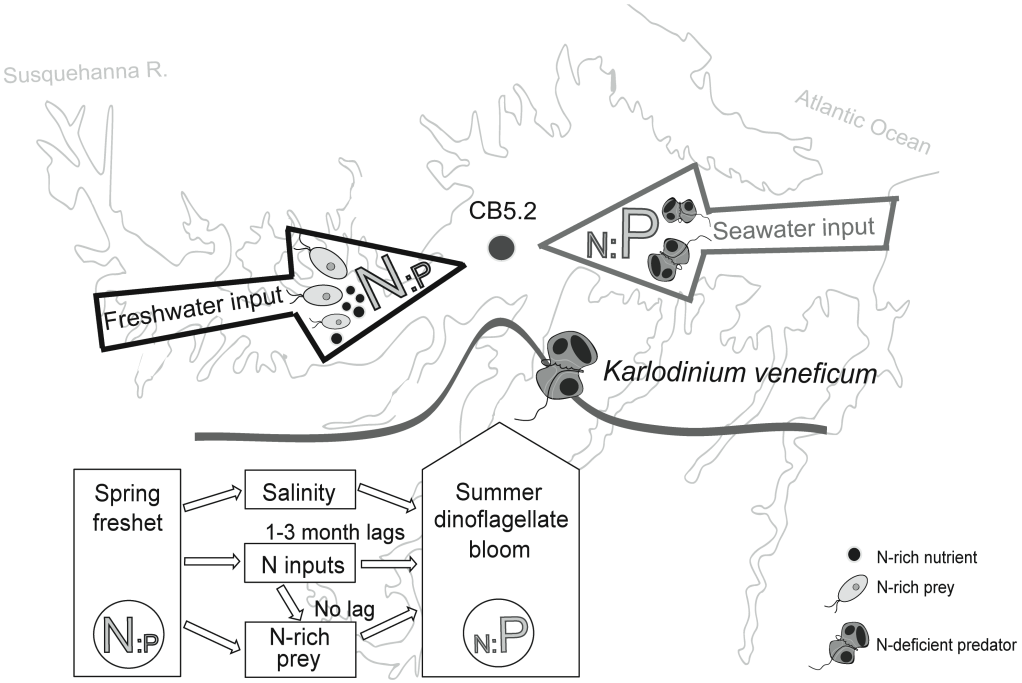

Appendix I: Supplemental Material Chapter 2

Fig. AI.1. Nutrient concentration time series with significant trends ($p < 0.05$, triangles) and non-significant trends ($p > 0.05$, circles) over 7 stations in the Chesapeake Bay from 2002 to 2011. A loess curve (solid line) is fitted with 95 % confidence interval (grey band).

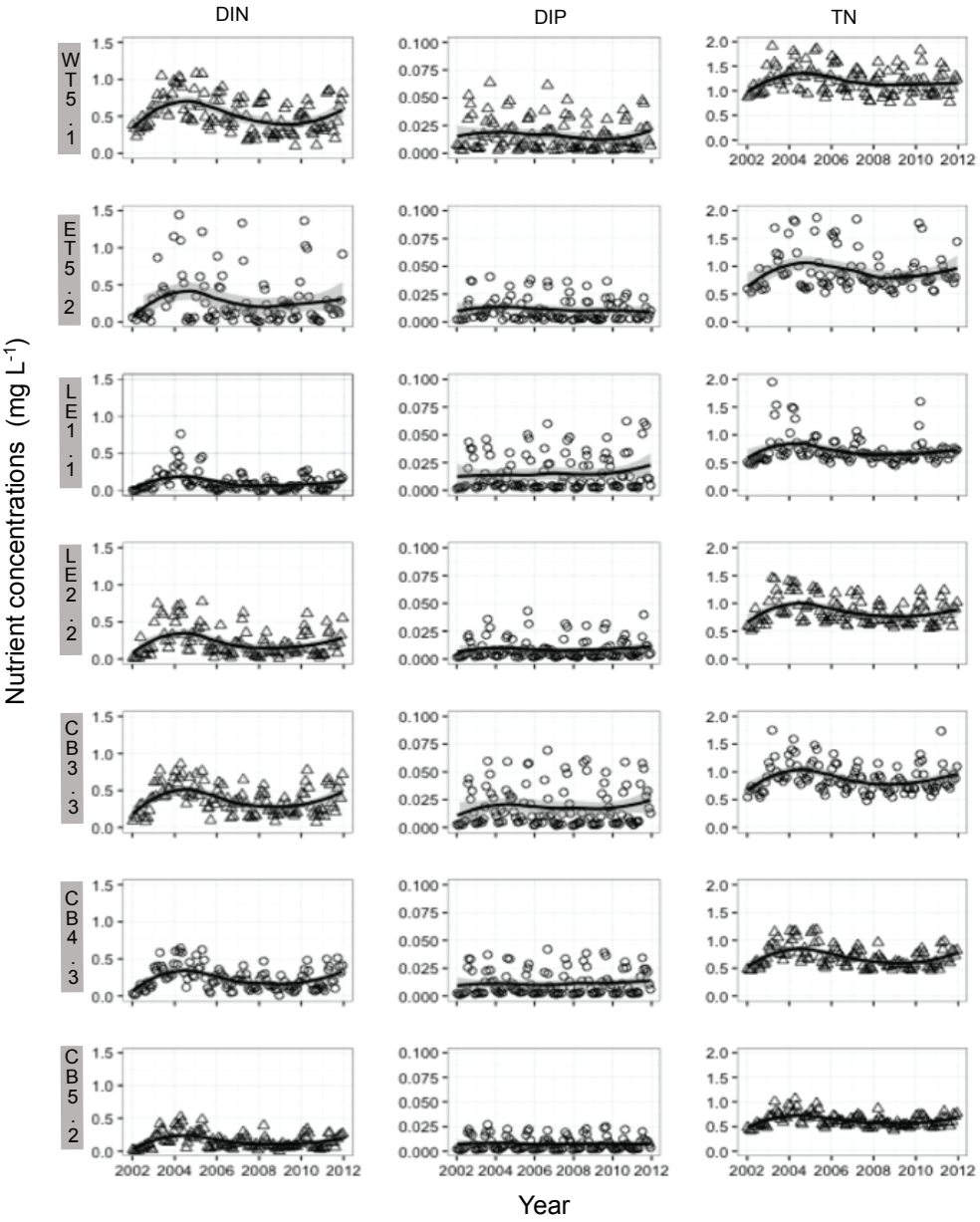

Fig. AI.1. (Continued)

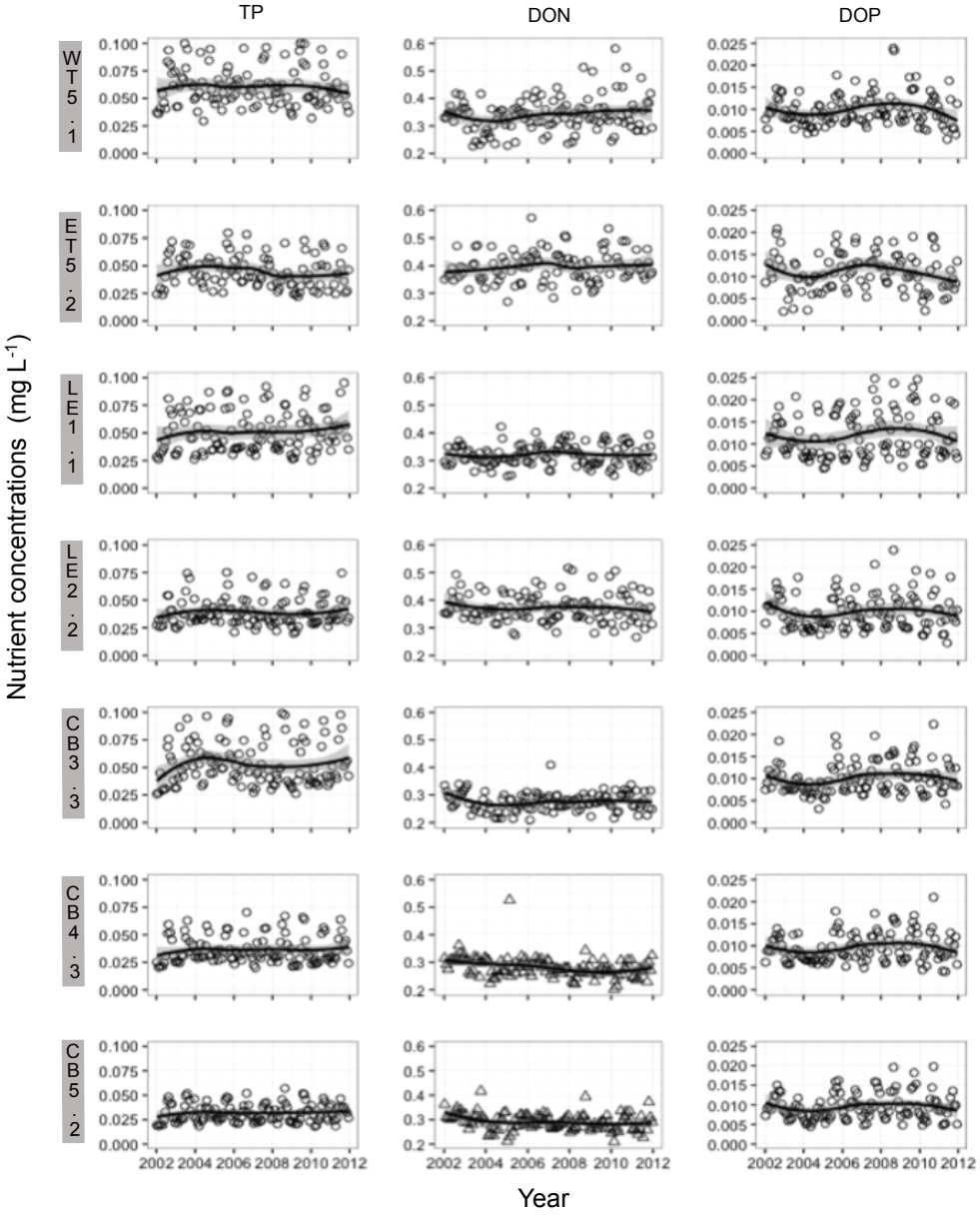

Fig. AI. 2. Phytoplankton time series with significant trends ($p < 0.05$, squares) and non-significant trends ($p > 0.05$, circles) over 7 stations in the Chesapeake Bay from 2002 to 2011. A loess curve (solid line) is fitted with 95 % confidence interval (grey band).

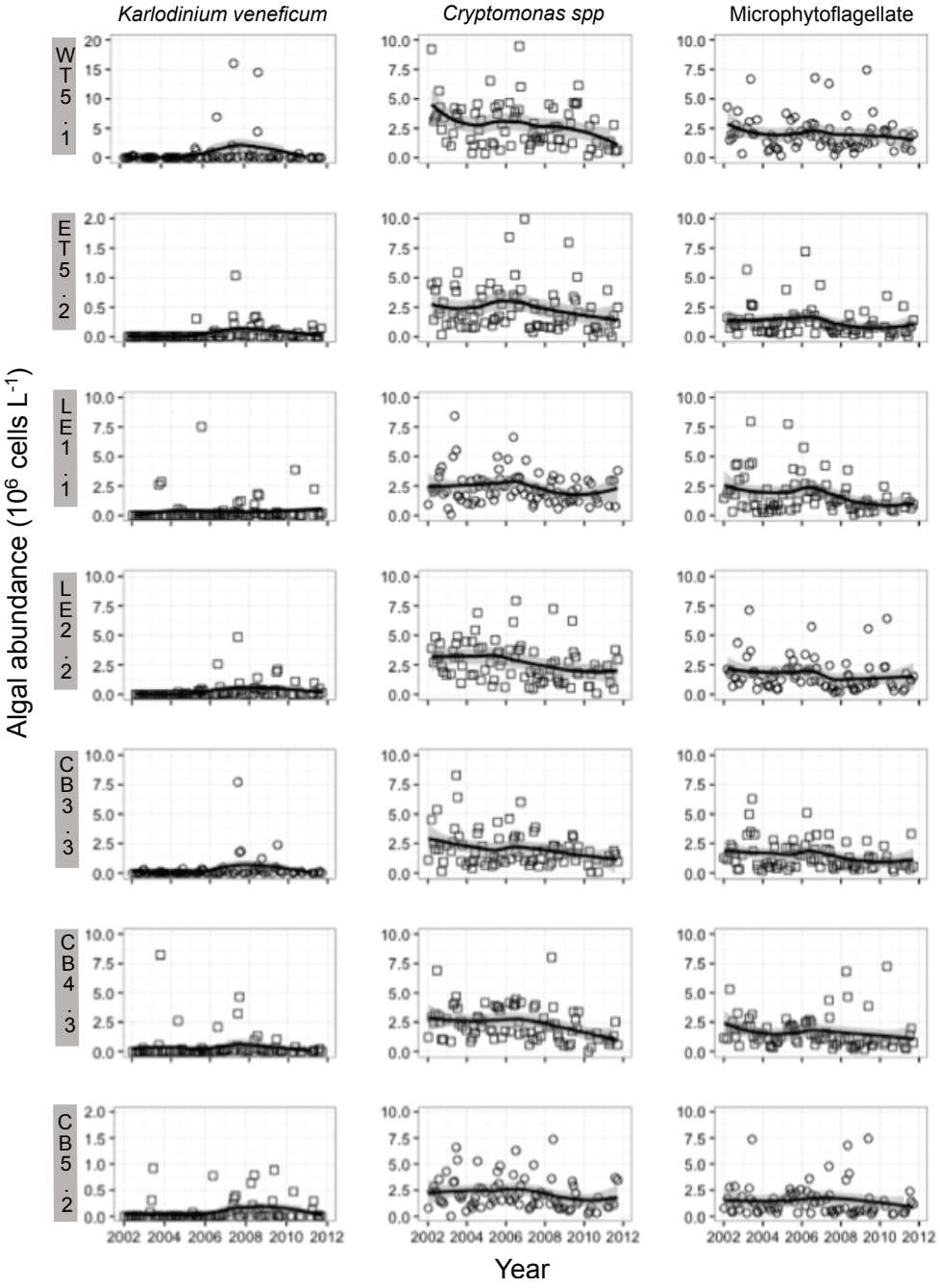

Chapter 3: *Karlodinium veneficum* feeding responses and effects on larvae of the eastern oyster *Crassostrea virginica* under variable nitrogen:phosphorus stoichiometry[2]

Abstract

Mixotrophic feeding can be promoted by nutrient-enriched prey, a nutritional strategy which can provide benefits to some toxic microalgae under nutrient-imbalanced conditions. However, it is unclear how the nutritional condition of the predator or the prey affects the mixotrophy and toxicity of toxin-producing mixotrophs. Laboratory experiments were conducted to measure growth and feeding rates of *Karlodinium veneficum* with addition of *Rhodomonas salina* as prey under varied nitrogen (N):phosphorus (P) stoichiometry (molar N:P of 4, 16 and 32) of both predator and prey and with *K. veneficum* initially in different growth phases (exponential and stationary). Growth rates of initially exponential- and stationary-phase *K. veneficum* were enhanced in the presence of prey with reciprocal nutrient conditions. Feeding rates (measured as prey death rates) were highest for low-NP *K. veneficum* initially growing exponentially and mixed with N-rich prey. Maximum feeding rates of low-NP *K. veneficum* on N-rich prey during exponential growth were ~4-fold higher than the rates of high-NP *K. veneficum* on N-rich prey. The nutritionally different *K. veneficum* were tested with larvae of the eastern oyster *Crassostrea virginica* to compare putative toxicity. Larval mortality was significantly increased in 2 d exposures to high-NP *K. veneficum* monocultures in both growth

[2] Published as Lin et al. (2017). *Aquat. Microb. Ecol.* 79(2), 101-114. doi: 10.3354/ame01823.

phases. When mixed with N-rich prey, the presence of *K. veneficum* resulted in significantly enhanced larval mortality, but this was not the case for low-NP *K. veneficum* in exponential phase. Enhanced growth of *K. veneficum* and increased negative effects of *K. veneficum* on larval survival appeared to be highest when fed prey with higher N:P content.

Introduction

Mixotrophy, the process by which algae gain nutrition from both phototrophy and phagotrophy, is a ubiquitous phenomenon in freshwater as well as marine systems from oligotrophic to eutrophic waters (Jeong et al., 2005a,b; Burkholder et al., 2008; Zubkov and Tarran, 2008; Stoecker et al., 2009; Flynn et al., 2013). Phagotrophic algae appear to be common among chrysophytes, dinoflagellates and haptophytes; most of these organisms are capable of deriving a substantial proportion of their carbon (C) by ingestion of prey compared to C acquisition from photosynthetic reactions (Schnepf and Elbrächter, 1992; Graneli and Carlsson, 1998; Legrand, 2001; Adolf et al., 2006; Raven et al., 2009; Jeong et al., 2010; Hansen, 2011; Granéli et al., 2012). The understanding that many algae can benefit from prey ingestion and that this metabolic pathway is ecological important is rapidly advancing (Stoecker et al., 2009; Flynn et al., 2013; Mitra et al., 2014, 2016), but questions of how mixotrophic metabolism can be advantageous to organisms living under varying environmental conditions remain. In particular, linkages between conditions when organisms experience inorganic nutrient and light limitation and/or changes in cellular nutrient content and mixotrophic nutrition are not well understood (Stoecker et al., 1997; Li et al., 2000b; Smalley et al., 2003; Carvalho and Granéli, 2010;

Lundgren et al., 2016). Although the importance of mixotrophic metabolism is regulated by prey quantity and quality (Hansen et al., 2000), detailed examinations of how these factors affect physiological states of mixotrophic organisms are scarce (Carvalho and Granéli, 2010; Lundgren et al., 2016).

Mixotrophic nutrition has been shown to be significant for growth of the dinoflagellate *Karlodinium veneficum* (Li, 1996; Adolf et al., 2006; Calbet et al., 2011). This species can produce hemolytic, cytotoxic and ichthyotoxic compounds, named karlotoxins (Kempton et al., 2002), and growth-limited conditions (e.g., stationary growth phase) have been associated with higher cellular quotas of karlotoxin (Adolf et al., 2009). This species is also capable of forming high-biomass blooms of up to 10^5 cells mL^{-1} (e.g., Adolf et al., 2008; Place et al., 2012) leading to fish and shellfish mortality, illness of aquatic organisms and human health concerns (Deeds et al., 2002). Blooms of *K. veneficum* are distributed worldwide in estuaries and coasts from South Africa (Braarud, 1957) to Europe (Bjornland and Tangen, 1979), China (Dai et al., 2013), Australia (Ajani et al., 2001; Adolf et al., 2015) and the United States (Li et al., 2000a; Adolf et al., 2008; Hall et al., 2008). The importance of mixotrophy to this species under highly variable environments in terms of nutrient availability and its association with toxigenic abilities may contribute to its global success (Adolf et al., 2009; Place et al., 2012).

In the United States, *K. veneficum* is known to be an important member of the Chesapeake Bay phytoplankton community (reviewed in Marshall et al., 2005), and this dinoflagellate is frequently present at levels of $> 4 \times 10^3$ cells mL^{-1} (Li et al., 2015). It may be distributed throughout the bay through annual subsurface transport

from southern bay to nutrient-poor surface waters in the middle and upper bay (Li et al., 2000a). This species co-occurs with cryptophytes and develops high concentrations, particularly in the salinity range of 7 to 18 (Li et al., 2000a). It also has been shown to occur during the period in which a median value of ambient dissolved inorganic nitrogen (N): phosphate (P) ratios bracket the Redfield ratio (~16) in summer, but blooms may also be found during periods well in excess of Redfield proportions (Li et al., 2015). The ability to use organic nutrients, including particulate nutrients via mixotrophy, appears to be essential to the growth and maintenance of high abundances of this species under nutrient limitation. For example, grazing of phycoerythrin-containing cryptophytes by *K. veneficum* based on food vacuoles contents, is commonly found (Li, 1996), and daily removal of up to 4 % of the cryptophyte population in Chesapeake Bay has been observed (Li et al., 2001). Growth rates of *K. veneficum* in its mixotrophic mode (~0.52 – 0.57 d^{-1}) have been reported to be ~2-fold larger than those in autotrophic mode (~0.22 – 0.27 d^{-1}) (Li et al., 1999; Adolf et al., 2006; Calbet et al., 2011). The nutritional supply from feeding to the growth of mixotrophic *K. veneficum* in Chesapeake Bay can be significant, as they can gain 10 % of their C, 11 % of their N and 17 % of their P requirements through consumption of cryptophyte biomass (Li, 1998). These data support the hypothesis that feeding contributes important nutrient sources to the formation and persistence of *K. veneficum* blooms when inorganic nutrients are limited in supply (Adolf et al., 2008), especially under P-limited environments (Li et al., 2000b).

Cellular toxicity also has implications for *K. veneficum* bloom formation and/or maintenance under varying environments. The toxins (alleochemicals) are

found to aid the mixotrophic feeding of *K. veneficum* (Adolf et al., 2008) by inhibiting movement of prey, and negative effects of toxin on other planktonic organisms, including grazers, can be a mechanism for bloom promotion (Mitra and Flynn, 2006). Additional nutrient sources via feeding are promoted by these toxic substrates that immobilize prey and enhance the efficiency of prey capture (Place et al., 2012). As *K. veneficum* has the ability to produce toxins that are involved in allelopathic interactions, its temporal and spatial overlap with oyster spawning in Chesapeake Bay has drawn attention to potential impacts of these toxins on oyster larvae (Glibert et al., 2007). Although laboratory studies with a low toxin level strain have examined the adverse effects on early development of oyster larvae as a function of the abundance of *K. veneficum* (Glibert et al., 2007; Stoecker et al., 2008), questions of whether or not alleochemicals produced by this species change with the physiological state of its growth or that of its prey due to varying nutrient supply as well as how such changes may affect their interactions with oyster larvae remain largely unanswered.

Studies of other mixotrophic algae have demonstrated that high N:P stoichiometry is often associated with increases in cellular toxicity (Granéli and Johansson, 2003; Granéli and Flynn, 2006; Hardison et al., 2012; Lundgren et al., 2016). Many toxic compounds are N and/or C rich, so production of toxins under high enrichment conditions might be considered as a dissipatory mechanism such that cells release the nutrients (N or C) that are not needed (Glibert and Burkholder, 2011) or produce secondary metabolites through metabolic processes that may not go to completion via the normal pathway. Toxin production by *K. veneficum* is coupled

with cellular C acquisition (Staunton and Weissman, 2001) through photosynthesis and it has been shown that these cells produce toxin and only eat during the light period (Adolf et al., 2008), but the link between this observation and that of N and P nutrition is unknown. A link between feeding and toxicity might be explained by situations in which nutrient limitation triggers nutritional switches, which in turn contribute to production of toxins (Stoecker et al., 2006). From this reasoning, *K. veneficum* would likely be more phagotrophic and more toxic under conditions of nutrient imbalance.

The objective was to examine if growth rates of *K. veneficum*, or death rates of its cryptophyte prey, change when it and its prey are under different stoichiometric conditions (as defined by N:P ratio). Bioassay experiments with oyster larvae were used to test the hypothesis that under nutrient-imbalanced conditions, *K. veneficum* will increase its mixotrophic metabolism and toxin production, enhancing the detrimental effects on oyster larvae. In all, my data contribute to the understanding of how different growth phases and nutritional conditions of *K. veneficum* affect oyster larval growth under varying environmental conditions.

Materials and Methods

Algal cultures

Non-axenic strains of *Karlodinium veneficum* (CCMP1975, isolated from Chesapeake Bay, Maryland, USA) and *Rhodomonas salina* were provided by the National Center for Marine Algae and Microbiota (NCMA) and the Oyster Hatchery of Horn Point Laboratory (HPL), respectively. Strains were first grown in *f*/2 media

(Guillard, 1975) at 22 ^{o}C with a light intensity of 430 μmol photos m^{-2} s^{-1} on a 14 h light:10 h dark cycle. Culture media were prepared with autoclaved artificial water (salinity of 10). Once the cultures (both experimental species) reached high cell densities but were still growing exponentially, the cells were inoculated into new growth media adjusted to give variable N:P ratios. The nitrate (NO_3^-) concentration was held constant at *f*/2 proportions, but different PO_4^{3-} concentrations were added to achieve 3 nutrient conditions for both species: low-NP (molar N:P = 4, [N] = 88 μM, [P] = 22 μM); Redfield ratio (molar N:P = 16, [N] = 88 μM, [P] = 5.5 μM) and high-NP (molar N:P = 32, [N] = 88 μM, [P] = 2.75 μM). Trace metals, iron, vitamins (B12, biotin and thiamine) were added to the cultures at levels corresponding to *f*/2 media. The objective was to establish cultures with variable stoichiometry, not true N or P limitation.

Experimental design

Experimental treatments were designed as 3 by 3 crossmatches of different nutrient conditions of *K. veneficum* and *R. salina* for each growth state of *K. veneficum*. Specifically, experiments were performed using *K. veneficum* grown under 3 N:P ratios (low NP, Redfield ratio and high NP, see 'Algal cultures' above) and in 2 growth phases (exponential and stationary) and with *R. salina* grown under the same N:P conditions but always under exponential growth. Culture flasks containing 250 mL of new growth media (i.e. N:P ratio of 4, 16 and 32) were inoculated with *K. veneficum* and *R. salina* cells to a final concentration of 1500 and 5000 cells mL^{-1}, respectively. The *R. salina* cells were centrifuged at 6000 rpm (1000 × g) for 10 min to remove the culture medium and inorganic nutrients and added into

culture flasks with *K. veneficum* cultures. Control treatments, of individual species only, were also conducted for the 3 nutrient conditions of each *K. veneficum* and *R. salina*. Thus, this study consisted of 15 treatments, in duplicates, totalling 30 culture flasks for each growth state of *K. veneficum*.

The mixed-culture experiments with *K. veneficum* inoculated during both exponential and stationary phase lasted for 72 and 96 h, respectively. During this time, aliquots (5 mL) were collected for cell enumeration at 0, 6, 12, 24, 36, 48 and 72 h after homogenization from each flask and were preserved with diluted acid Lugol's solution. Additional water samples (40 mL) were collected at the beginning (t_0) and the end (t_f) of the time courses and filtered for the analysis of NO_3^- and PO_4^{3-}. Samples of water and cells were also collected at the end of the experiments to perform the toxicity bioassays with oyster larvae (see 'Bioassay determination of putative toxicity' below).

Cell counts and nutrient analyses

Samples of *K. veneficum* and *R. salina* cells were enumerated using light microscopy at 100× magnification using a Sedgewick-Rafter chamber (Guillard, 1978). Replicate counts per sample were performed on 20 random fields for representative cell concentrations (expressed as cells mL^{-1}). Analyses of NO_3^- and PO_4^{3-} were performed on samples that were filtered through precombusted GF/F filters (pore size 0.47 μm). Colorimetric analyses were conducted using 96-well micro-assay plates, based on the methods of Doane & Horwáth (2003) for NO_3^- and Ringuet et al. (2011) for PO_4^{3-}.

Growth, death rates and nutrient consumption

Cell-specific growth rates (d^{-1}) of *K. veneficum* were calculated from the slopes of the regressions of natural log-transformed data during periods of maximum changes in cell densities.

Cell-specific death rates of *R. salina* (Rs *K. veneficum*$^{-1}$ d^{-1}) were determined as the difference between growth rates of prey in the control and experimental flasks with the corresponding nutrient conditions, based on the equations of Frost (1972) and Heinbokel (1978) to account for grazer growth. Death rates of *R. salina* were reported rather than ingestion rates because of the difficulty in differentiating between cells that were actually grazed and those cells that may have burst due to putative toxic effects.

Rates of consumption of NO_3^- and PO_4^{3-} were calculated based on the change in concentration from t_1 to t_2 in order to determine the extent to which the NO_3^-: PO_4^{3-} drawdown ratio varied between the different growth phases of the predator and between the different nutritional status of both predator and prey cells in the mixed cultures.

Bioassay determination of putative toxicity

Oyster larvae (provided by the Oyster Hatchery at HPL) were used as bioassay organisms to assess alleged *Karlodinium* toxicity. Spawning oysters were collected in filtered natural seawater with a salinity of 10 and a temperature of 28 ^oC. The larvae were tested within 4 h of fertilization, in triplicate, in 3 mL 12-well culture plates with flat bottoms.

Cells were obtained at t_0 and t_f of the mixed-culture experiments to initiate the bioassay tests. The oyster larvae (60 larvae cells mL^{-1}) were exposed to a fixed density of *K. veneficum* (9×10^2 cell mL^1) obtained from the 3 monoculture treatments and the 9 mixed-culture treatments from each growth phase. After 48 h of exposure of the larvae to the algal cultures, each well was fixed with dilute acid Lugol's solution, and the samples were analyzed using an Utermöhl chamber (Edler and Elbrächter, 2010) through an inverted light microscope (Nikon Eclipse TE2000-U) at 100×. Both live and dead larvae were counted to estimate larval mortality.

Statistical analyses

All statistical analyses were performed with R. The Shapiro-Wilk test was used to check normality of the data, while the Levenes' test was used to assess the homogeneity of variance. Maximal growth rates of *K. veneficum* were compared for statistical differences in slopes of regression of natural log-transformed data among the variables measured in the replicates of the treatments during the same periods of time (ANCOVA test). Comparisons between the 2 growth-phase conditions considering a single variable were verified using the Student's *t*-test, while correlations between 2 variables were estimated by significance of the Pearson's product moment coefficients. Differences among the larval mortality in the triplicate monocultures and mixed cultures were analyzed using an ANOVA test followed by Tukey's HSD test for pairwise comparison.

Results

Cell densities, growth and prey death rates

Mixed-culture experiments were performed using stock cultures of *Karlodinium veneficum* grown under 3 N:P ratios (low-NP, Redfield ratio and high-NP conditions), and cells were inoculated during the exponential and stationary phase (Fig. 3.1). Since the variable N:P growth conditions did not initially yield N or P limitation, similar patterns of growth of *K. veneficum* from exponential phase to early stationary phase were observed (Fig. 3.1). The specific growth rates of monocultures of *K. veneficum* under the 2 growth phases and 3 nutrient conditions ranged from 0.25 to 0.50 d^{-1} (Table 3.1). While monocultures of exponential-phase *K. veneficum* had similar growth rates when transferred to low-NP, Redfield ratio and high-NP growth media, the cultures of stationary-phase *K. veneficum* showed significantly different cell densities and growth rates when transferred into different media (ANCOVA test, $p < 0.01$; Fig. 3.2). Maximum growth rates increased when cells were transferred into the high-NP media compared to the other 2 conditions when *K. veneficum* was initially in stationary phase (Fig. 3.2).

With additions of prey, cell densities and growth rates of *K. veneficum* changed with time for both conditions of *K. veneficum* cells, exponentially growing and stationary phase (Fig. 3.3). After transfer to the plus-prey condition, maximal growth rates of initially exponential-phase *K. veneficum* cultures under low-NP condition (0.70 ± 0.10 d^{-1}) and initially stationary-phase *K. veneficum* cultures under high-NP condition (0.66 ± 0.16 d^{-1}) were similar (Table 3.1). Specific growth rates between the monoculture and mixed culture treatments were compared, and it was

found that there was a significant increase in growth when exponentially-growing, low-NP *K. veneficum* cells were mixed with prey of high-NP (ANCOVA test, $p < 0.05$) and when high-NP *K. veneficum* cells were mixed with Redfield ratio prey (ANCOVA test, $p < 0.01$). In contrast, significant increased growth rates of initially stationary-phase *K. veneficum,* when transferred into all nutrient conditions, were found only when cells were mixed with prey that were low NP compared to monocultures (ANCOVA test, $p < 0.05$ for all tests).

The effects of the nutrient condition of the prey on growth rates of *K. veneficum* were determined as the slope of the rate of changes over the exposure time course, and it was found that the rate of change was higher in initially exponential-phase *K. veneficum* than in initially stationary-phase *K. veneficum* (Fig. 3.3). In particular, exponential-phase *K. veneficum* grown under both Redfield ratio and low-NP conditions had significantly different growth rates with nutritionally distinct prey (ANCOVA test, $p < 0.01$; Table 3.1), while only the growth rates of stationary-phase *K. veneficum* under high NP responded differently to nutritional distinct prey *R. salina* (ANCOVA test, $p < 0.1$; Table 3.1).

Regardless of the nutritional status of *R. salina* or *K. veneficum*, death rates of prey were significantly higher when *K. veneficum* was initially in stationary phase compared to exponential phase (*t*-test for all comparison, $p < 0.01$; Table 3.2) and were the same regardless of the nutritional status of the prey (ANOVA test, $p > 0.01$; Table 3.2). In addition, the maximal growth rates of initially exponential-phase *K. veneficum* were positively correlated with prey death rates ($r = 0.77$, $n = 18$, $p < 0.01$; Fig. 3.4), while those of the mixed-cultures for initially stationary-phase *K. veneficum*

showed a negative relationship with prey death rates ($r = -0.65$, $n = 18$, $p < 0.05$; Fig. 3.4). When looking only at the initially exponential-phase *K. veneficum,* highest prey death rates were observed when low-NP *K. veneficum* were combined with high-NP *R. salina* (ANOVA test, $p < 0.01$; Table 3.2).

Nutrient depletion

The ratios of consumption of NO_3^- and PO_4^{3-} (drawdown ratios) in monoculture and mixed cultures varied between preconditioned exponential- and stationary-grown *K. veneficum*, and there were also slight differences in the nutrient consumption ratios of the monocultures of *K. veneficum* compared to nutritional distinct prey *R. salina* (Fig. 3.5). In mixed cultures, the NO_3^-:PO_4^{3-} drawdown ratios of initially stationary-phase *K. veneficum* were significantly higher than those of exponential-phase *K. veneficum* (Student's *t*-test for all comparison, $p < 0.01$) and ~2-fold greater than the Redfield ratio of 16 (Fig. 3.5B).

Putative toxic effects of Karlodinium veneficum *on larval growth*

The monocultures of *K. veneficum* grown under high-NP (i.e. N-rich) media in both exponential and stationary phases induced high larval mortality (on average 76 ± 15 %, n = 12) under most growth conditions (Fig. 3.6A, C). However, stationary-phase *K. veneficum* grown on low-NP media, and exponentially-growing *K. veneficum* initially grown on all media combinations, did not induce significant mortality greater than the larvae-only controls (Fig. 3.6A, C). Overall, larval mortality rates caused by the exponential-phase *K. veneficum* (on average 75 ± 21 % for the 3 culture media) were ~ 2-fold higher than those of stationary-phase *K. veneficum* (43 ±

26 %, $p < 0.001$) at t_0. In contrast, by t_f, *K. veneficum* monocultures showed a different pattern of larval mortality depending on their growth phase, with the highest mortality (82 ± 4 %) found for cultures grown in high-NP media (Fig. 3.6C). Overall, larval mortality rates were lower for the exponential-phase *K. veneficum* treatments (54 ± 4 %) compared to those of the stationary-phase *K. veneficum* (66 ± 18 %) at the end of experiments, but there was not a significant difference (Student's *t*-test, $p = 0.11$).

In the presence of *R. salina*, the bioassay tests with both exponential- and stationary-phase *K. veneficum* indicated increases in larval mortalities, except for the condition of N-deficient *K. veneficum* mixed-cultures in exponential phase (Fig. 3.6B, D). Mixed-cultures (irrespective of their nutrient conditions) resulted in high larval mortality in exponential phase (Fig. 3.6B) but even higher rates of mortality in stationary phase under most nutrient conditions (Fig. 3.6D). In exponential phase, only low-NP *K. veneficum* mixed cultures resulted in low larval mortality (Fig. 3.6B). With the presence of *R. salina* with low-NP condition excepted, stationary-phase *K. veneficum* mixed cultures exhibited significantly higher larval mortality rates (average of 81 ± 7 %) compared to those exponential-phase *K. veneficum* mixed cultures (average of 67 ± 12 %; Student's *t*-test, $p < 0.001$). Highest larval mortalities typically occurred with the presence of high-NP (i.e. N-rich) *R. salina* when exponential- and stationary-phase *K. veneficum* was under Redfield ratio and high-NP conditions, respectively (Fig. 3.6B, D).

Discussion

Mixotrophy is clearly far more common in dinoflagellates than previous recognized (Jeong et al., 2005a,b; Flynn et al., 2013) and has advantages to the cells with synergistic, not just additive, effects of phototrophic and heterotrophic growth (Mitra and Flynn, 2010). Even though mixotrophic nutrition has been emphasized as a major mode for harmful algal species in eutrophic environments and feeding has been linked to toxin production (Adolf et al., 2008; Burkholder et al., 2008), there is still much we do not fully understand about why foods of certain nutritional content are eaten, what the effects of variable nutrition are on growth and putative toxicity and how nutrition or physiological state affect growth of the harmful algal bloom or other organisms (e.g., oyster larvae) under eutrophic conditions. The experiments show that the intracellular balance of nutrients and growth phases of the mixotroph as well as its prey have important effects on the growth of *Karlodinium veneficum* blooms and on the development of oyster larvae.

Growth and grazing responses of mixotrophic Karlodinium veneficum

Mixotrophic nutrition can yield significantly enhanced growth rates compared to those achievable in autotrophic mode (Li et al., 1999; Jeong et al., 2005a,b; Adolf et al., 2006; Glibert et al., 2009). The growth rates of *K. veneficum* cultures that were grown only phototrophically or mixotrophically with additions of *Rhodomonas salina* (Table 3.1) were similar to those reported for different strains of *K. veneficum* by a wide range of investigators in batch cultures (Li et al., 1999; Adolf et al., 2006; Calbet et al., 2011). The growth benefit of mixotrophy to *K. veneficum* has been shown to be upwards of 2- to 3-fold. For example, Li et al. (1999) measured

maximum autotrophic growth rates of *K. veneficum* strain CCMP1974 (maintained at 20 ^{o}C at a salinity of 10) of 0.32 ± 0.02 d^{-1} but rates of 0.94 ± 0.06 d^{-1} in mixotrophic cultures with the presence of the cryptophyte *Storeatula major*. In the present study, growth of *K. veneficum* strain CCMP 1975 with additions of *R. salina* had a maximal increase of ~2.8-fold for exponentially growing *K. veneficum* under low-NP condition compared to monoculture growth (Table 3.1).

Growth rates of *K. veneficum* have shown to be dependent on their food source and its quality. Previous investigators have also found that nutrient availability is one of the triggering factors for mixotrophy in this dinoflagellate. For example, feeding appears under nutrient-replete conditions but increases when under N and/or P deficiency (Li et al., 2000b). The growth rates of *K. veneficum* for both exponentially growing *K. veneficum* under low-NP condition (0.70 ± 0.10 d^{-1}) and stationary-phase *K. veneficum* under high-NP condition (0.66 ± 0.17 d^{-1}) were significantly enhanced in the presence of prey with reciprocal nutritional status when compared to maximal autotrophic growth in exponential phase (0.25 ± 0.07 d^{-1}) and stationary phase (0.50 ± 0.07 d^{-1}), respectively (Table 3.1). These results suggest that enhanced growth performance of *K. veneficum* depends on both prey and predator nutritional status (defined here in terms of N:P ratio) and is ultimately determined through a dynamic balance between internal factors of *K. veneficum* cells under different growth phases and external nutrient supplies (e.g., culture media and high quality food).

It has been shown for other species that mixotrophy can be influenced by both cellular and external nutrient concentrations and ratios as well as prey quality

(Smalley et al., 2003; Lundgren et al., 2016). The results showed significant increases in growth performance for exponentially-growing *K. veneficum* in mixed cultures when supplied with high levels of inorganic P and/or N-rich prey (Table 3.1); however, the growth rates of exponentially growing *K. veneficum* in monocultures were not profoundly influenced by the N:P ratio of the culture media (Fig. 3.2A). This indicates that when the N was depleted in the ambient culture media, exponentially growing *K. veneficum* presumably resorted to feeding on N-rich *R. salina* to compensate. In contrast, the growth performance of initially stationary-phase *K. veneficum* was strongly influenced by N:P ratio of culture media in monocultures, and the highest growth rates were also found when stationary-phase *K. veneficum* grown with P-rich prey when resupplied with a high level of inorganic N (Table 3.1). In particular, it is recognized that N:P drawdown ratios for monoculture exponentially growing *K. veneficum* were higher than those *K. veneficum* in stationary phase; those conditions were enhanced in the mixed cultures, although in the latter the contributions between prey and predator to total inorganic nutrient consumption were difficult to distinguish from each other (Fig. 3.5). Those results might suggest that the N and P in proportions incorporated into particulate matter of *K. veneficum* from the ambient culture media are different regarding the different cellular metabolic and structure requirements of the different growth phases. Nielsen (1996) assessed the cellular composition of *Gymnodinium galatheanum,* a harmful algal bloom species regarded as a synonym of *K. veneficum,* and found a comparatively larger capability for P storage compared to that of other dinoflagellates. This stored P consequently is thought to allow them to survive long

periods in stationary phases under conditions not otherwise conducive for sustaining growth. With internally stored P, stationary-phase *K. veneficum* can survive a condition of high N:P in the external media. Such a strategy has also been suggested for other dinoflagellates, including *Prorocentrum minimum* and *Ostreopsis* cf. *ovata*, both of which appear to be sustained for long period of time when P is seemingly depleted in its natural waters (Glibert et al. 2012, Accoroni et al. 2015). Although significant higher prey death rates were observed with *K. veneficum* in stationary-phase than those in exponential-phases, the short-term benefits of the mixotrophy on the growth rates were mainly observed in the latter phase (Fig. 3.4). The data suggest that feeding by exponential-phase *K. veneficum* could improve growth performance immediately compared to stationary-phase cells in which metabolic processes are generally slower. In this regard, nutritional or metabolic status of *K. veneficum* may play an important role in determining the capability to absorb particulate and/or use dissolved organic material released from prey (Glibert and Legrand, 2006), as well as to produce algal toxins with which it can immobilize or kill its prey as part of its nutritional strategy (Sheng et al., 2010; Place et al., 2012). Thus, these differential relationships between exponential-phase and stationary-phase *K. veneficum* could have implications for bloom formations due to different responses and strategies in utilization of nutrient supplies.

The concept that N is preferably obtained through feeding is supported by some studies on haptophyte *Prymensium parvum* (Legrand, 2001; Lindehoff et al., 2010; Lundgren et al., 2016). Lundgren et al. (2016) found that mortality rates are higher when prey is N-rich, regardless of the nutritional states of *P. parvum*. The

study herein agreed with the works involving *P. parvum* of varying nutritional states, as evidenced by the highest values of prey death rates that occurred when mixed with high-NP *R. salina* for both *K. veneficum* in both growth phases (Table 3.2). However, only low-NP *K. veneficum* had high feeding rates of N-rich prey in exponential phase (0.68 ± 0.07 Rs Kv^{-1} d^{-1}), a likely consequence of prey selection that can serve to rectify nutrient deficiency (Mitra and Flynn, 2005).

Moreover, incidences of feeding in mixotrophic dinoflagellates seem to be influenced by ambient nutrient concentration and ratios (Li et al., 2000a,b; Smalley and Coats, 2002). In Chesapeake Bay, feeding in *Ceratium furca* and *K. veneficum* (referred to as *Gyrodinium galatheanum* by the author) are enhanced when N:P ratio deviate from the Redfield ratio with either N or P deficiency (Li et al., 2000b; Smalley and Coats, 2002). The present study agreed with these observations. If only considering the feeding on Redfield ratio prey, increased prey death rates were observed when initially exponential- and stationary-phase *K. veneficum* were grown under high-NP and low-NP condition, respectively (Table 3.2). However, the effects of inorganic nutrient on feeding responses of *K. veneficum* were inversed, which suggests feeding is mediated through the cellular status of the initial growth phase. In fact, *K. veneficum* have shown a 95% increase in fatty acid content, as high quality lipids, during stationary compared to exponential phase growth (Fuentes-Grünewald et al., 2009), so the cellular nutrient stoichiometry and energy metabolism might have changed between the distinct growth phases. This underscores that the intracellular nutrient history and growth conditions of mixotrophic dinoflagellate can influence the ability to utilize different nutrient supplies and supports the study of Smalley et al

(2003) in terms of difficulty of inferring feeding dynamics based on inorganic nutrient data alone.

The difference between prey cells that were actually grazed and involved in burst release due to allelopathic interactions is difficult to resolve for the mixed algae cultures (Carvalho and Granéli, 2006; Lundgren et al., 2016). Further studies on the mechanisms of allelopathic interactions among microalgae may be warranted, especially considering the varying nutritional status and different toxin production during different growth phases as well as how they may be involved in prey capture. For example, karlotoxins of the dinoflagellate *K. veneficum* released into the surrounding media have been shown to cause prey immobilization and improve the ingestion rates (Adolf et al., 2007; Place et al., 2012).

Implication for natural blooms and oyster restoration

In Chesapeake Bay, *K. veneficum* blooms mostly occur during summer from June to September when the ambient dissolved inorganic phosphate is high and N:P ratio is lower than the Redfield ratio (N:P = 1:16; Li et al., 2000b; Li et al., 2015). This study, in which higher P consumption rates for exponential-phase *K. veneficum* were observed, supports the field observations and suggests that the first phases of the bloom (i.e., when cells are in exponential phase) often occur at N:P ratios lower than 16 but still with measurable N in the water column. In contrast, in the latter phases of *K. veneficum* blooms (i.e., when cells are in stationary phase), cells appear to have adaptive physiological mechanisms involving mixotrophic and/or allelopathic interactions that enable them to be maintained at less than maximal growth rates and at higher N:P ratios (Glibert et al., 2012; Accoroni et al., 2015), as is the case with

Prorocentrum minimum and *Ostreopsis* cf. *ovata*. Abundances of *K. veneficum* have been related to patterns in subsurface transport from southern Bay to upper and middle regions of the bay (Li et al., 2000a), and well-mixed conditions in the shallow upper bay could bring low-NP oceanic waters into the waters of reciprocal nutrient conditions (e.g., high-NP freshwater). Also, the dinoflagellates may encounter cryptophytes of differing nutritional content if they have originated in one of the tributaries with different patterns of nutrient loading. In this regard, according to my experiments, the possibility exists for improvement in the growth performance of *K. veneficum* inoculated from southern waters if chance encounters with prey with reciprocal nutrient content should occur in the northern reaches of the bay.

Nutrient-limited growth conditions for *K. veneficum* have previously been shown to be associated with toxin production (Adolf et al., 2009) and impacts on larval mortality (Stoecker et al., 2008). The overlap of *K. veneficum* bloom in space and time with larval spawning has emphasized the need for understanding growth of mixotrophic *K. veneficum* and its negative effects on oyster larvae survival and development of embryos and young larvae (Glibert et al., 2007). Herein, the bioassay experiments indicated that both exponential- and stationary-phase *K. veneficum* caused higher mortality when cells were grown under N-rich (i.e., P-deficient) conditions (Fig. 3.6A, C). These findings suggest that growth-limiting conditions, especially under P-deficiency conditions, would enhance the adverse effects on larval survival. In addition, rates of larval mortality were generally enhanced with the presence of prey and when *K. veneficum* was inoculated from initially stationary-phase growth compared to rates in the presence of *K. veneficum* from exponential

phase. In particular, P-deficient *K. veneficum* mixed with N-rich prey resulted in the highest oyster larval mortality at stationary phase (Fig. 3.6 B,D). In this regard, the potential for this dinoflagellate to inhibit larval growth seems to be high when shellfish spawning coincides with late-stage blooms (i.e., cells is at stationary growth phase) and with prey of nonreciprocal nutrient status. Although these links have not yet been tested in the field, the relationships between eutrophication and *Crassostrea virginica* need to be highlighted especially in subregions of estuaries such as Chesapeake Bay, which have excessive N inputs and a succession from dense cryptophytes blooms to *K. veneficum* blooms (Adolf et al., 2008).

References

Accoroni, S., Glibert, P.M., Pichierri, S., Romagnoli, T., Marini, M., Totti, C., 2015. A conceptual model of annual *Ostreopsis* cf. *ovata* blooms in the northern Adriatic Sea based on the synergic effects of hydrodynamics, temperature, and the N: P ratio of water column nutrients. Harmful Algae 45, 14-25.

Adolf, J.E., Bachvaroff, T., Place, A.R., 2008. Can cryptophyte abundance trigger toxic *Karlodinium veneficum* blooms in eutrophic estuaries? Harmful Algae 8(1), 119-128.

Adolf, J.E., Bachvaroff, T.R., Deeds, J.R., Place, A.R., 2015. Ichthyotoxic *Karlodinium veneficum* (Ballantine) J Larsen in the Upper Swan River Estuary (Western Australia): Ecological conditions leading to a fish kill. Harmful Algae 48, 83-93.

Adolf, J.E., Bachvaroff, T.R., Place, A.R., 2009. Environmental modulation of karlotoxin levels in strains of the cosmopolitan dinoflagellate, *Karlodinium veneficum*. J. Phycol. 45(1), 176-192.

Adolf, J.E., Krupatkina, D., Bachvaroff, T., Place, A.R., 2007. Karlotoxin mediates grazing by *Oxyrrhis marina* on strains of *Karlodinium veneficum*. Harmful Algae 6(3), 400-412.

Adolf, J.E., Stoecker, D.K., Harding, L.W., 2006. The balance of autotrophy and heterotrophy during mixotrophic growth of *Karlodinium micrum* (Dinophyceae). J. Plankt. Res. 28(8), 737-751.

Ajani, P., Hallegraeff, G., Pritchard, T., 2001. Historic overview of algal blooms in marine and estuarine waters of New South Wales, Australia. Proc. Linn. Soc. N. S. W. 123, 1-22.

Bjornland, T., Tangen, K., 1979. Pigmentation and morphology of a marine *Gyrodinium* (Dinophyceae) with a major carotenoid different from peridinin and fucoxanthin. J. Phycol. 15, 457-463.

Braarud, T., 1957. A red water organism from Walvis Bay (*Gymnodinium galatheanum* n. sp.). Galathea Deep Sea Exped. 1, 137-138.

Burkholder, J.M., Glibert, P.M., Skelton, H.M., 2008. Mixotrophy, a major mode of nutrition for harmful algal species in eutrophic waters. Harmful Algae 8(1), 77-93.

Calbet, A., Bertos, M., Fuentes-Grünewald, C., Alacid, E., Figueroa, R., Renom, B., Garcés, E., 2011. Intraspecific variability in *Karlodinium veneficum*: Growth rates, mixotrophy, and lipid composition. Harmful Algae 10(6), 654-667.

Carvalho, W.F., Granéli, E., 2006. Acidotropic probes and flow cytometry: a powerful combination for detecting phagotrophy in mixotrophic and heterotrophic protists. Aquat. Microb. Ecol. 44(1), 85-96.

Carvalho, W.F., Granéli, E., 2010. Contribution of phagotrophy versus autotrophy to *Prymnesium parvum* growth under nitrogen and phosphorus sufficiency and deficiency. Harmful Algae 9(1), 105-115.

Dai, X., Lu, D., Guan, W., Wang, H., He, P., Xia, P., Yang, H., 2013. Newly recorded *Karlodinium veneficum* dinoflagellate blooms in stratified water of the East China Sea. Deep Sea Res. II 101, 237-243.

Deeds, J.R., Terlizzi, D.E., Adolf, J.E., Stoecker, D.K., Place, A.R., 2002. Toxic activity from cultures of *Karlodinium micrum* (= *Gyrodinium galatheanum*)(Dinophyceae)—a dinoflagellate associated with fish mortalities in an estuarine aquaculture facility. Harmful Algae 1(2), 169-189.

Doane, T.A., Horwáth, W.R., 2003. Spectrophotometric determination of nitrate with a single reagent. Anal. Lett. 36(12), 2713-2722.

Edler, L., Elbrächter, M., 2010. The Utermöhl method for quantitative phytoplankton analysis, In: Karlson, B., Cusack, C., Bresnan, E. (Eds.), Microscopic and Molecular Methods for Quantitative Phytoplankton Analysis. IOC UNESCO, Paris, pp. 13-20.

Flynn, K.J., Stoecker, D.K., Mitra, A., Raven, J.A., Glibert, P.M., Hansen, P.J., Granéli, E., Burkholder, J.M., 2013. Misuse of the phytoplankton–zooplankton dichotomy: the need to assign organisms as mixotrophs within plankton functional types. J. Plankt. Res. 35(1), 3-11.

Frost, B.W., 1972. Effects of size and concentration of food particles on the feeding behavior of the marine planktonic copepod *Calanus Pacificus*. Limnol. Oceanogr. 17, 805-815.

Fuentes-Grünewald, C., Garcés, E., Rossi, S., Camp, J., 2009. Use of the dinoflagellate *Karlodinium veneficum* as a sustainable source of biodiesel production. J. Ind. Microbiol. Biotechnol. 36(9), 1215-1224.

Glibert, P.M., Alexander, J., Meritt, D.W., North, E.W., Stoecker, D.K., 2007. Harmful algae pose additional challenges for oyster restoration: Impacts of the harmful algae *Karlodinium veneficum* and *Prorocentrum minimum* on early life stages of the oysters *Crassostrea virginica* and *Crassostrea ariakensis*. J. Shellfish Res. 26(4), 919-925.

Glibert, P.M., Burkholder, J.M., 2011. Harmful algal blooms and eutrophication:"strategies" for nutrient uptake and growth outside the Redfield comfort zone. Chin. J. Oceanol. Limnol. 29(4), 724-738.

Glibert, P.M., Burkholder, J.M., Kana, T.M., 2012. Recent insights about relationships between nutrient availability, forms, and stoichiometry, and the distribution, ecophysiology, and food web effects of pelagic and benthic *Prorocentrum* species. Harmful Algae 14, 231-259.

Glibert, P.M., Burkholder, J.M., Kana, T.M., Alexander, J., Skelton, H., Shilling, C., 2009. Grazing by *Karenia brevis* on *Synechococcus* enhances its growth rate and may help to sustain blooms. Aquat. Microb. Ecol. 55(1), 17-30.

Glibert, P.M., Legrand, C., 2006. The diverse nutrient strategies of harmful algae: focus on osmotrophy, In: Granéli, E., Turner, J.T. (Eds.), Ecology of Harmful Algae, 1st ed., Ecological Studies. Springer Berlin/Heidelberg, pp.163-175.

Graneli, E., Carlsson, P., 1998. The ecological significance of phagotrophy in photosynthetic flagellates, In: Anderson, D., Cambella, A., Hallegraeff, G. (Eds.), Physiological Ecology of Harmful Algal Blooms, NATO ASI Series., 539-557 ed. Springer, Berlin/Heidelberg, pp. 539-557.

Granéli, E., Edvardsen, B., Roelke, D.L., Hagström, J.A., 2012. The ecophysiology and bloom dynamics of *Prymnesium* spp. Harmful Algae 14, 260-270.

Granéli, E., Flynn, K., 2006. Chemical and physical factors influencing toxin content, In: Granéli, E., Turner, J.T. (Eds.), Ecology of Harmful Algae, 1st ed., Ecological Studies. Springer, Berlin/Heidelberg, pp. 229-241.

Granéli, E., Johansson, N., 2003. Increase in the production of allelopathic substances by *Prymnesium parvum* cells grown under N-or P-deficient conditions. Harmful Algae 2(2), 135-145.

Guillard, R.R., 1975. Culture of phytoplankton for feeding marine invertebrates, In: Smith, W.L., Chanley, M.H. (Eds.), Culture of Marine Invertebrate Animals. Plenum Press, New York, pp. 29-60.

Guillard, R.R., 1978. Counting slides, In: Sournia, A. (Ed.), Phytoplankton manual Monographs on Oceanographic Methodology. UNESCO, Paris, pp. 182-189.

Hall, N.S., Litaker, R.W., Fensin, E., Adolf, J.E., Bowers, H.A., Place, A.R., Paerl, H.W., 2008. Environmental factors contributing to the development and

demise of a toxic dinoflagellate (*Karlodinium veneficum*) bloom in a shallow, eutrophic, lagoonal estuary. Estuar. Coast. 31(2), 402-418.

Hansen, P.J., 2011. The role of photosynthesis and food uptake for the growth of marine mixotrophic dinoflagellates. J. Eukaryot. Microbiol. 58(3), 203-214.

Hansen, P.J., Skovgaard, A., Glud, R.N., Stoecker, D.K., 2000. Physiology of the mixotrophic dinoflagellate *Fragilidium subglobosum*. II. Effects of time scale and prey concentration on photosynthetic performance. Mar. Ecol. Prog. Ser. 201, 137-146.

Hardison, D.R., Sunda, W.G., Wayne Litaker, R., Shea, D., Tester, P.A., 2012. Nitrogen limitation increases brevetoxins in *Karenia brevis* (Dinophyceae): implications for bloom toxicity[1]. J. Phycol. 48(4), 844-858.

Heinbokel, J.F., 1978. Studies on the functional role of tintinnids in the Southern California Bight. I. Grazing and growth rates in laboratory cultures. Mar. Biol. 47(2), 177-189.

Jeong, H.J., Du Yoo, Y., Kim, J.S., Seong, K.A., Kang, N.S., Kim, T.H., 2010. Growth, feeding and ecological roles of the mixotrophic and heterotrophic dinoflagellates in marine planktonic food webs. Ocean. Sci. J. 45(2), 65-91.

Jeong, H.J., Park, J.Y., Nho, J.H., Park, M.O., Ha, J.H., Seong, K.A., Jeng, C., Seong, C.N., Lee, K.Y., Yih, W.H., 2005a. Feeding by red-tide dinoflagellates on the cyanobacterium *Synechococcus*. Aquat. Microb. Ecol. 41(2), 131-143.

Jeong, H.J., Yoo, Y.D., Park, J.Y., Song, J.Y., Kim, S.T., Lee, S.H., Kim, K.Y., Yih, W.H., 2005b. Feeding by phototrophic red-tide dinoflagellates: five species

newly revealed and six species previously known to be mixotrophic. Aquat. Microb. Ecol. 40(2), 133-150.

Kempton, J.W., Lewitus, A.J., Deeds, J.R., Law, J.M., Place, A.R., 2002. Toxicity of *Karlodinium micrum* (Dinophyceae) associated with a fish kill in a South Carolina brackish retention pond. Harmful Algae 1(2), 233-241.

Legrand, C., 2001. Phagotrophy and toxicity variation in the mixotrophic *Prymnesium patelliferum* (Haptophyceae). Limnol. Oceanogr. 46(5), 1208-1214.

Li, A., 1998. The feeding physiology and ecology of the mixotrophic dinoflagellate *Gyrodinium galatheanum*, Marine, Estuarine, Environmental Sciences Graduate Program. University of Maryland, College Park, MD.

Li, A., 1996. Ingestion of fluorescently labeled and phycoerythrin-containing prey by mixotrophic dinoflagellates. Aquat. Microb. Ecol. 10, 139-147.

Li, A., Stoecker, D.K., Adolf, J.E., 1999. Feeding, pigmentation, photosynthesis and growth of the mixotrophic dinoflagellate *Gyrodinium galatheanum*. Aquat. Microb. Ecol. 19, 163-176.

Li, A., Stoecker, D.K., Coats, D.W., 2000a. Spatial and temporal aspects of *Gyrodinium galatheanum* in Chesapeake Bay: distribution and mixotrophy. J. Plankt. Res. 22(11), 2105-2124.

Li, A., Stoecker, D.K., Coats, D.W., 2000b. Mixotrophy in *Gyrodinium galatheanum* (Dinophyceae): grazing responses to light intensity and inorganic nutrients. J. Phycol. 36(1), 33-45.

Li, A., Stoecker, D.K., Coats, D.W., 2001. Use of the 'food vacuole content'method to estimate grazing by the mixotrophic dinoflagellate *Gyrodinium galatheanum* on cryptophytes. J. Plankt. Res. 23(3), 303-318.

Li, J., Glibert, P.M., Gao, Y., 2015. Temporal and spatial changes in Chesapeake Bay water quality and relationships to *Prorocentrum minimum*, *Karlodinium veneficum*, and CyanoHAB events, 1991–2008. Harmful Algae 42, 1-14.

Lindehoff, E., Granéli, E., Glibert, P.M., 2010. Influence of prey and nutritional status on the rate of nitrogen uptake by *Prymnesium parvum* (Haptophyte). J. Am. Water Resour. Assoc. 46(1), 121-132.

Lundgren, V.M., Glibert, P.M., Granéli, E., Vidyarathna, N.K., Fiori, E., Ou, L., Flynn, K.J., Mitra, A., Stoecker, D.K., Hansen, P.J., 2016. Metabolic and physiological changes in *Prymnesium parvum* when grown under, and grazing on prey of, variable nitrogen: phosphorus stoichiometry. Harmful Algae 55, 1-12.

Marshall, H.G., Burchardt, L., Lacouture, R., 2005. A review of phytoplankton composition within Chesapeake Bay and its tidal estuaries. J. Plankt. Res. 27(11), 1083-1102.

Mitra, A., Flynn, K.J., 2005. Predator–prey interactions: is 'ecological stoichiometry'sufficient when good food goes bad? J. Plankt. Res. 27(5), 393-399.

Mitra, A., Flynn, K.J., 2006. Promotion of harmful algal blooms by zooplankton predatory activity. Biol. Lett. 2(2), 194-197.

Mitra, A., Flynn, K.J., 2010. Modelling mixotrophy in harmful algal blooms: More or less the sum of the parts? J. Mar. Syst. 83(3), 158-169.

Mitra, A., Flynn, K.J., Burkholder, J., Berge, T., Calbet, A., Raven, J.A., Granéli, E., Glibert, P.M., Hansen, P.J., Stoecker, D.K., 2014. The role of mixotrophic protists in the biological carbon pump. Biogeosciences 10(8), 13535-13562.

Mitra, A., Flynn, K.J., Tillmann, U., Raven, J.A., Caron, D., Stoecker, D.K., Not, F., Hansen, P.J., Hallegraeff, G., Sanders, R., 2016. Defining planktonic protist functional groups on mechanisms for energy and nutrient acquisition: incorporation of diverse mixotrophic strategies. Protist 167(2), 106-120.

Nielsen, M.V., 1996. Growth and chemical composition of the toxic dinoflagellate *Gymnodinium galatheanum* in relation to irradiance, temperature and salinity. Mar. Ecol. Prog. Ser. 136, 205-211.

Place, A.R., Bowers, H.A., Bachvaroff, T.R., Adolf, J.E., Deeds, J.R., Sheng, J., 2012. *Karlodinium veneficum* —The little dinoflagellate with a big bite. Harmful Algae 14, 179-195.

Raven, J.A., Beardall, J., Flynn, K.J., Maberly, S.C., 2009. Phagotrophy in the origins of photosynthesis in eukaryotes and as a complementary mode of nutrition in phototrophs: relation to Darwin's insectivorous plants. J. Exp. Bot. 60(14), 3975-3987.

Ringuet, S., Sassano, L., Johnson, Z.I., 2011. A suite of microplate reader-based colorimetric methods to quantify ammonium, nitrate, orthophosphate and silicate concentrations for aquatic nutrient monitoring. J. Environ. Monit. 13(2), 370-376.

Schnepf, E., Elbrächter, M., 1992. Nutritional strategies in dinoflagellates: a review with emphasis on cell biological aspects. Eur. J. Protistol. 28(1), 3-24.

Sheng, J., Malkiel, E., Katz, J., Adolf, J.E., Place, A.R., 2010. A dinoflagellate exploits toxins to immobilize prey prior to ingestion. Proc. Natl. Acad. Sci. 107(5), 2082-2087.

Smalley, G.W., Coats, D.W., 2002. Ecology of the red-tide dinoflagellate *Ceratium furca*: Distribution, mixotrophy, and grazing impact on ciliate populations of Chesapeake Bay. J. Eukaryot. Microbiol. 49(1), 63-73.

Smalley, G.W., Coats, D.W., Stoecker, D.K., 2003. Feeding in the mixotrophic dinoflagellate *Ceratium furca* is influenced by intracellular nutrient concentrations. Mar. Ecol. Prog. Ser. 262, 137-151.

Staunton, J., Weissman, K.J., 2001. Polyketide biosynthesis: a millennium review. Nat. Prod. Rep. 18(4), 380-416.

Stoecker, D., Li, A., Coats, D.W., Gustafson, D., Nannen, M., 1997. Mixotrophy in the dinoflagellate *Prorocentrum minimum*. Mar. Ecol. Prog. Ser. 152(1), 1-12.

Stoecker, D., Tillmann, U., Graneli, E., 2006. Phagotrophy in harmful algae, In: Graneli, E., Turner, J.T. (Eds.), Ecology of Harmful Algae, 1st ed., Ecological Studies. Springer, Verlag, Berlin/Heidelberg, pp. 177-187.

Stoecker, D.K., Adolf, J.E., Place, A.R., Glibert, P.M., Meritt, D.W., 2008. Effects of the dinoflagellates *Karlodinium veneficum* and *Prorocentrum minimum* on early life history stages of the eastern oyster (*Crassostrea virginica*). Mar. Biol. 154(1), 81-90.

Stoecker, D.K., Johnson, M.D., de Vargas, C., Not, F., 2009. Acquired phototrophy in aquatic protists. Aquat. Microb. Ecol. 57, 279-310.

Zubkov, M.V., Tarran, G.A., 2008. High bacterivory by the smallest phytoplankton in the North Atlantic Ocean. Nature 455(7210), 224-226.

Tables

Table 3. 1. Specific growth rates (μ, d^{-1}) calculated from the slopes of the regression of cell density vs. time for initially exponential- and stationary-phase *K. veneficum*. ANCOVA were used to compare statistical differences in slopes for the low NP, Redfield ratio and high NP *R. salina* additions of each predator growth conditions.

Nutritional status of predator	Prey addition	Slope ± SE	r^2	n	*p*-value
Exponential-phase culture					
Low-NP *K. veneficum*	+ no prey	0.25 ±0.07	0.70	8	
	+ low NP *R. salina*	0.28 ±0.09	0.53	8	
	+ Redfield ratio *R. salina*	0.50 ±0.08	0.85	8	< 0.01
	+ high NP *R. salina*	0.70 ±0.10	0.83	8	
Redfield ratio *K. veneficum*	+ no prey	0.26 ±0.05	0.48	14	
	+ low NP *R. salina*	0.35 ±0.05	0.82	14	
	+ Redfield ratio *R. salina*	0.45 ±0.04	0.90	14	< 0.01
	+ high NP *R. salina*	0.23 ±0.01	0.82	14	
High-NP *K. veneficum*	+ no prey	0.36 ±0.07	0.73	14	
	+ low NP *R. salina*	0.32 ±0.04	0.64	14	
	+ Redfield ratio *R. salina*	0.44 ±0.05	0.87	14	0.12
	+ high NP *R. salina*	0.30 ±0.06	0.50	14	
Stationary-phase culture					
Low-NP *K. veneficum*	+ no prey	0.28 ±0.06	0.63	12	
	+ low NP *R. salina*	0.47 ±0.10	0.62	12	
	+ Redfield ratio *R. salina*	0.17 ±0.07	0.64	12	0.25
	+ high NP *R. salina*	0.33 ±0.08	0.59	12	
Redfield ratio *K. veneficum*	+ no prey	0.37 ±0.04	0.89	12	
	+ low NP *R. salina*	0.51 ±0.21	0.36	12	
	+ Redfield ratio *R. salina*	0.42 ±0.09	0.69	12	0.17
	+ high NP *R. salina*	0.33 ±0.07	0.71	12	
High-NP *K. veneficum*	+ no prey	0.50 ±0.07	0.80	12	
	+ low NP *R. salina*	0.66 ±0.16	0.62	12	
	+ Redfield ratio *R. salina*	0.25 ±0.05	0.37	12	0.09
	+ high NP *R. salina*	0.43 ±0.12	0.56	12	

Table 3. 2. Death rates of prey, *R. salina* (Rs Kv^{-1} d^{-1}), based on equations of Frost (1972) and Heinbokel (1978) to account for *Karlodinium veneficum* growth. Significant differences in prey death rates between three nutritional states of prey are marked as different letters (ANOVA test, $p < 0.01$).

Nutritional status of predator	Prey addition	Exponential phase	Stationary phase
Low-NP *K. veneficum*	+ low NP *R. salina*	0.35 ±0.02[a]	0.70 ±0.04[a]
	+ Redfield ratio *R. salina*	0.28 ±0.01[a]	1.24 ±0.22[a]
	+ high NP *R. salina*	0.68 ±0.07[b]	1.21 ±0.66[a]
Redfield ratio *K. veneficum*	+ low NP *R. salina*	0.35 ±0.04[a]	0.70 ±0.26[a]
	+ Redfield ratio *R. salina*	0.35 ±0.05[a]	1.06 ±0.09[a]
	+ high NP *R. salina*	0.20 ±0.07[a]	0.47 ±0.08[a]
High-NP *K. veneficum*	+ low NP *R. salina*	0.25 ±0.13[a]	0.51 ±0.03[a]
	+ Redfield ratio *R. salina*	0.59 ±0.15[a]	1.00 ±0.75[a]
	+ high NP *R. salina*	0.18 ±0.12[a]	0.63 ±0.92[a]

Figures

Fig. 3. 1. Growth curves of the stock cultures of *Karlodinium veneficum* grown on low-NP, Redfield ratio and high-NP media. Inocula of *K. veneficum* cells were transferred to the mixed-culture experiments on day 5 (exponential growth) and day 11 (stationary phase growth).

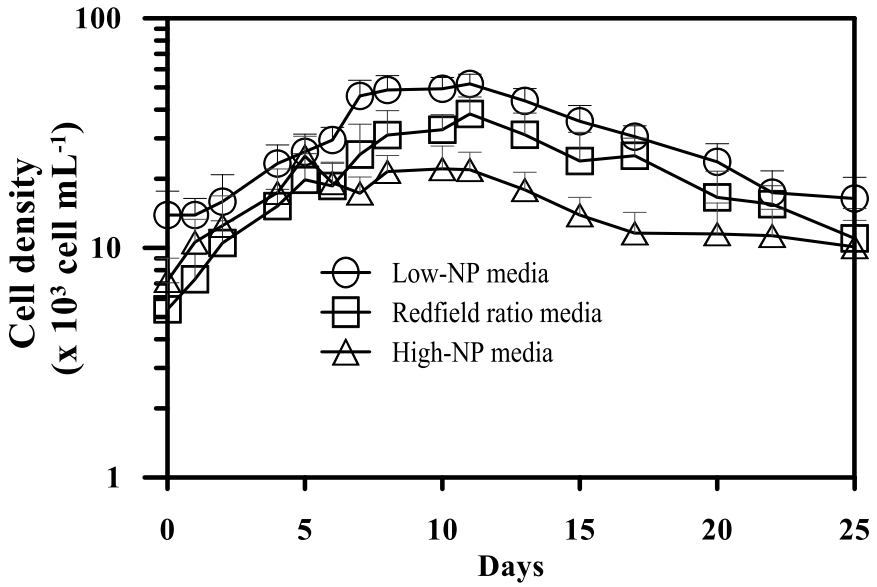

Fig. 3. 2. Growth curves of initially (A) exponential-phase and (B) stationary-phase *Karlodinium veneficum* when transferred into low-NP, Redfield ratio and high-NP culture media during monoculture experiments.

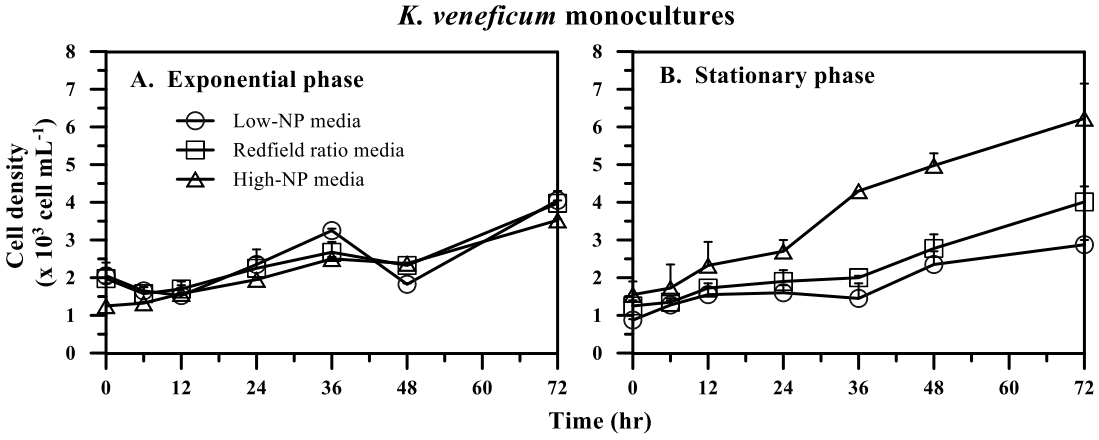

Fig. 3. 3. Growth curves of initially exponential-phase *Karlodinium veneficum* transferred into (A) low-NP, (B) Redfield ratio and (C) high-NP conditions and of initially stationary-phase *K. veneficum* transferred into (D) low-NP, (E) Redfield ratio and (F) high-NP conditions and provided with low-NP, Redfield ratio and high-NP prey *Rhodomonas salina* during mixed-culture experiments.

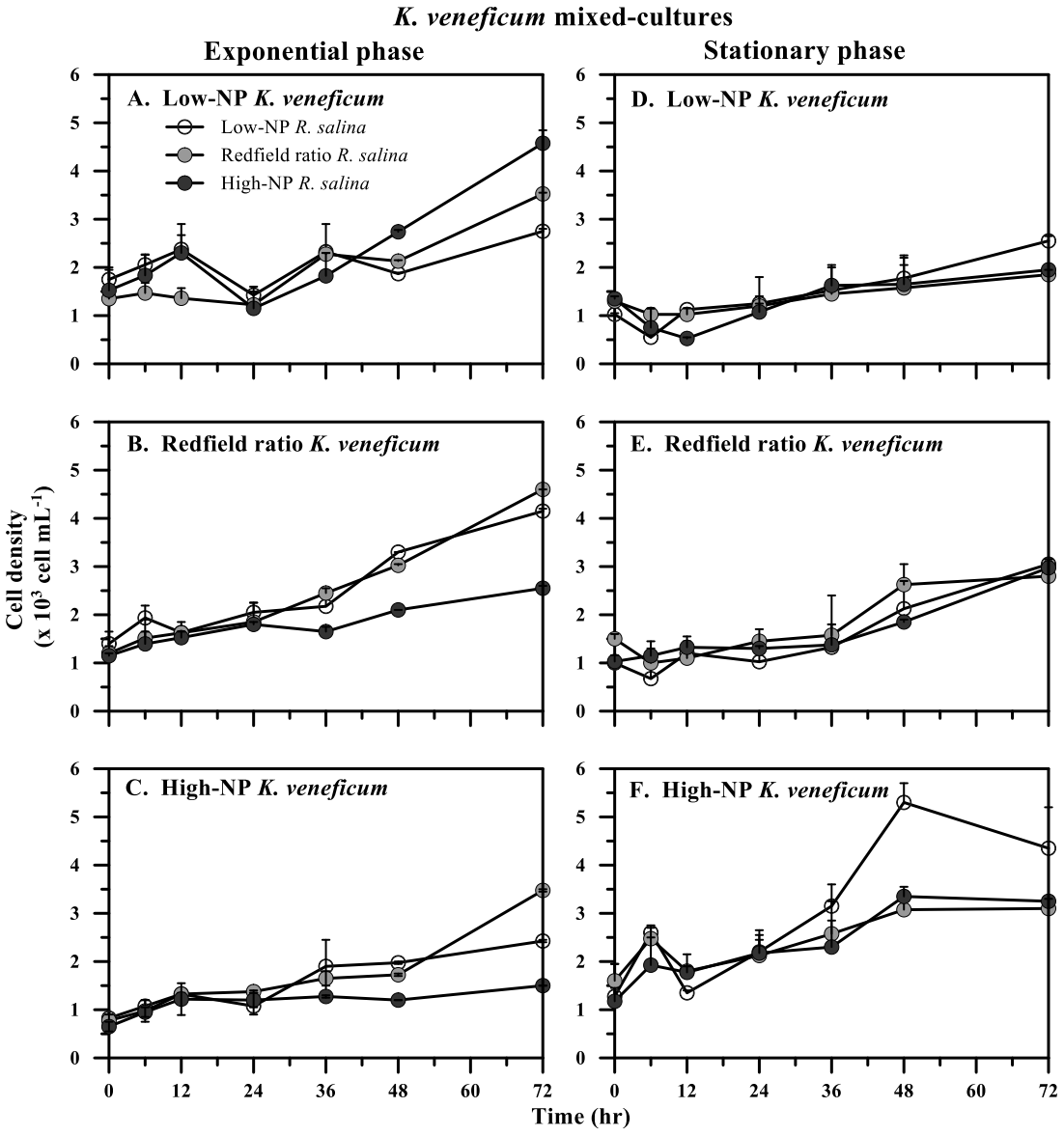

Fig. 3. 4. Relationship between death rates of *Rhodomonas salina* (Rs) prey relative to *Karlodinium veneficum* (Kv) specific growth for *K. veneficum* that were initially grown to (A) exponential-phase and (B) stationary-phase.

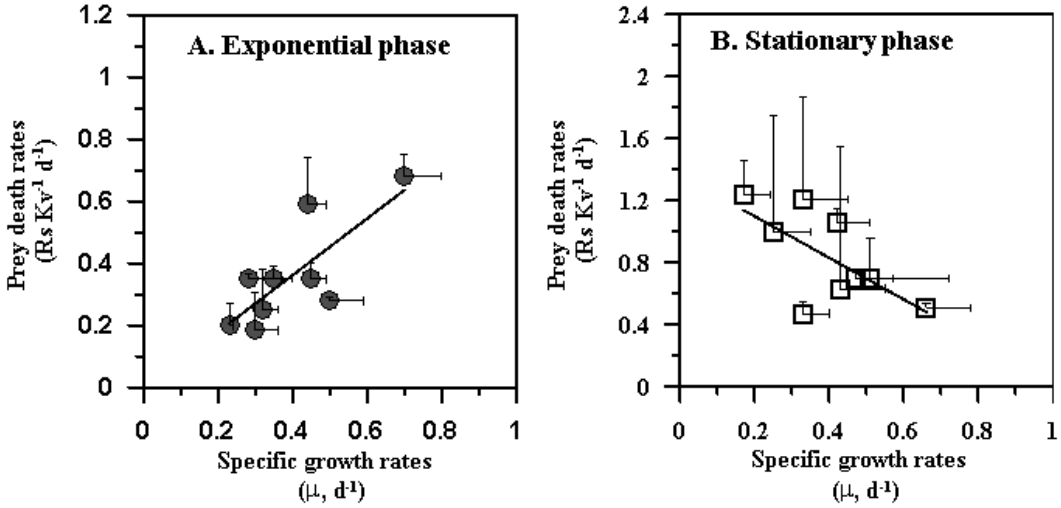

Fig. 3. 5. Relationship between the concentrations of nitrate (NO_3^-) and phosphate (PO_4^{3-}) for *Karlodinium veneficum* (Kv) and *Rhodomonas salina* (Rs) in (A) monocultures and (B) mixed cultures for both initially exponential and stationary phase of *K. veneficum*. The Redfield proportion of 16:1 is included for reference (dashed line).

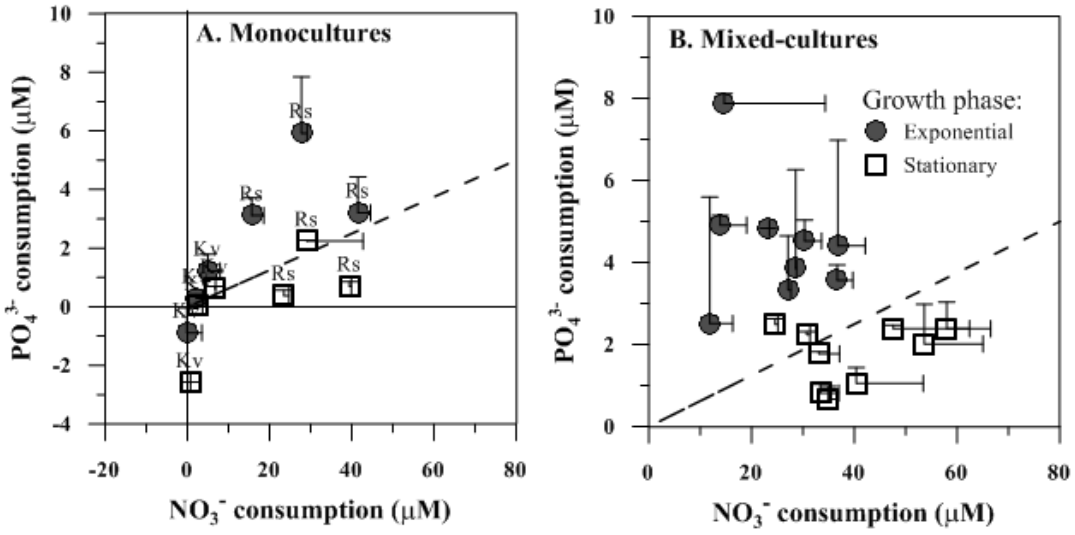

Fig. 3. 6. Mortality of *Crassostrea virginia* larvae after 2 d of exposure to low-NP, Redfield ratio and high-NP *Karlodinium veneficum* at the final concentrations (0.9×10^3 cell mL^{-1}) in the absence and presence of low-NP, Redfield and high-NP prey *Rhodomonas salina.* Monocultures of (A) initially exponential-phase and (C) stationary-phase *K. veneficum* with three nutrient conditions were collected for larval bioassay test at t_0 and t_f. Mixed-cultures of (B) initially exponential-phase and (D) stationary-phase *K. veneficum* were collected for larval test at t_f. Control treatments (ctr) contained *C. virginia* larvae alone. Statistical tests were conducted separately for the monocultures and mixed-cultures of three nutrient conditions. Different letters show significant differences between treatments (ANOVA test, $p < 0.01$).

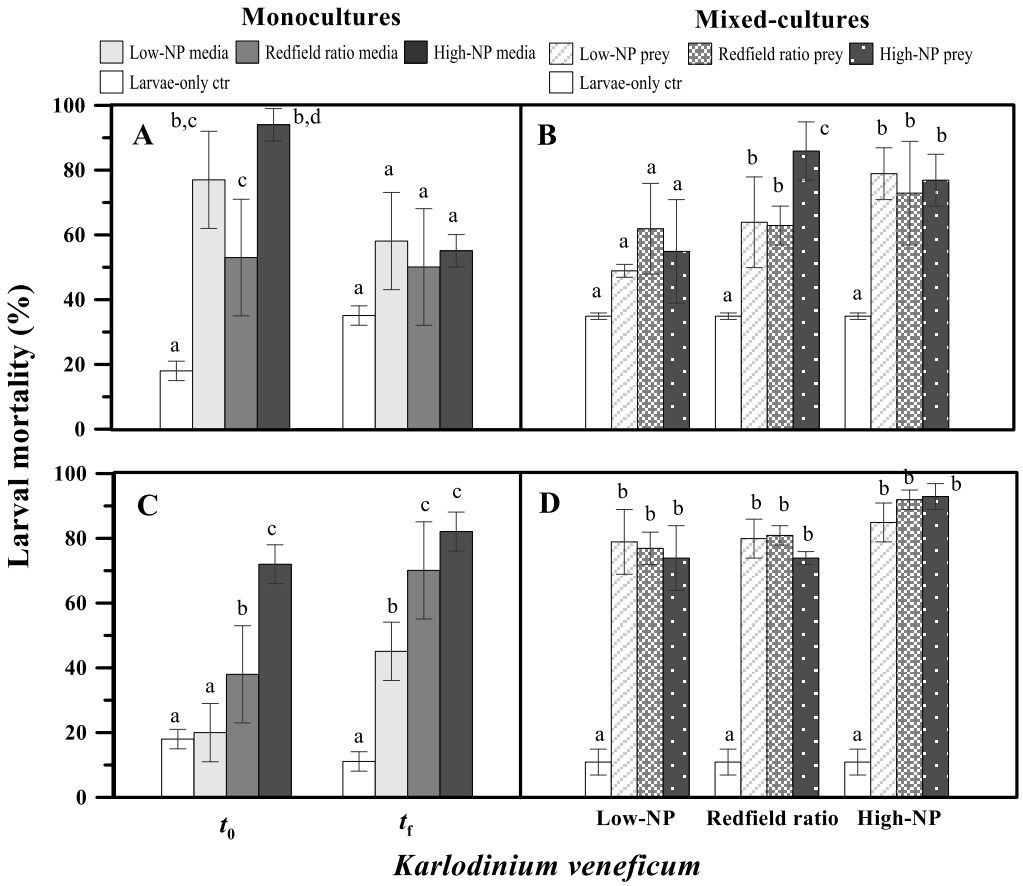

Chapter 4: Mixotrophy with multiple prey species measured with a multiwavelength-excitation PAM fluorometry: case study of *Karlodinium veneficum*[3]

Abstract

Grazing studies were conducted on the mixotrophic dinoflagellate, *Karlodinium veneficum,* in the presence of single prey species, the cryptophyte *Rhodomonas salina,* or a phycocyanin strain of the cyanobacterium, *Synechococcus* sp., and when prey were mixed in varying proportions. A multiwavelength PAM fluorometer was used for non-invasive biomass estimates and to detect changes in photophysiology. Rates of grazing by, and growth of, *K. veneficum* increased as the function of increasing prey concentrations of *R. salina*, regardless of whether the prey was provided as a single prey item or in a mixed prey community. With *Synechococcus* as the prey, in single or mixed prey assemblages, it was poorly grazed, and growth rates of the mixotroph declined. The maximal quantum yields of PSII fluorescence (F_v/F_m) of the mixotroph declined when *Synechococcus* was the prey but remaining unchanged when fed on *R. salina*. The F_v/F_m of *R. salina* declined by about 60% as it was consumed, while that of *Synechococcus* sp. increased as mixotroph growth declined. Robust relationships were established between flow cytometry-based cell counts and PAM fluorometry-based chlorophyll measurements, validating the usefulness of this rapid and non-intrusive quantification approach for

[3] Lin and Glibert. *J. Plankt. Res.* Submitted.

measuring mixotrophy in predator-prey interactions among multiple differently pigmented species.

Introduction

Mixotrophic nutrition (i.e., the combination of autotrophy and phagotrophy) is widespread among many photosynthetic algal species, in particular, phototrophic chrysophytes, dinoflagellates, and haptophytes (Jeong et al., 2005a,b; Burkholder et al., 2008; Flynn et al., 2013). Mixotrophs are known to play important roles in plankton dynamics (Stickney et al., 2000; Tittel et al., 2003) and both experimental and numerical studies have indicated that there are growth advantages to being mixotrophic in dynamic environmental conditions (Sanders, 1991; Stoecker, 1999; Jeong et al., 2005a; Glibert et al., 2009; Stoecker et al., 2017). For instance, planktonic mixotrophy has been found in oligotrophic habitats where limiting nutrients are often concentrated in microbial prey compared to the water column (Jones, 1994) and eutrophic estuaries where light can be limiting and/or where nutrients are sufficient but not in balanced proportions (Burkholder et al., 2008; Glibert and Burford, 2017; Millette et al., 2017). Phagotrophy in algae can provide an alternative or supplement to photosynthesis as sources of carbon (C), or dissolved substrates, nitrogen (N) and/or phosphorus (P), and through the acquisition of food, particularly high quality food, mixotrophs can enhance their growth rates relative to their autotrophic growth (Li et al. 2000; Jeong et al., 2005a,b; Adolf et al., 2008; Glibert et al., 2009; Lin et al., 2017).

There are several approaches for the measurement of mixotrophy and most of these involve manipulation with a tracer. Prey may be labeled using an isotope (^{14}C, ^{15}N), or artificial prey (for example, beads) may be added and over time, the accumulation of tracer in the mixotroph is measured (e.g., Hall et al., 1993; Smalley et al., 1999; Adolf et al., 2006; Lundgren et al., 2016). Alternatively, enumerations of changes in predator and/or prey may be made through microscopy or other enumeration approaches (Carvalho and Granéli, 2006; Lin et al., 2017). Tracer labeling techniques and/or feeding trials with artificial substrates (beads) may lead to artifacts due to various manipulations or artificial food required.

Pulse-amplitude-modulated (PAM) fluorescence is a widely used tool for determining the maximum quantum efficiency of photosystem (PS) II fluorescence (F_v/F_m), a commonly reported measure of phytoplankton physiological state (Kolber et al., 1988; Geider et al., 1993; Goto et al., 2008). The Phyto-PAM II (Walz, Germany) incorporates multiple modulating beams set to different excitation spectra and therefore can measure different groups of phytoplankton simultaneously in the same solution. With appropriate calibration and deconvolution of signals, the dark-adapted, minimal fluorescent signal (F_0) can also be used as a measure of biomass (chlorophyll) and thus this instrument allows the simultaneous measurement of the abundance of different phytoplankton groups in a mixed sample. Given the spectral composition of the 5 available excitation wavelengths, differentiation of phytoplankton groups is optimal between cyanobacteria, green algae, diatoms/dinoflagellates, and phycoerythrin-containing cells such as cryptophytes. Here, the Phyto-PAM II was used to characterize the change in abundance of a

mixotroph, the dinoflagellate *Karlodinium veneficum*, in the presence of prey, including the cryptophyte, *Rhodomonas salina*, and a phycocyanin-containing cyanobacterium, *Synechococcus* sp. that is also a prey of the cryptophyte (e.g., Urabe et al., 2000; Izaguirre et al., 2012). The mechanisms for feeding on cryptophytes by *K. veneficum* have been extensively examined in the field and laboratory (Li et al., 2000; Adolf et al., 2008), while some *Synechococcus* have been found to be readily grazed by other gymnodinoid dinoflagellate (Jeong et al., 2005a; Glibert et al., 2009). This study addressed the hypothesis that feeding by the mixotroph may be enhanced when provided multiple prey sources compared with feeding rates on single species of prey due to the combination of increasing prey concentrations and multiple prey species choice. The goal herein is not only to assess rates of mixotrophy and physiological state of this important dinoflagellate in the presence of multiple prey species and in different proportions, but also to demonstrate the effectiveness of this variable fluorescence approach.

Materials and Methods

Phytoplankton cultures

Non-axenic cultures of the dinoflagellate *Karlodinium veneficum* (CCMP1975) and the cryptophyte *Rhodomonas salina,* provided by the National Center for Marine Algae and Microbiota and the Oyster Hatchery of Horn Point Laboratory, respectively, were grown in *f*/2 media (Guillard, 1975) with a light intensity of ~184 μmol photons m^{-2} s^{-1}. A Chesapeake isolate, CB0101, of a phycocyanin (PC)-rich

cyanobacteria *Synechococcus* sp., was obtained from Dr. Feng Chen at University of Maryland Institute of Marine and Environmental Technology. It was subsequently grown in SN media (Waterbury et al., 1986) using the same light conditions as the other cultures. All culture media were prepared with 0.2 μm filtered Choptank River (a tributary of Chesapeake Bay) water (salinity of 10) and sterilized by autoclaving. All three species were maintained in batch cultures at 22°C on a 12 h light: 12 h dark cycle.

Mixed-culture experimental design

Mixed-culture experiments were conducted to examine the feeding and growth responses of *K. veneficum* to two different types of prey in different proportions. Two-species mixtures with *K. veneficum* (as a predator) and *R. salina* or *Synechococcus* sp. (as prey) were conducted. For convenience, the experimental treatments are referred to herein by culture volume: volume ratios (see Table 4.1 for cell concentrations). For the two-species mixtures, experiments were conducted at predator-to-prey ratios of 3:1, 2:1, 1:1 and 1:2, and for three-species mixtures experiments were conducted at predator-to-prey ratios of 3:1:1, 2:1:1, 1:1:1 and 1:2:1 for *K. veneficum*, *R. salina,* and *Synechococcus*. Together with controls of individual species for each set of mixtures, this study thus consisted of 25 treatments, in triplicate, with a total of 75 culture flasks (Fig. 4.1). The mixed-cultured treatments were sampled at 12 h intervals over 96 h, with each sampling period being 1-2 h after lights on/lights off.

For each sampling, flasks were gently mixed, and 3 ml aliquots were withdrawn and analyzed, after 30 min of dark adaptation, with the Phyto-PAM II to

yield minimal fluorescence (F_0) and maximal fluorescence (F_m) for each taxa. Taxon-specific variable fluorescence ($F_v = F_m - F_0$) and its yield (F_v/F_m) parameters were also obtained. At each time point, samples (0.5 ml) were also preserved in 1% paraformaldehyde and held at 4 °C for later cell enumeration via flow cytometry.

Chlorophyll a fluorescence validation/calibration

The F_0-based chlorophyll (Chl) *a* concentrations were validated with the acetone-extracted method using single, and two- and three-species in mixed cultures in preliminary trials. Firstly, the acetone-based Chl *a* measurements were used to establish the reference of each algal strain for the purpose of instrument calibration. Secondly, mixtures of each algal group were made in 1:1 and/or 1:1:1 stock volume proportions. While fully aware of the differences in cell size and potential for Chl *a*:cell to vary substantially, as a first order assumption for cultures in the same state of growth, 1:1 mixtures were presumed to reflect 50 % of the Chl *a* from each algal group, while those in the 1:1:1 mixtures were presumed to reflect 33 % of the Chl *a* from each species. Finally, filtered Choptank River water was added to dilute the single- and mixed-culture stock cultures by 80 %, 60 %, 40 % and 20 % prior to extraction to obtain a concentration gradient. Samples were extracted with acetone for 12 h at 4ºC following the method of Arar and Collins (1997) and measured with a calibrated Turner Designs AU-10 fluorometer.

Flow cytometry comparisons/validation

The F_0-based Chl *a* concentrations of the mixed species cultures were also compared with flow cytometry-based cell counts using combinations of two- and

three-species (see mixed-culture experimental designs). The preserved samples collected at each time point were analyzed within a week using a BD Accurri C6 flow cytometry with dual excitation: 488 nm (blue laser) and 640 nm (red laser). The cells were identified and gated based on their size, shapes and structural complexity using forward scatter (FSC) and side scatter (SSC) light threshold. In addition, 3 photomultipliers including FL2 (phycoerythrin, PE), FL3 (peridinin chlorophyll protein complex) and FL4 (allophycocyanin, APC) filters were used to measure cell auto-fluorescence. Absolute cell counts were determined by volume flow rates, which were fixed at 14 μL min^{-1}.

Photosynthetic activities

To assess physiological states of *K. veneficum* and its prey, F_v/F_m values were measured using the Phyto-PAM II. Fluorescence signals from five color wavelengths (440, 480, 540, 590 and 625 nm) were deconvoluted to the three algal groups by calibrating Chl *a* fluorescence for each taxa.

Calculations and statistical analyses

In separate calculations, changes in taxon-specific biomass based on PAM-derived F_0 values, calibrated with extracted Chl *a*, and those derived by flow cytometry, were used to calculate the growth of the mixotroph and death rates of its prey. Cell-specific growth rates (d^{-1}) of *K. veneficum* were determined based on the slopes of the regression of natural log-transformed biomass data for the experimental periods (96 h). Cell-specific death rates of *R. salina* (Rs cells *K. veneficum*$^{-1}$ d^{-1}) were calculated as the difference between growth rates of prey in the control and mixed-

cultures flasks, based on the equations of Frost (1972) and Heinbokel (1978) to account for grazer growth. Death rates of the prey are reported rather than ingestion rates because of the difficulty in differentiating between cells that were actually grazed and those cells that may have burst due to putative toxic effects (e.g., Lin et al., 2017). Low grazing rates on *Synechococcus* precluded the comparable calculation of death rates of this prey species.

All statistical analyses were performed with R. The Shapiro-Wilks test was used to check normality, while the Levene's test was used to assess the equality of variance. Comparisons of the methods of measurement for Chl *a* (PAM fluorometry and acetone extraction), and rates of growth and death determined by Chl *a* fluorescence from PAM fluorometry and cell density by flow cytometry were conducted using linear Pearson's product moment coefficient, and the correlation coefficients were assessed using the Fisher r-to-z transformation. Differences in cell-specific growth rates of *K. veneficum,* as well as death rates of prey and F_v/F_m of individual species (e.g., predator and two prey species) in the monocultures and two- and three-species mixed cultures, were analyzed using ANOVA tests followed by Tukey's HSD tests for pairwise comparisons.

Results

Calibration and verification of chlorophyll a

Values of Chl *a* based on F_o (hereafter Chl_{F0}) agreed well with those of extracted Chl *a*. The coefficient of determination between the combined values for all

treatments was 0.83 ($p < 0.001$, n = 35), but the slope did deviate from 1.0 and there was a positive intercept (y = 0.68x + 37.01; Table 4.2, Fig. 4.2). Total Chl *a* concentrations up to ~ 220 μg L^{-1} for single *K. veneficum* and *R. salina* algal cultures were reliably determined by Chl_{F0}. The monoculture of *Synechococcus* sp. also obtained a sufficiently reliable determination using F_o, but total Chl *a* concentrations were at the lower end of the calibration curve, 120 μg L^{-1}. Values of Chl_{F0} in two or three species mixed-cultures deviated from the 1:1 line at Chl *a* concentrations > 200 μg L^{-1} and < 20 μg L^{-1} (Fig. 4.2). When treatments were compared independently, all 7-treatment conditions yielded comparable estimates between the two methods with slope values of ~ 0.8, except for the two-species mixed cultures that included *Synechococcus* sp. (Table 4.2). In two-species mixtures, an approximately equal amount of total Chl *a* was attributed to *K. veneficum* (52 ± 3 %) and *R. salina* (48 ± 3 %). *Synechococcus* sp. was generally underestimated when mixed with *K. veneficum* and/or *R. salina*. When mixed with *K. veneficum,* it accounted for 41 ± 3 % of total Chl *a* and *K. veneficum* accounted for 59 ± 3 % of total Chl *a*. When the two prey were mixed, *R. salina* represented 67 ± 2 % of total Chl *a*, whereas *Synechococcus* sp. represented 33 ± 2 % of the Chl *a*. In the three-species mixtures, *K. veneficum*, *R. salina*, and *Synechococcus* sp. contributed 36 ± 5 %, 41 ± 5 % and 23 ± 5 % of the Chl *a*, respectively. Given the large disparity in cell size between *Synechococcus* sp. and the other taxa, the strength of these relationships is surprisingly strong.

Growth and death rates of the mixotroph and prey: method comparison

Cell-specific growth rates of *K. veneficum* with additions of *R. salina* and/or *Synechococcus* and death rates of *R. salina* based on the changes in Chl_{F0} were in

good agreement with those based on algal cell densities (Fig. 4.3). The regression line for *K. veneficum* growth rates based on cell numbers and Chl_{FO} has a slope of 0.94, indicating that rate estimates using Phyto-PAM II were slightly lower than those calculated by cell numbers (Table 4.3). The observed results from mixed-culture treatments with *R. salina* clearly deviated from the 1:1 line, but results were closer to the 1:1 line when three-species mixtures were compared (Fig. 4.3A). Although not significant, rates of grazing for *K. veneficum* on *R salina* based on Chl_{F0} were less than those measured by flow cytometry. On the other hand, death rates of *R. salina* showed a slope of > 1 with an r^2 of 0.96 (Fig. 4.3B) and the highest death rate values (6.49 ± 1.22 Rs cells *K. veneficum*$^{-1}$ d^{-1}) were found when values were based on Chl_{F0} (Table 4.4). The points deviating from the line were found in the mixed cultures with proportionally higher prey *R. salina* culture volume at a predator-to-prey ratios of 1:2 and/or 1:2:1.

Two species mixtures: Karlodinium *and* Rhodomonas

Karlodinium veneficum consistently grazed *Rhodomonas salina*, and consistently grew at a rate approaching double the rate in the monoculture without prey. Rates of grazing were independent of the amount of prey provided, suggesting that even the lowest proportion of prey added was sufficient to saturate the rate of feeding by the mixotroph (Table 4.3, Fig. 4.4).

A number of patterns were revealed by comparison of the culture mixtures. The highest cell density and Chl_{F0} concentrations of *K. veneficum* were reached when it was mixed with *R. salina* at a 1:2 volume ratio (Fig. 4.4A, C). The time period at which Chl_{F0} of *R. salina* became undetectable due to grazing was 24 h in the mixed

culture with predators at a 3:1 volume ratio but was proportionately longer, 48, 72 and 96 h, respectively, when predators were in volume ratios of 2:1, 1:1 and 1:2 (Fig. 4.4B). In terms of cell densities of *R. salina,* values fell to near zero after 36 and 60 h when it was mixed with predators in volume ratios of 3:1 and 2:1, respectively, but were maintained at detectable levels over entire experimental time course with higher prey abundance (1:1 and 1:2 volume ratios; Fig. 4.4D).

Two species mixtures: Karlodinium *and* Synechococcus

Overall, *K. veneficum* did not grow well on *Synechococcus* sp. (Table 4.3). There were, however, several trends revealed in the time series (Fig. 4.5). In all treatments, cell densities and/or Chl_{F0} of *K. veneficum* increased during the first 24–48 h of incubations and then declined. For the treatments with the highest prey proportions (1:1 and 1:2 predator: prey), both abundance and Chl_{F0} of the mixotroph declined to very low levels, suggesting substantial cell stress, but those mixotrophs with lower prey abundance (2:1 and 3:1) did not decline to the same degree, at least maintaining their abundance and Chl_{F0} at levels comparable to controls without prey (Fig. 4.5A, C). Cell densities of *Synechococcus* sp. increased in the treatments with the highest predator proportions through 48 h and then remained relatively stable during 48–96 h, while Chl_{F0} of *Synechococcus* sp. consistently increased through the entire time series in all treatments except the control for which increases were seen only in the last 12 h (Fig. 4.5B, D). The difference between Chl_{F0} and cell abundance suggests that photoacclimation of Chl *a* likely occurred as culture densities increased.

Two species mixtures: Rhodomonas *and* Synechococcus

In the mixtures of the two prey species, *R. salina* grew very well with the presence of *Synechococcus* sp., and the growth rates (0.17 – 0.23 d^{-1}) were higher compared to monoculture growth (0.10 d^{-1}). In all treatments, cell densities and/or Chl_{F0} of *R. salina* remained unchanged during the first 36 h and then dramatically increased, except for treatment with the highest *Synechoccoccus* proportions (1:2 *Rhodomonas*: *Synechococcus*; Fig. 4.6A,C). In contrast, both abundance and Chl_{F0} of *Synechococcus* consistently declined after 48 h, suggesting potential grazing pressure by *R. salina* in all treatments.

Comparison of growth and death rates in two and three-species mixed cultures

For three-species mixed cultures, there were some parallel responses to those observed in the two-species treatments, and also some differences (Fig. 4.7). In the two-species mixtures with *R. salina*, Chl_{F0} and cell abundance of *K. veneficum* consistently increased, and the same pattern was seen with the three species combined, except in the presence of *Synechococcus* at a 1:2:1 volume ratio (Fig. 4.7A, D). In all of the mixtures, growth rates of *K. veneficum,* when feeding on *R. salina*, ranged from 0.25 d^{-1} to 0.37 d^{-1} (based on changes in cell densities) and from 0.16 d^{-1} to 0.22 d^{-1} (based on changes in Chl_{F0}; Table 4.3). The relationship between *Rhodomonas* cell density and *K. veneficum* growth rate based on cell densities were not significantly different from those based on by Chl_{F0} ($z = 1.58$, $p = 0.11$; Fig. 4.8A).

With *Synechococcus* alone, growth rates of *K. veneficum* remained unchanged and/or declined (Table 4.3). In three-species mixtures, cell densities of

Synechococcus increased through the entire time series in the presence of *R. salina* and predator when in proportions of 2:1:1 and 3:1:1 (Fig. 4.7C, F). At a *Synechococcus* prey abundance of > 270×10^8 cells L^{-1}, or of biomass > 25 Chl_{F0} μg L^{-1}, *K. veneficum* exhibited negative growth (Fig. 4.8B). The relationship between *Synechococcus* cell density and *K. veneficum* growth rate determined based on cell numbers was significantly different from that estimated by Chl_{F0} ($z = 2.4$, $p < 0.05$; Fig. 4.8B), likely reflecting the change in Chl: cell of *Synechococcus*. When specific growth rates between mixed culture treatments of two- and three-species conditions were compared, there were significant increases in growth based on cell densities and/or Chl_{F0} when *R. salina* was the only prey compared with when it was combined with *Synechococcus* (Table 4.3).

In contrast to growth rates of *K. veneficum*, death rates of *R. salina* showed no difference between two- and three-species mixed cultures, suggesting effective feeding of *R. salina* was sustained despite the presence of *Synechococcus* sp. (Table 4.4). Across all treatments, death rates of *R. salina* caused by feeding of *K. veneficum* increased with increasing prey concentrations and the correlation coefficients were not different for rates determined with the cell-based and fluorescence-based methods ($z = 0.28$, $p = 0.78$; Fig. 4.8C).

Plastid functionality of Karlodinium, Rhodomonas *and* Synechococcus

Values of the F_v/F_m appeared to be species-specific for each taxa in monoculture (ANOVA, $p < 0.01$, Fig. 4.9). The measured F_v/F_m for *K. veneficum* was about 0.55 over the first 72 h and decreased to 0.41 at the end of the experiment. By comparison, the prey species *R. salina* and *Synechococcus* sp. in monocultures

showed no significant changes in F_v/F_m and remained about 0.60 and 0.20 throughout the experiment, respectively.

In the two-species mixed cultures with *K. veneficum* and *R. salina*, the value of F_v/F_m for *K. veneficum* remained at ~ 0.55 over entire experimental periods (Fig. 4.9A). In the first 12 h of the mixed-culture experiments, F_v/F_m of *R. salina* increased up to ~ 0.75 and then rapidly decreased to 0 as cells were consumed over the next 24–48 h in the treatments with the highest predator proportion (2:1 and 3:1 predator: prey). In addition, a pattern of decrease-increase-rapidly decrease in F_v/F_m values for *R. salina* was found under the high prey condition (Fig. 4.9B).

When mixed only with *Synechococcus*, F_v/F_m of *K. veneficum* rapidly decreased after 24 h incubation in the 1:2 and 1:1 predator: prey mixtures (Fig. 4.8C). In contrast, *Synechococcus* sp. displayed increasing F_v/F_m values, reaching ~ 0.40 after 36-48 h and then gradually declined to 0.12 at the end of the mixed culture experiment (Fig. 4.8D). Overall, an average F_v/F_m value of 0.39 for *K. veneficum* was found in the two-species mixed cultures with *Synechococcus,* which was significantly different from the measured value in the monoculture and in the two-species mixed cultures with *R. salina* (Table 4.5).

In two-prey species mixed cultures, the value of F_v/F_m for *R. salina* remained at ~ 0.6 over the entire experimental periods, comparable with the single species control (Fig. 4.9E, Table 4.5). In contrast, *Synechococcus* sp. showed declining F_v/F_m values after 12 h, reaching zero in all treatments with *R. salina*. Overall, an average F_v/F_m value of 0.13 for *Synechococcus* was observed in the two-prey species mixed cultures (Fig. 4.9F), which was significantly different from the values in the

monocultures and in two- and three-species mixed cultures with *K. veneficum* (Table 4.5).

In the three-species mixed cultures, the F_v/F_m values over time for *Synechococcus* and *K. veneficum* were mostly comparable to those in the respective two-species mixed cultures (Fig. 4.9, Table 4.5). No differences in averaged F_v/F_m values for *Synechococcus* sp. were found between with- and without-predator cultures. There was little variation in the measured values of F_v/F_m for *K. veneficum*, except that F_v/F_m decreased in the presence of *Synechococcus* when in the 1:2:1 volume ratio. Overall, the average values of F_v/F_m for *K. veneficum* showed significant differences among culture conditions, particularly in the presence of *Synechococcus* (Table 4.5). Unlike in the two-species mixed culture, however, the F_v/F_m for *R. salina* was not enhanced but remained at ~ 0.60 throughout the experiment when in proportions of 1:1:1 and 1:2:1, while F_v/F_m values in *Synechococcus* sp. increased up to ~ 0.4 in first 24 h of mixed cultures and gradually decreased to zero under higher *R. salina* proportions of 1:2:1 ratio. The F_v/F_m for *R. salina* on average was significantly reduced (by about 60%) in two- and three-species mixed cultures compared to monocultures.

Discussion

In this study, different approaches were brought to bear in measuring grazing and photophysiology of *Karlodinium veneficum* and multiple prey when provided in different proportions. Multiwavelength PAM fluorometry proved to be an effective tool to rapidly assess both biomass changes and changes in photosynthetic

physiological state. In keeping with previous findings (e.g., Jeong et al., 2005b; Adolf et al., 2008; Calbet et al., 2011; Lin et al., 2017), the mixotroph readily grazed the cryptophyte *Rhodomonas salina*, but in contrast to other studies of gymnodinoid dinoflagellates, *K. veneficum* did not appear to substantially graze *Synechococcus*. In contrast to more traditional methods of assessing mixotrophy, the photosynthetic efficiency of predator and prey were also assessed. Photosynthetic efficiency of the mixotroph differed on the different prey species, declining when *Synechococcus* was the prey but not when *R. salina* was the prey.

The lack of substantial grazing on *Synechococcus* by *K. veneficum* is interesting given that other gymnodinoids have been reported to graze substantially on *Synechococcus,* albeit different strains (e.g., Jeong et al., 2005a; Glibert et al., 2009). There are several possible reasons why feeding on this species was not observed to any significant degree. First, the specific strain selected for use in these experiments may not be preferred. This strain was chosen because, as a PC-rich cyanobacterium, it could be differentiated using the multiwavelength PAM. It is possible that a PE-rich or other type of picoplankton may be grazed by *K. veneficum*, but there are no reports to date substantiating this. Second, the effects of predation on this prey may not have been effectively detected with PAM fluorometry because a relatively high abundance of prey is necessary for the minimal detection of F_0 (16 Chl *a* μg L^{-1}, equal to 135×10^8 cell L^{-1} is the minimum detection limit; Fig. 4.2). The *Synechococcus* prey: predator (cell: cell) ratios used herein, in general, were higher than in previous studies that had ranges of 180 to 500 (Jeong et al., 2005a) and 0.7 to 226 (Glibert et al., 2009). While high cell densities of *Synechococcus* were used, in

Chesapeake Bay, from which *Synechococcus* was isolated and for which *K. veneficum* is a common bloom-former, these PC-containing picocyanobacteria can exceed 10^9 cells L^{-1} (e.g., Ray et al., 1989; Affronti and Marshall, 1994). These high *Synechococcus* cell abundances may have lead to C-limitation and high pH stress in these cultures.

In contrast to *K. veneficum* that decreased in growth when provided *Synechococcus*, the cryptophyte *R. salina* appeared to readily feed on *Synechococcus* in two-species mixtures, but not in three-species mixtures. Many nano-planktonic cryptophyte species have been revealed to be mixotrophic, grazing on co-occurring cyanobacteria (e.g., Izaguirre et al., 2012; Yoo et al., 2017). These findings suggest a complex trophic relationship exist between cyanobacteria, cryptophyte and dinoflagellate. Multiple stage trophic relationships have been reported for other mixotrophs, such as the heterotrophic dinoflagellate genus *Dinophysis* that feeds on the ciliate *Myrionecta rubra* which, in turn, feeds on cryptophytes (e.g., Park et al., 2006).

Compared to *Synechococcus*, *R. salina* was readily consumed by *K. veneficum*, as previously observed (Jeong et al., 2005b; Adolf et al., 2008; Calbet et al., 2011; Lin et al., 2017), and rates were within the medium-low range of previous investigations, ranging from 0.17 to 0.50 d^{-1} (~3 fold variation; Lin et al., 2017) and/or from 0.16 to 0.40 d^{-1} (Calbet et al., 2011). In general, mixotrophic growth herein was somewhat lower than the average value of 0.42 ± 0.09 d^{-1} obtained from feeding experiments with 12 different cryptophyte strains reported in Adolf et al. (2008). The magnitude of *K. veneficum* growth (~2 fold) observed here with varying

prey quantity was lower than the magnitude of the change in growth rates of this same species when provided the same prey *R. salina* but in variable nutrient conditions (Lin et al., 2017). The nutritional quality of prey thus appears to outweigh prey quantity in regulating feeding rates. Interestingly, growth rates of *K. veneficum* with multiple species were comparable to those in the two-species mixtures as feeding was dominated by *R. salina* as prey.

When feeding on *R. salina*, the F_v/F_m of *K. veneficum* did not change substantially, but it did decline with time when feeding on *Synechococcus* as the sole prey. On the other hand, the two types of prey species showed different patterns in F_v/F_m when being fed upon (Fig. 4.9). For *R. salina,* F_v/F_m varied between 0.6 and 0.8 but declined rapidly as it was consumed (Fig. 4.9B). An independent trial (not shown) confirmed that the F_v/F_m change in *R. salina* was a function of the degradation of its phycoerythrin in the presence of the predator, but not necessarily due to direct grazing; rather it appeared to be due to the possible presence of toxin, although toxin was not measured in the study herein or in this independent experiment. In the case of *Synechococcus*, the F_v/F_m remained in a range of 0.2-0.4 throughout the grazing period. The F_v/F_m values of *Synechococcus*, while substantially lower than those of *R. salina*, are in the range of previously reported cyanobacteria (Raateoja et al., 2004; Hung et al., 2013), which tend to be consistently lower than reported for other taxa in a physiologically healthy state. The increases of photosynthetic efficiency in the mixed cultures may have been due to increased availability of recycled nutrients when the predator *K. veneficum* cells were under stress conditions (Fig. 4.9C, D).

In conclusion, growth and physiological states of *K. veneficum* have fundamentally different responses to individual prey species. Variable Chl fluorescence parameters can provide robust measures of the role of mixotrophy in predator-prey interactions with multiple prey species and in different proportions. A substantial increase in growth of *K. veneficum* was achieved with increasing prey concentrations of *R. salina*. While photosynthetic status of the mixotoroph was not affected by feeding, that of its primary prey (e.g., cryptophyte *R. salina*) declined with substantial predation pressure. No substantial feeding by *K. veneficum* was detected on *Synechococcus* sp., and this prey did not alter its photosynthetic status in the presence of the predator *K. veneficum*. This picoplanktonic prey species was consumed by the primary prey, which was able to maintain its photosynthetic efficiency when acting as a predator. This study further advances the use of Phyto-PAM II for assessing rates of mixotrophy as well as in photosynthetic status of algal cells in multiple prey-predator interactions.

References

Adolf, J.E., Bachvaroff, T., Place, A.R., 2008. Can cryptophyte abundance trigger toxic *Karlodinium veneficum* blooms in eutrophic estuaries? Harmful Algae 8(1), 119-128.

Adolf, J.E., Stoecker, D.K., Harding, L.W., 2006. The balance of autotrophy and heterotrophy during mixotrophic growth of *Karlodinium micrum* (Dinophyceae). J. Plankt. Res. 28(8), 737-751.

Affronti, L.F., Marshall, H.G., 1994. Using frequency of dividing cells in estimating autotrophic picoplankton growth and productivity in the Chesapeake Bay. Hydrobiologia 284(3), 193-203.

Arar, E.J., Collins, G.B., 1997. *In vitro* determination of chlorophyll a and pheophytin a in marine and freshwater algae by fluorescence. Method 445.0, National Exposure Research Laboratory, EPA, Cincinnati, OH.

Burkholder, J.M., Glibert, P.M., Skelton, H.M., 2008. Mixotrophy, a major mode of nutrition for harmful algal species in eutrophic waters. Harmful Algae 8(1), 77-93.

Calbet, A., Bertos, M., Fuentes-Grünewald, C., Alacid, E., Figueroa, R., Renom, B., Garcés, E., 2011. Intraspecific variability in *Karlodinium veneficum*: Growth rates, mixotrophy, and lipid composition. Harmful Algae 10(6), 654-667.

Carvalho, W.F., Granéli, E., 2006. Acidotropic probes and flow cytometry: a powerful combination for detecting phagotrophy in mixotrophic and heterotrophic protists. Aquat. Microb. Ecol. 44(1), 85-96.

Flynn, K.J., Stoecker, D.K., Mitra, A., Raven, J.A., Glibert, P.M., Hansen, P.J., Granéli, E., Burkholder, J.M., 2013. Misuse of the phytoplankton–zooplankton dichotomy: the need to assign organisms as mixotrophs within plankton functional types. J. Plankt. Res. 35(1), 3-11.

Frost, B.W., 1972. Effects of size and concentration of food particles on the feeding behavior of the marine planktonic copepod *Calanus Pacificus*. Limnol. Oceanogr. 17, 805-815.

Geider, R.J., Roche, J., Greene, R.M., Olaizola, M., 1993. Response of the photosynthetic apparatus of *Phaeodactylum tricornutum* (Bacillariophyceae) to nitrate, phosphate, or iron starvation. J. Phycol. 29(6), 755-766.

Glibert, P.M., Burford, M.A., 2017. Globally changing nutrient loads and harmful algal blooms: Recent advances, new paradigms, and continuing challenges. Oceanogr. 30(1), 58-69.

Glibert, P.M., Burkholder, J.M., Kana, T.M., Alexander, J., Skelton, H., Shilling, C., 2009. Grazing by *Karenia brevis* on *Synechococcus* enhances its growth rate and may help to sustain blooms. Aquat. Microb. Ecol. 55(1), 17-30.

Goto, N., Kihira, M., Ishida, N., 2008. Seasonal distribution of photosynthetically active phytoplankton using pulse amplitude modulated fluorometry in the large monomictic Lake Biwa, Japan. J. Plankt. Res. 30(10), 1169-1177.

Guillard, R.R., 1975. Culture of phytoplankton for feeding marine invertebrates, In: Smith, W.L., Chanley, M.H. (Eds.), Culture of Marine Invertebrate Animals. Plenum Press, New York, pp. 29-60.

Hall, J.A., Barrett, D.P., James, M.R., 1993. The importance of phytoflagellate, heterotrophic flagellate and ciliate grazing on bacteria and picophytoplankton sized prey in a coastal marine environment. J. Plankt. Res. 15(9), 1075-1086.

Heinbokel, J.F., 1978. Studies on the functional role of tintinnids in the Southern California Bight. I. Grazing and growth rates in laboratory cultures. Mar. Biol. 47(2), 177-189.

Hung, S.-H., Chung, C.-C., Liao, C.-W., Gong, G.-C., Chang, J., 2013. Sequence diversity and expression levels of *Synechococcus* phosphate transporter gene in the East China Sea. J. Exp. Mar. Biol. Ecol. 440, 90-99.

Izaguirre, I., Sinistro, R., Schiaffino, M.R., Sánchez, M.L., Unrein, F., Massana, R., 2012. Grazing rates of protists in wetlands under contrasting light conditions due to floating plants. Aquat. Microb. Ecol. 65(3), 221-232.

Jeong, H.J., Park, J.Y., Nho, J.H., Park, M.O., Ha, J.H., Seong, K.A., Jeng, C., Seong, C.N., Lee, K.Y., Yih, W.H., 2005a. Feeding by red-tide dinoflagellates on the cyanobacterium *Synechococcus*. Aquat. Microb. Ecol. 41(2), 131-143.

Jeong, H.J., Yoo, Y.D., Park, J.Y., Song, J.Y., Kim, S.T., Lee, S.H., Kim, K.Y., Yih, W.H., 2005b. Feeding by phototrophic red-tide dinoflagellates: five species newly revealed and six species previously known to be mixotrophic. Aquat. Microb. Ecol. 40(2), 133-150.

Jones, R.I., 1994. Mixotrophy in planktonic protists as a spectrum of nutritional strategies. Mar. Microb. Food Webs 8, 87-96.

Kolber, Z., Zehr, J., Falkowski, P., 1988. Effects of growth irradiance and nitrogen limitation on photosynthetic energy conversion in photosystem II. Plant Physiol. 88(3), 923-929.

Li, A., Stoecker, D.K., Coats, D.W., 2000. Mixotrophy in *Gyrodinium galatheanum* (Dinophyceae): grazing responses to light intensity and inorganic nutrients. J. Phycol. 36(1), 33-45.

Lin, C.-H., Accoroni, S., Glibert, P.M., 2017. *Karlodinium veneficum* feeding responses and effects on larvae of the eastern oyster *Crassostrea virginica*

under variable nitrogen: phosphorus stoichiometry. Aquat. Microb. Ecol. 79(2), 101-114.

Lundgren, V.M., Glibert, P.M., Granéli, E., Vidyarathna, N.K., Fiori, E., Ou, L., Flynn, K.J., Mitra, A., Stoecker, D.K., Hansen, P.J., 2016. Metabolic and physiological changes in *Prymnesium parvum* when grown under, and grazing on prey of, variable nitrogen: phosphorus stoichiometry. Harmful Algae 55, 1-12.

Millette, N.C., Pierson, J.J., Aceves, A., Stoecker, D.K., 2017. Mixotrophy in *Heterocapsa rotundata*: A mechanism for dominating the winter phytoplankton. Limnol. Oceanogr. 62(2), 836-845.

Park, M.G., Kim, S., Kim, H.S., Myung, G., Kang, Y.G., Yih, W., 2006. First successful culture of the marine dinoflagellate *Dinophysis acuminata*. Aquat. Microb. Ecol. 45(2), 101-106.

Raateoja, M., Seppälä, J., Ylöstalo, P., 2004. Fast repetition rate fluorometry is not applicable to studies of filamentous cyanobacteria from the Baltic Sea. Limnol. Oceanogr. 49(4), 1006-1012.

Ray, R.T., Haas, L.W., Sieracki, M.E., 1989. Autotrophic picoplankton dynamics in a Chesapeake Bay sub-estuary. Mar. Ecol. Prog. Ser., 273-285.

Sanders, R.W., 1991. Mixotrophic protists in marine and freshwater ecosystems. J. Eukaryotic Microbiol. 38(1), 76-81.

Smalley, G.W., Coats, D.W., Adam, E.J., 1999. A new method using fluorescent microspheres to determine grazing on ciliates by the mixotrophic dinoflagellate *Ceratium furca*. Aquat. Microb. Ecol. 17(2), 167-179.

Stickney, H.L., Hood, R.R., Stoecker, D.K., 2000. The impact of mixotrophy on planktonic marine ecosystems. Ecol. Modell. 125(2-3), 203-230.

Stoecker, D.K., 1999. Mixotrophy among dinoflagellates[1]. J. Eukaryotic Microbiol. 46(4), 397-401.

Stoecker, D.K., Hansen, P.J., Caron, D.A., Mitra, A., 2017. Mixotrophy in the marine plankton. Annu. Rev. Mar. Sci. 9, 311-335.

Tittel, J., Bissinger, V., Zippel, B., Gaedke, U., Bell, E., Lorke, A., Kamjunke, N., 2003. Mixotrophs combine resource use to outcompete specialists: implications for aquatic food webs. Proc. Natl. Acad. Sci. 100(22), 12776-12781.

Urabe, J., Gurung, T.B., Yoshida, T., Sekino, T., Nakanishi, M., Maruo, M., Nakayama, E., 2000. Diel changes in phagotrophy by *Cryptomonas* in Lake Biwa. Limnol. Oceanogr. 45(7), 1558-1563.

Waterbury, J.B., Watson, S.W., Valois, F.W., Franks, D.G., 1986. Biological and ecological characterization of the marine unicellular cyanobacterium *Synechococcus*, In: Platt, T., Li, W.K.W. (Eds.), Photosynthetic Picoplankton. Can. Bull. Fish. Aquat. Sci., Toronto, pp. 71-120.

Yoo, Y.D., Seong, K.A., Jeong, H.J., Yih, W., Rho, J.R., Nam, S.W., Kim, H.S., 2017. Mixotrophy in the marine red-tide cryptophyte *Teleaulax amphioxeia* and ingestion and grazing impact of cryptophytes on natural populations of bacteria in Korean coastal waters. Harmful algae 68, 105.

Tables

Table 4. 1. Summary of cell conversion based on culture volume: volume ratios in mixed culture experiments. All the culture flasks were derived from the stock cultures of individual taxa at same physiological status. n = 3.

Species composition	Treatments	Initial cell denisties (x 10^8 cell L^{-1})			*R. salina*: *K. veneficum* cell: cell ratio	*Synechococcus*: *K. veneficum* cell: cell ratio	*Synechococcus*: *R. salina* cell: cell ratio
		K. veneficum	*R. salina*	*Synechococcus*			
Monoculture	Control	1.48	9.67	418.94	-	-	-
Two-species mixtures:	1:2	0.53	8.14	-	15.38	-	-
Kv:Rs ratio	1:1	0.72	6.29	-	8.70	-	-
	2:1	0.71	3.45	-	4.85	-	-
	3:1	0.77	2.41	-	3.11	-	-
Two-species mixtures:	1:2	0.12	-	337.43	-	2902.70	-
Kv:Syn ratio	1:1	0.26	-	284.81	-	1110.46	-
	2:1	0.42	-	200.78	-	478.46	-
	3:1	0.47	-	142.45	-	300.29	-
Two-species mixtures:	1:2	-	3.71	325.94	-	-	87.85
Rs:Syn ratio	1:1	-	5.73	344.40	-	-	60.10
	2:1	-	6.84	173.14	-	-	25.31
	3:1	-	8.45	171.27	-	-	20.27
Three-species mixtures:	1:2:1	0.24	3.82	135.93	15.91	565.91	35.56
Kv:Rs:Syn ratio	1:1:1	0.28	2.87	164.07	10.31	588.21	57.08
	2:1:1	0.36	1.73	135.75	4.82	379.45	78.66
	3:1:1	0.51	1.77	135.21	3.47	264.99	76.28

Table 4. 2. Summary of linear regression equations of Phyto-PAM II chlorophyll *a* autofluorescence (Chl_{F0}) against acetone-extracted Chl *a* concentrations (μg L^{-1}) over serial (0, 20, 40, 60 and 80 %) diluted conditions for single algal culture, and two-species and/or three-species mixed cultures. For the full model, all data were considered.

Species compositions	Regression analysis				
	Slope ± SE	y-Intercept	n	r^2	*p*-value
Karlodinium veneficum (Kv)	0.74 ± 0.11	37.43	5	0.94	0.005
Rhodomonas salina (Rs)	0.81 ± 0.05	48.82	5	0.99	<0.001
Synechococcus sp. (Syn)	0.76 ± 0.06	30.29	5	0.98	<0.001
Two species mixtures (Kv+Rs)	0.72 ± 0.08	38.12	5	0.96	0.003
Two species mixtures (Kv+Syn)	1.15 ± 0.10	13.68	5	0.98	0.001
Two species mixtures (Rs+Syn)	0.47 ± 0.03	37.36	5	0.98	<0.001
Three species mixtures (Kv+Rs+Syn)	0.78 ± 0.12	1.53	5	0.94	0.006
Full model	0.68 ± 0.05	37.01	35	0.83	<0.001

Table 4. 3. Specific growth rates (μ, d^{-1}) calculated from the slopes of the regressions of the changes in Phyto-PAM II chlorophyll *a* and flow cytometric measurements of cell density with time for monocultures, two-species and three-species mixed cultures of *Karlodinium veneficum* in multiple treatments at varying predator-to-prey volume ratios. ANCOVA was used to compare statistical differences in slopes for Group I, II, III and IV of each predator growth condition.

Groups	Species composition	Treatments	Flow cytometry (cell)				Phyto-PAM II (Chl_{F0})			
			Growth rates of *K. veneficum* (d^{-1})				Growth rates of *K. veneficum* (d^{-1})			
			Slope ± SE	r^2	*p*-value	Effect	Slope ± SE	r^2	*p*-value	Effect
I.	Monoculture	Control	0.15 ± 0.03	0.58	<0.001	Groups:	0.12 ± 0.02	0.67	<0.001	Groups:
II.	Two-species mixtures:	1:2	0.37 ± 0.03	0.85	<0.001	I > II > IV> III	0.22 ± 0.03	0.64	<0.001	I > II > IV> III
	Kv:Rs ratio	1:1	0.31 ± 0.04	0.84	<0.001	F = 81.416	0.16 ± 0.02	0.53	<0.001	F = 15.04
		2:1	0.32 ± 0.03	0.81	<0.001	p < 0.0001	0.20 ± 0.02	0.76	<0.001	p < 0.0001
		3:1	0.30 ± 0.05	0.61	<0.001		0.17 ± 0.03	0.62	<0.001	
III.	Two-species mixtures:	1:2	-1.03 ± 0.17	0.74	<0.001		-1.22 ± 0.18	0.69	<0.001	
	Kv:Syn ratio	1:1	-0.84 ± 0.13	0.62	<0.001		-0.65 ± 0.11	0.58	<0.001	
		2:1	0.09 ± 0.05	0.11	0.106		0.04 ± 0.04	0.07	0.205	
		3:1	0.12 ± 0.06	0.63	0.061		0.06 ± 0.03	0.11	0.111	
IV.	Three-species mixtures:	1:2:1	-0.54 ± 0.07	0.57	<0.001		-0.63 ± 0.11	0.73	<0.001	
	Kv:Rs:Syn ratio	1:1:1	0.25 ± 0.06	0.55	<0.001		0.17 ± 0.04	0.50	<0.001	
		2:1:1	0.30 ± 0.06	0.56	<0.001		0.19 ± 0.03	0.66	<0.001	
		3:1:1	0.27 ± 0.04	0.64	<0.001		0.19 ± 0.03	0.64	<0.001	

Table 4. 4. Death rates of prey, *Rhodomonas salina* (DR: Rs cell *Karlodinium veneficum*$^{-1}$ d^{-1}), estimated based on equations of Frost (1972) and Heinbokel (1978) using Phyto-PAM II chlorophyll *a* measurements applied with cell-to-Chl correction factors vs. flow cytometric assay of cell density for two- and/or three-species mixtures in multiple treatments at predator-to-prey volume ratio. Differences in prey death rates between two groups are compared (ANOVA *F*-test).

Groups	Species composition	Treatments	Flow cytometry (cell)		Phyto-PAM II (Chl_{F0})	
			Death rates of *R. salina*		Death rates of *R. salina*	
			DR ± SE	Effect	DR ± SE	Effects
I.	Two-species mixtures:	1:2	4.83± 0.30	Groups:	6.49 ± 1.22	Groups:
	Kv:Rs ratio	1:1	3.27 ± 0.03	I > II	3.89 ± 0.26	I > II
		2:1	1.76 ± 0.15	F = 2.753	1.37 ± 0.36	F = 3.843
		3:1	1.28 ± 0.05	p = 0.114	0.68 ± 0.04	p = 0.065
II.	Three-species mixtures:	1:2:1	-4.41 ± 0.15		-4.64 ± 0.85	
	Kv:Rs:Syn ratio	1:1:1	2.33 ± 0.17		1.80 ± 0.08	
		2:1:1	1.94 ± 0.43		1.77 ± 0.50	
		3:1:1	1.42 ± 0.12		1.42 ± 0.03	

Table 4. 5. Measurements of the maximum quantum yield of PS II fluorescence (F_v/F_m) in monocultures, and two- and three-species mixed cultures of *Karlodinium veneficum*, *Rhodomonas salina*, and *Synechococcus*. Differences in F_v/F_m between groups are marked as different letters (ANOVA *F*-test).

Groups	*Fv/Fm*		
	K. veneficum	*R. salina*	*Synechococcus* sp.
Monocultures of each species	0.55 ± 0.02^{a} (n=24)	0.60 ± 0.01^{a} (n=24)	0.20 ± 0.02^{a} (n=24)
Two-species mixtures (Kv+Rs)	0.54 ± 0.01^{a} (n=96)	0.38 ± 0.06^{b} (n=96)	-
Two-species mixtures (Kv+Syn)	0.39 ± 0.04^{b} (n=96)	-	0.27 ± 0.02^{a} (n=96)
Two-species mixtures (Rs+Syn)	-	0.58 ± 0.01^{a} (n=96)	0.13 ± 0.01^{b} (n=96)
Three-species mixtures (Kv+Rs+Syn)	$0.48 \pm 0.02^{a,b}$ (n=96)	0.38 ± 0.05^{b} (n=96)	0.23 ± 0.02^{a} (n=96)
ANOVA			
F	4.698	5.693	8.291
p-value	0.004	0.001	<0.001

Figures

Fig. 4. 1. Schematic of the experimental design. There were 25 individual culture treatments, each with 3 replicates, and sampled every 12 h for 96 h. Here, the proportions of the culture mixtures are indicated by the respective number of colored tubes.

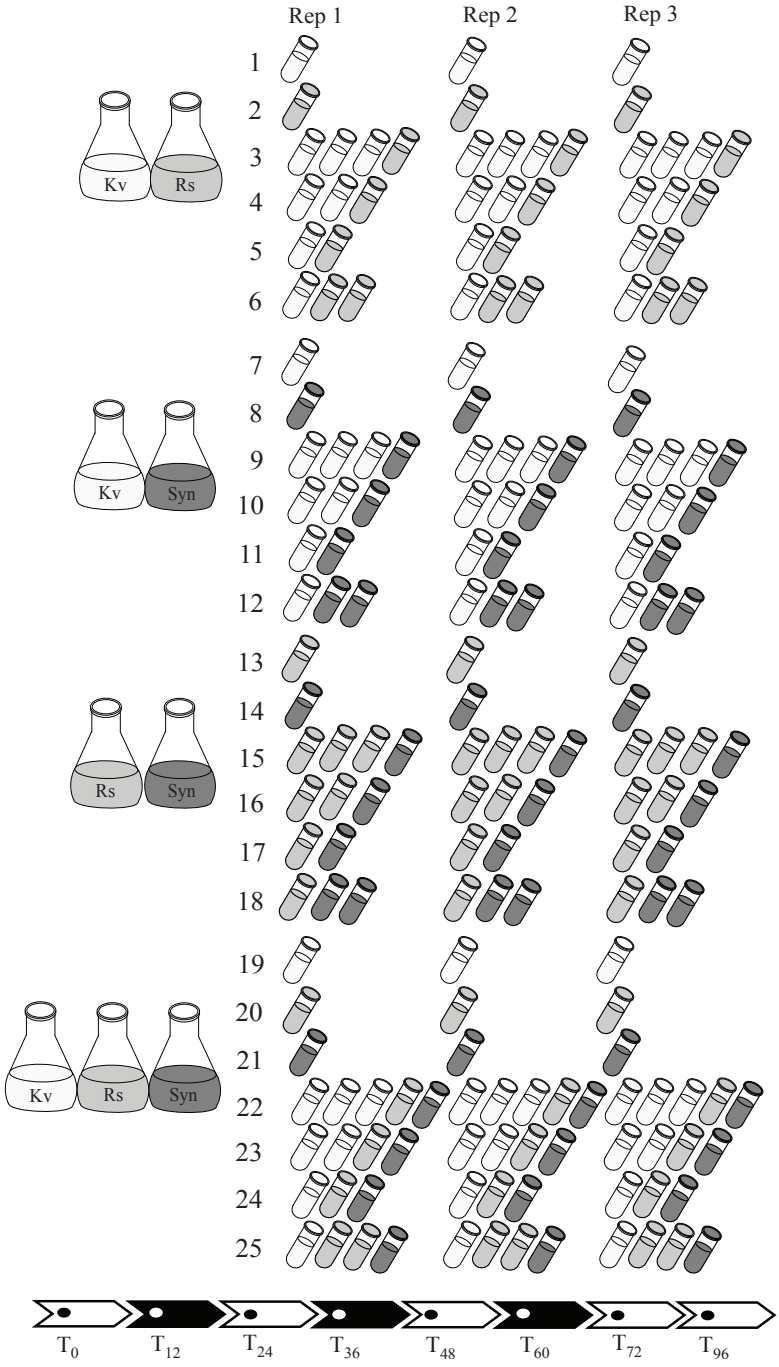

Fig. 4. 2. Relationship between fluorescence-based Chl *a* (Phyto-PAM II) and acetone-extracted Chl *a* concentrations (μg L^{-1}) in single cultures of individual algal strains (open symbols; *Karlodinium veneficum,* circles; *Rhodomonas salina,* squares; *Synechococcus* sp., triangles), and in mixed cultures of two species (solid symbols; *K. veneficum* plus *R. salina,* circles; *K. veneficum* plus *Synechococcus* sp., squares; *R salina* plus *Synechococcus* sp., triangles) and/or three species (cross wheel symbols). The overall regression line is shown; regression statistics of individual mixtures are given in Table 4.2. Dashed line represents the 1:1 relationship. Note that the Phyto-PAM II overestimates that measured by acetone extraction at low chlorophyll levels and underestimates it at values > 100 μg L^{-1}.

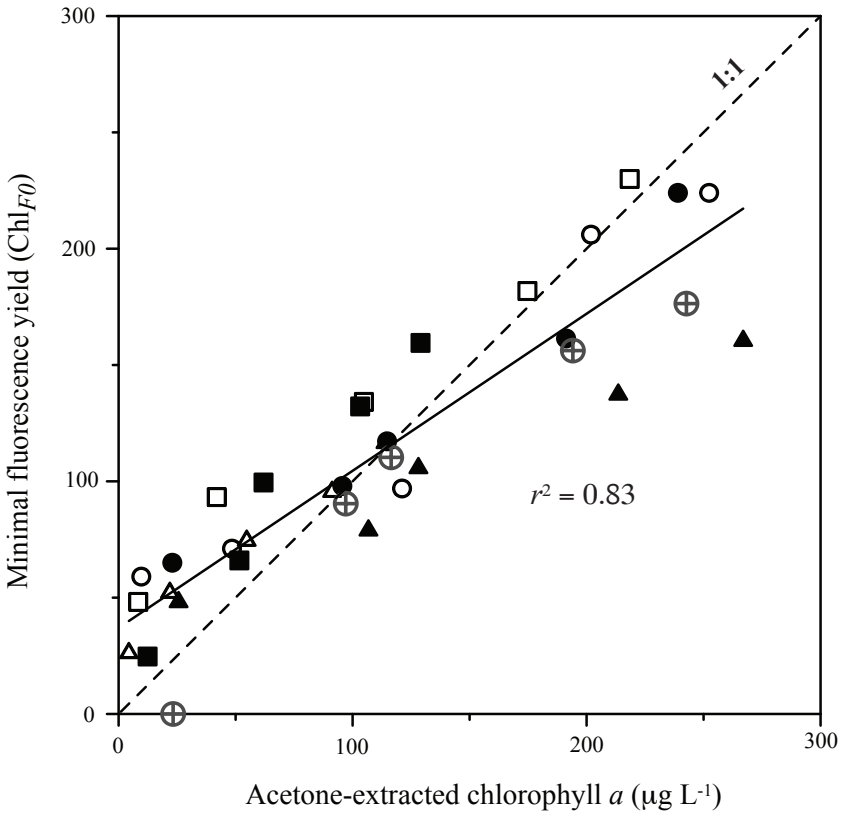

Fig. 4. 3. Relationship between cell-specific growth rates of *Karlodinium veneficum* (A) and death rates of *Rhodomonas salina* (B) based on variable fluorescence using Phyto-PAM II vs. cell densities using flow cytometry over 96 h.

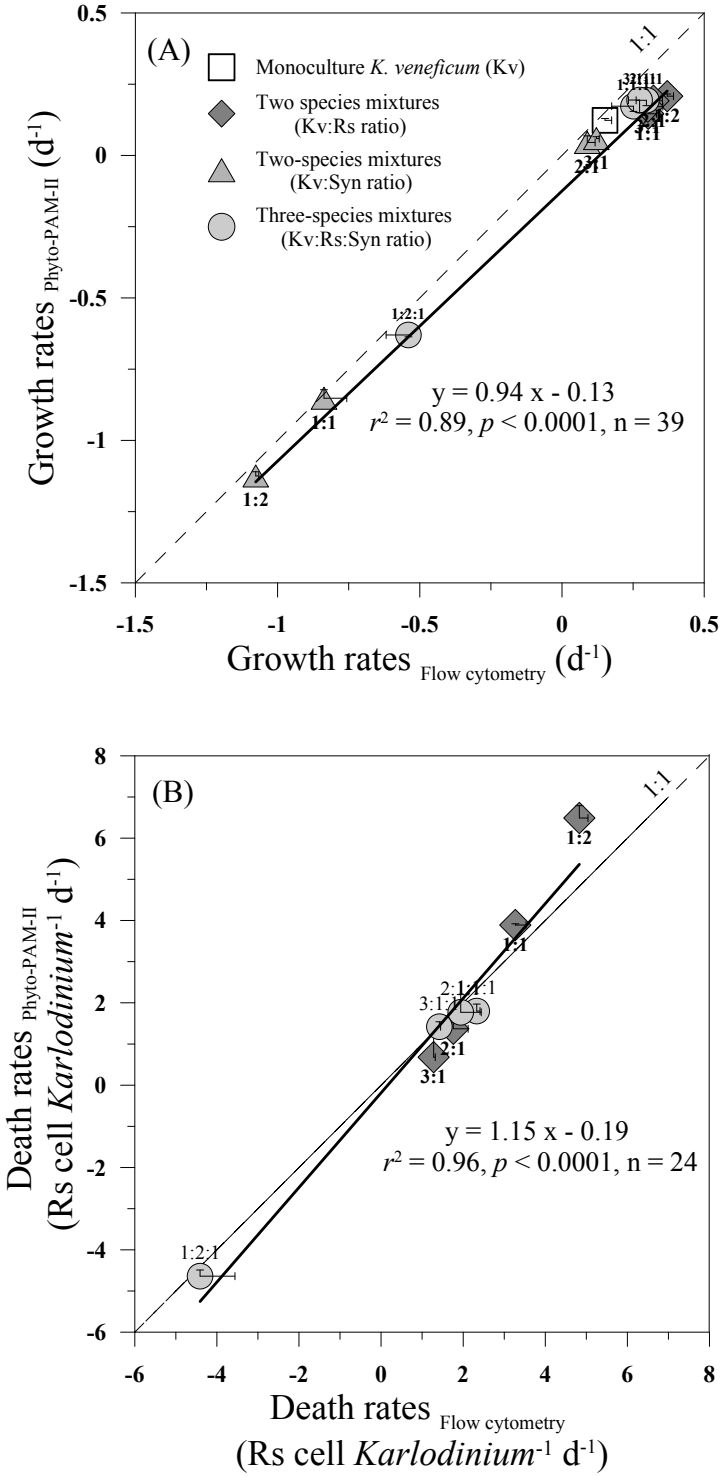

Fig. 4. 4. Changes over time in Chl *a* based on variable fluorescence (A, B), and cell densities based on flow cytometric measurements (C, D) of *Karlodinium veneficum* (circles) mixed with *Rhodomonas salina* (triangles) in monocultures (open symbols), and two-species mixed cultures (filled symbols). The intensity of the shading of the symbols indicates increasingly predator: prey proportions. For calibration purposes, the Chl concentrations and cell densities in mixed-cultures were multiplied by the dilution factors (culture volume: volume ratios) to allow comparison between those measurements in monocultures.

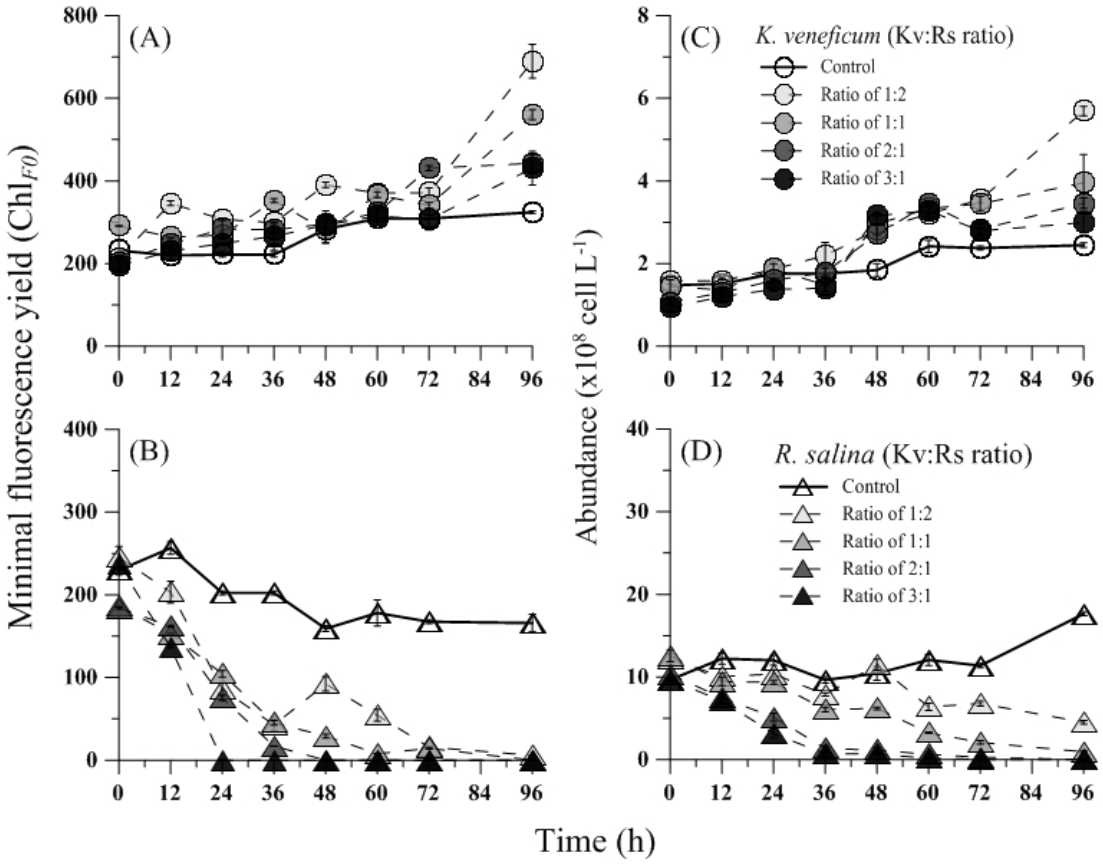

Fig. 4. 5. Changes over time in Chl *a* based on variable fluorescence (A, B), and cell densities based on flow cytometric measurements (C, D) of *Karlodinium veneficum* (circles) mixed with *Synechococcus* sp. (squares) in monocultures (open symbols), and two-species mixed cultures (filled symbols). The intensity of the shading of the symbols indicates increasingly predator: prey proportions. For calibration purposes, the Chl concentrations and cell densities in mixed-cultures were multiplied by the dilution factors (culture volume: volume ratios) to allow comparison between those measurements in monocultures.

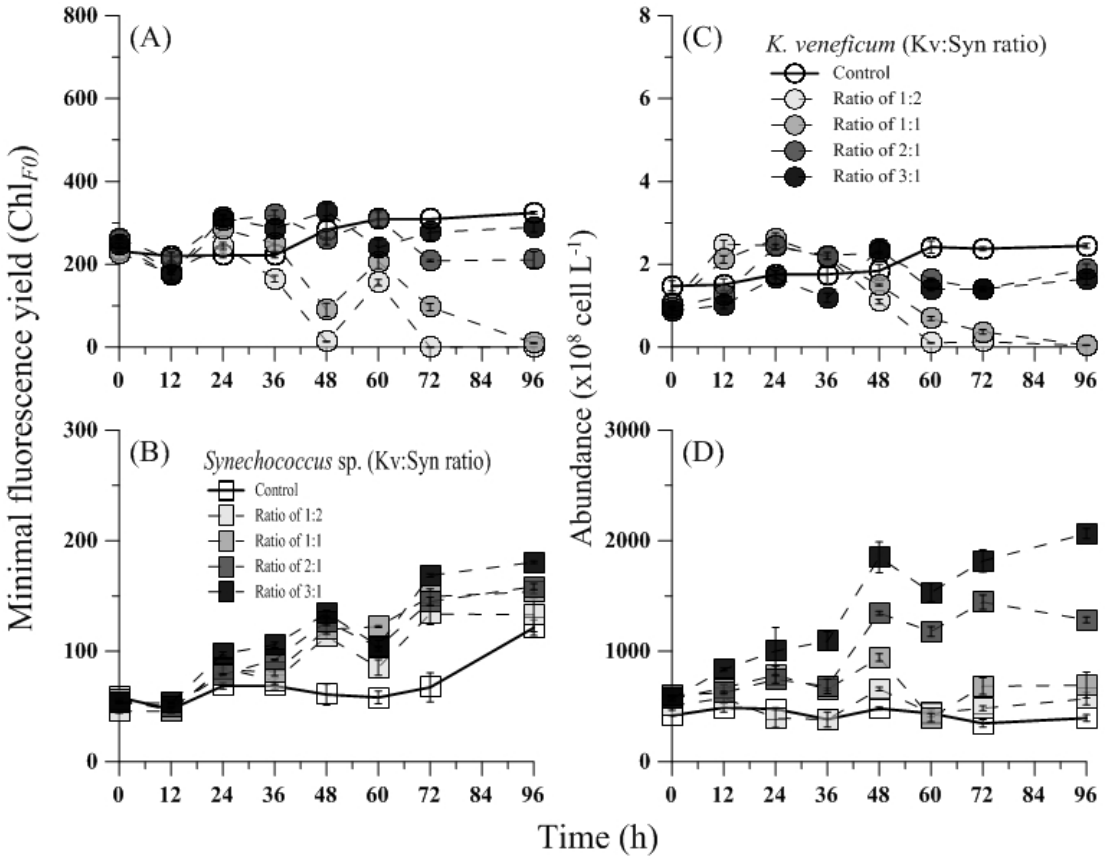

Fig. 4. 6. Changes over time in Chl *a* based on variable fluorescence (A, B), and cell densities based on flow cytometric measurements (C, D) of *Rhodomonas salina* (triangles) mixed with *Synechococcus* sp. (squares) in monocultures (open symbols), and two-species mixed cultures (filled symbols). The intensity of the shading of the symbols indicates increasingly predator: prey proportions. For calibration purposes, the Chl concentrations and cell densities in mixed-cultures were multiplied by the dilution factors (culture volume: volume ratios) to allow comparison between those measurements in monocultures.

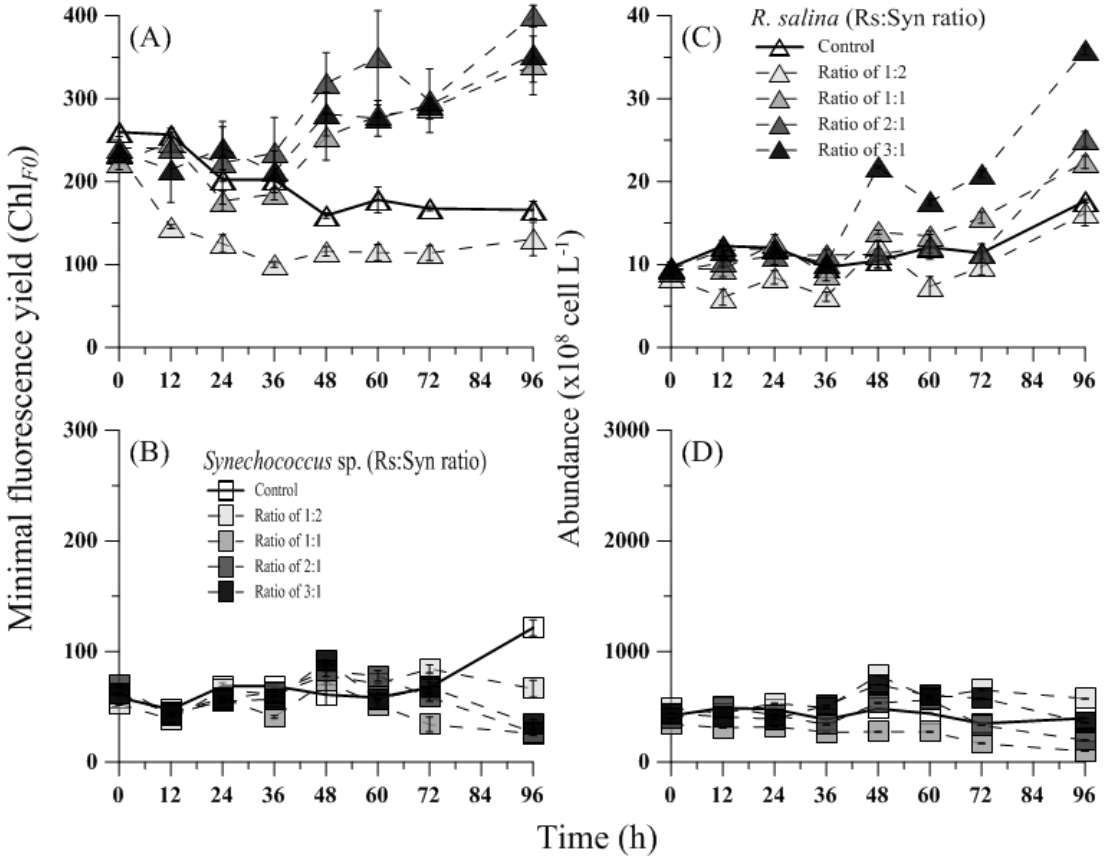

Fig. 4. 7. Changes over time in Chl *a* based on variable fluorescence (A, B, C), and cell densities based on flow cytometric measurements (D, E, F) of *Karlodinium veneficum* (circles) mixed with *Rhodomonas salina* (triangles) and *Synechococcus* sp. (squares) in monocultures (open symbols), and three-species mixed cultures (filled symbols). The intensity of the shading of the symbols indicates increasingly predator: prey proportions. For calibration purposes, the Chl concentrations and cell densities in mixed-cultures were multiplied by the dilution factors (culture volume: volume ratios) to allow comparison between those measurements in monocultures.

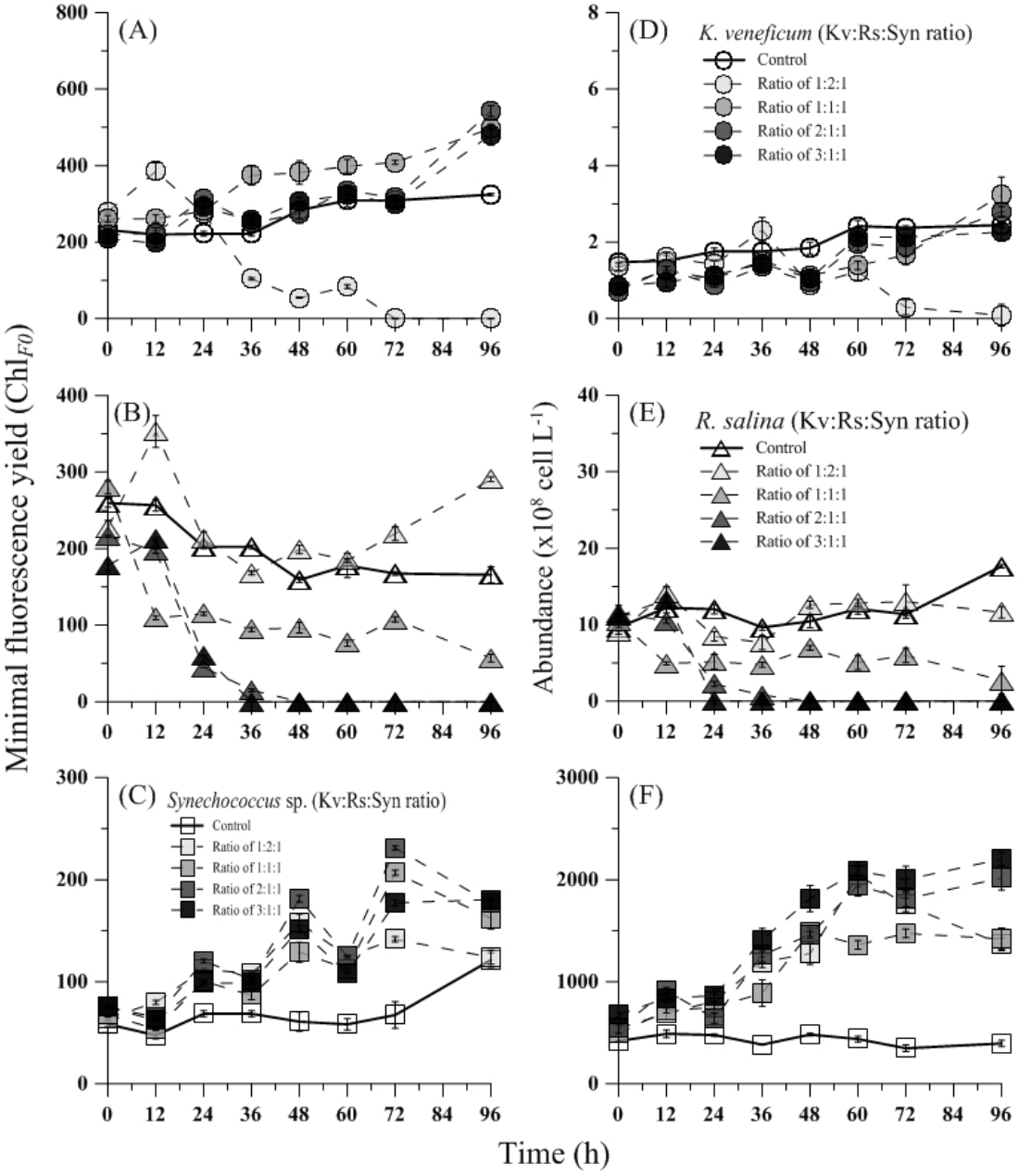
(A)
(B)
(C) Synechococcus sp. (Kv:Rs:Syn ratio)
(D) K. veneficum (Kv:Rs:Syn ratio)
(E) R. salina (Kv:Rs:Syn ratio)
(F)
Control
Ratio of 1:2:1
Ratio of 1:1:1
Ratio of 2:1:1
Ratio of 3:1:1
Minimal fluorescence yield (Chl$_{F0}$)
Abundance (x10^8 cell L^{-1})
Time (h)

Fig. 4. 8. Cell-specific growth rates of *Karlodinium veneficum* (A, B) and death rates of *Rhodomonas salina* (C) as a function of prey concentrations of *R. salina* (circles) and *Synechococcus* sp. (triangles) based on variable fluorescence using Phyto-PAM II (open symbols) vs. cell densities using flow cytometry (filled symbols). The cell-to-Chl *a* correction factors are applied to the calculation of death rates in fluorescence-based Chl *a* (Chl_{F0}) measurements. The correlation coefficients were estimated and the outliers (e.g., Kv: Rs: Syn = 1:2:1) were removed from the analyses. Samples size n = 21 and error bars are standard deviations.

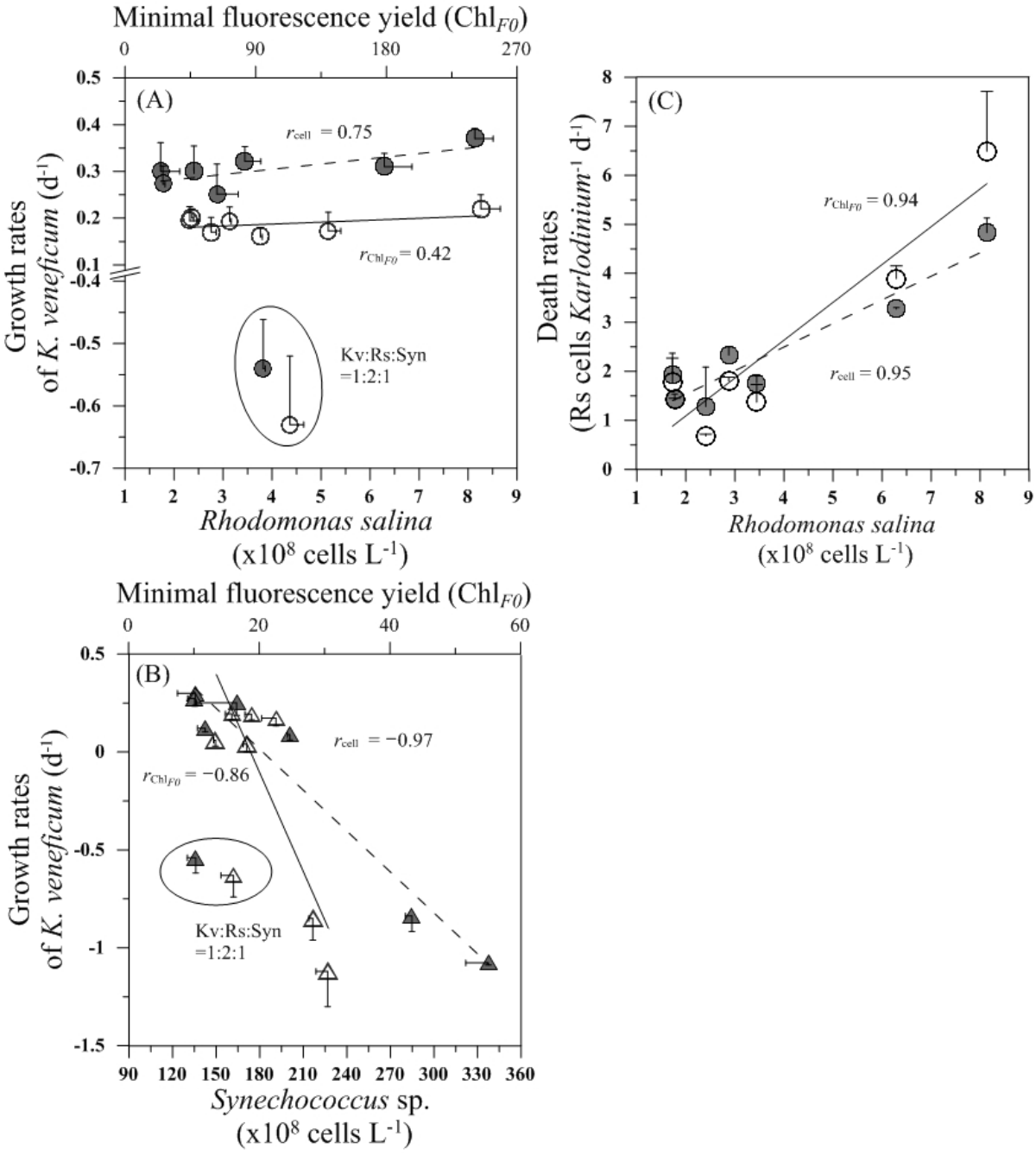
Minimal fluorescence yield (Chl$_{F0}$)
(A)
r_{cell} = 0.75
$r_{Chl_{F0}}$ = 0.42
Kv:Rs:Syn
=1:2:1
Growth rates
of *K. veneficum* (d^{-1})
Rhodomonas salina
(x10^8 cells L^{-1})
(C)
$r_{Chl_{F0}}$ = 0.94
r_{cell} = 0.95
Death rates
(Rs cells *Karlodinium*$^{-1}$ d^{-1})
Rhodomonas salina
(x10^8 cells L^{-1})
Minimal fluorescence yield (Chl$_{F0}$)
(B)
r_{cell} = −0.97
$r_{Chl_{F0}}$ = −0.86
Kv:Rs:Syn
=1:2:1
Growth rates
of *K. veneficum* (d^{-1})
Synechococcus sp.
(x10^8 cells L^{-1})

Fig. 4. 9. Changes in variable fluorescence of *Karlodinium veneficum* (circles) mixed with *Rhodomonas salina* (triangles) and *Synechococcus* sp. (squares) in monocultures (open symbols), and two-species mixed cultures (filled symbols) with time. The intensity of the shading of the symbols indicates increasingly predator: prey proportions.

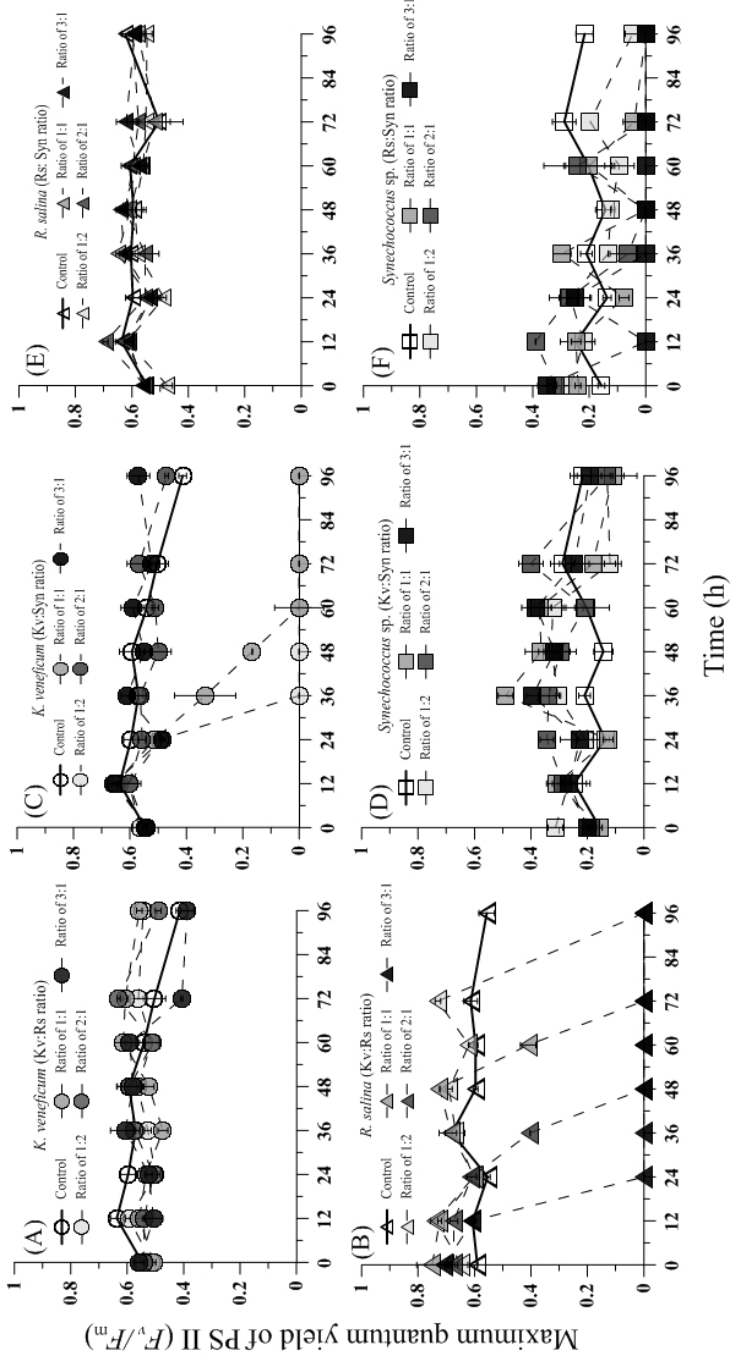

Fig. 4. 10. Changes in variable fluorescence of *Karlodinium veneficum* (circles) mixed with *Rhodomonas salina* (triangles) and *Synechococcus* sp. (squares) in monocultures (open symbols), and three-species mixed cultures (filled symbols) with time. The intensity of the shading of the symbols indicates increasingly predator: prey proportions.

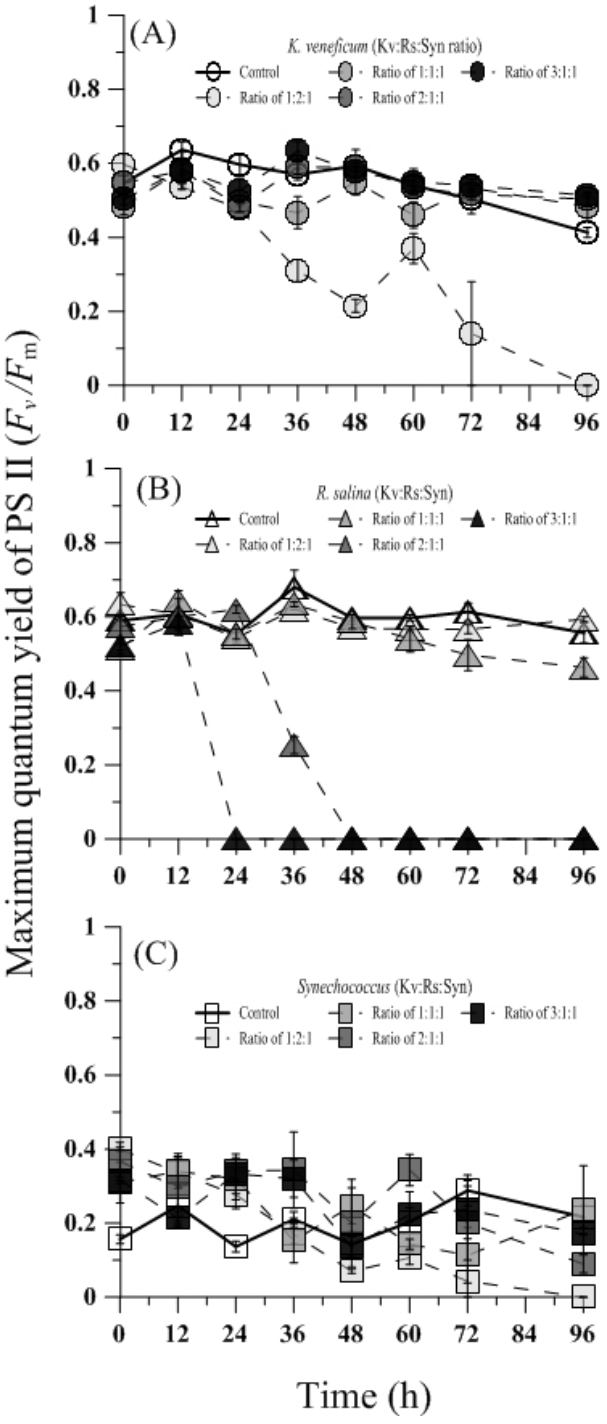

Chapter 5: Modeling effects of variable nutrient stoichiometry and temperature on mixotrophy in the harmful dinoflagellate *Karlodinium veneficum*[4]

Abstract

A dynamic mathematical model is presented simulating the growth of the harmful algal bloom (HAB) mixotrophic dinoflagellate *Karlodinium veneficum* and its algal prey, *Rhodomonas salina*. This model describes carbon-nitrogen-phosphorus-based interactions within the mixotroph, interlinking autotrophic and phagotrophic nutrition. The model was tuned to experimental data from these species grown under autotrophic conditions and in mixed batch cultures in which nitrogen:phosphorus stoichiometry (molar N:P of 4, 16 and 32) of both predator and prey varied. With a single set of parameter values defining mixotroph and prey physiology, a good fit was attained to all experimentally-derived carbon biomass data. The potential effects of temperature and nutrients changes on promoting growth of prey and thus *K. veneficum* bloom formation were explored using this simulation platform. The modeled biomass of *K. veneficum* was highest when they consumed prey under high N:P conditions. The modeled scenarios under low N:P conditions responded differently, and showed larger deviation between mixotrophic and autotrophic growth, depending on temperature. When inorganic nutrients were in balanced proportions, lower biomass of the mixotroph was attained at all temperatures in the

[4] Lin et al. *Front. Mar. Sci.* Submitted.

simulations, suggesting that natural systems might be more resilient against *Karlodinium* HAB development in warming temperatures if nutrients were available in balanced proportions. The models highlight the importance of consideration of particulate prey in modeling HAB dynamics. The simulations also imply that warmer, wetter springs that may bring more N, such as predicted under climate change for Chesapeake Bay, may be more conducive to development of these HABs. Prey availability may also increase with temperature due to differential growth temperature responses of *K. veneficum* and its common prey.

Introduction

In conjunction with the growing recognition that harmful algal blooms (HABs) are promoted by increasing nutrient loads to marine and freshwaters (e.g., Anderson et al., 2002; Glibert et al., 2005; Heisler et al., 2008; Glibert and Burford, 2017), there is also an enhanced appreciation for the importance of mixotrophy in the nutrition of many HAB taxa (Jeong et al., 2005a,b; Burkholder et al., 2008; Flynn et al., 2013; Stoecker et al., 2017). The complexities of studying blooms dominated by mixotrophs compound the already difficult study of autotrophic physiology (Flynn, 2009), especially in the context of HAB species (Mitra and Flynn, 2010; Ghyoot et al., 2017). Understanding the processes that promote the growth of toxigenic flagellates and the extent to which they depend on mixotrophy for their nutrition is of major importance for managing the problems of HABs. The involvement of mixotrophy in both biomass and toxin production requires that we reappraise simulation models of HAB species, to not only consider autotrophic factors (John and Flynn, 2002) but also those factors that promote or alter rates of (phago-) heterotrophy (Mitra and Flynn,

2010). At present, predictive capabilities that include the role of mixotrophy in bloom formation under varying environmental conditions are generally lacking (Flynn, 2005b, 2010; Glibert et al., 2010; Mitra et al., 2014; 2016; Flynn et al., 2018). The challenge in understanding HAB dynamics is greatly complicated by the involvement of mixotrophy, as it is necessary to not only understand the ecophysiology of the HAB species, but also of prey species.

Modeling relationships between nutrients and harmful algae is challenging as nutrient sources, both dissolved and particulate, vary in quantity and nutritional quality. Mixotrophy in protists is not a simple additive process of autotrophy plus phagotrophy, but rather a complex integration of physiological interactions (Flynn and Mitra, 2009; Mitra and Flynn, 2010). Studying mixotroph physiology, and the inclusion of these physiological processes in models, is further complicated by the need to simultaneously consider the growth of the prey species and their physiological status (Mitra and Flynn, 2005). Only a few physiological experiments (Lundgren et al., 2016; Lin et al., 2017)–and even fewer model constructs–consider the feedback function of rates of change during mixotrophic feeding, the nutritional status of both predator and prey, and linkages to cellular stoichiometric balancing between physiological interactions (Mitra and Flynn, 2006, 2010).

Among the environmental conditions that affect HABs are those associated with climate. Climate change is likely to be locally if not regionally significant and increases in temperature may expand the potential niches for harmful or toxic algal blooms (Hallegraeff, 2010; Fu et al., 2012; Wells et al., 2015; Glibert and Burkholder, 2018). The most direct effects of climate change are those associated

with rising temperatures, including the growth rates of the HABs, but also the consortium of organisms that co-occur with the HAB species, and which can be food sources for these mixotrophs (e.g., Fu et al., 2012; Wells et al., 2015; Glibert et al., 2018). The frequency and severity of blooms may be exacerbated due to temperature-driven competitive advantages for HAB species over non-HAB species (Hallegraeff, 2010) and other HAB-favorable conditions may expand, such as increased stratification or altered precipitation patterns that affect the timing of freshwater and associated nutrient delivery (e.g., Heisler et al., 2008; Moore et al., 2015; Glibert and Burkholder, 2018). The mixotrophic chrysophyte *Ochromonas* sp., for example, has been found to become more heterotrophic with increased temperature (Wilken et al., 2013). There is also evidence that ingestion, growth rates and cell volume of the heterotrophic dinoflagellate *Oxyrrhis marina* respond differently to temperature-prey interactions, indicating complex and non-linear predator-prey dynamics with increasing temperatures (Montagnes et al., 2003; Kimmance et al., 2006). However, many questions of whether or not physiology and nutrient acquisition of HAB species change with rising temperature, as well as how such changes may affect their interactions with that of its prey under varying nutrient conditions, remain.

The mixotrophic dinoflagellate *Karlodinium veneficum* (formerly *Gymnodinium galatheanum* and *K. micrum*) is a common toxigenic species that can produce a suite of unique polyketide compounds, karlotoxins (Van Dolah, 2000; Kempton et al., 2002). This species is a constitutive mixotroph (Mitra et al., 2016), processing the ability to make its own chloroplasts, and is capable of forming blooms of up to 10^7-10^8 cells L^{-1} (e.g., Adolf et al., 2008) that have been associated with fish

and shellfish mortality, both in natural waters and aquaculture farms worldwide (Braarud, 1957; Nielsen, 1993; Glibert and Terlizzi, 1999; Deeds et al., 2002; Stoecker et al., 2008; Zhou et al., 2011). Blooms of *K. veneficum* appear to be increasing in size and frequency of occurrence in estuaries such as Chesapeake Bay, USA (Li et al., 2015), and elsewhere worldwide (Place et al., 2012, and references therein; Dai et al., 2013; Adolf et al., 2015). Given the apparent increases in HABs and potential threats to natural resources around the world, improved forecasting and predictive ability would be an aid to managers.

Here, applying both previously published and newly acquired experimental data to models of mixotrophy, simulations were developed that predict the growth of the mixotroph *K. veneficum,* and its common prey, *Rhodomonas*, under varying nutrient and temperature conditions. The modeled simulations were used to address the hypothesis that growth of the mixotroph may increase due to the combination of increased nutrient concentrations, altered nutrient ratios, and raised temperature, conditions that may be expected under future climate conditions in eutrophic estuaries. Simulations using such models may help inform nutrient management plans under future climate conditions.

Materials and Methods

Overall approach

The overall approach taken here was to apply physiological knowledge of *Karlodinium veneficum* and its common prey *Rhodomonas salina* under autotrophic

and mixotrophic growth conditions in a mechanistic model of variable stoichiometry and temperature (Fig. 5.1). This mechanistic model was developed based on the framework of an existing cell quota-based, variable carbon-nitrogen-phosphorus (C-N-P), photo-acclimative mixotrophy model, namely the "perfect beast" model of Flynn and Mitra (2009). This describes carbon-nitrogen-phosphorus (C-N-P)-based interactions within a mixotroph cell, and builds upon the variable stoichiometric zooplankton model of Mitra (2006) and the photosynthesis model of Flynn (2001). For a full description and rationale for the base models, please see the respective original papers.

In brief, the "perfect beast" construst for the mixotroph has eight state variables (Fig. 5.2) describing C, N and P and chlorophyll (Chl) associated with the core mixotroph (m) biomass (mC, NC, PC, ChlC) and also the same constituents associated with the contents of the food (F) vacuole (namely, FC, FNC, FPC and FChlC) after the mixotroph have fed on algal prey. The amount of material associated with the food vacuole is relative to the core mC biomass. Thus, the total C associated with the mixotroph is mC·(1+FC) with the unit of gC L^{-1}. Here the mixotroph model was configured to be consistent with the status of *Karlodinium* as a constitutive mixotroph, with its own photoacclimative description of Chl:C. The prey was described using the variable stoichiometric photoacclimative phytoplankton model of Flynn (2001), as used to describe phytoplankton prey in the work of Flynn and Mitra (2009). The total model accounts for predator stoichiometry, prey stoichiometry (i.e., food quality) and their feedback interactions (Fig. 5.2). The full model equation is available in the appendix. The model operates using ordinary differential equations

(ODEs) using an Euler integration routine with a timestep of 0.0078125 d (11.25 min).

For this work the model was built, and simulations run, within the Powersim Constructor platform, with tuning (calibration) to experimental data performed using the evolutionary algorithm supported by Powersim Solver v2 (Isdalstø, Norway). This algorithm can maximize the likelihood of resolving a global, rather than a local, minimum that produces the fit closest to the presented data (Haefner, 2005). Most of the constants within the model are not tuned; they are used to modulate physiological feedback processes and the model is not sensitive to their precise value (see source papers for further details). See Tables AII.1,2 for values of constants used for these particular simulations.

To configure the total model describing both the mixotroph and its prey, the constants that constrain the autotrophic physiology of predator and prey were first determined from experimental data. Once rates of photosynthesis and inorganic nutrient uptake for these species were calculated for varying nutrient and temperatures, the parameters that control mixotrophic performance of the predator were then ascertained (again through reference to experimental data), for conditions in which predator and prey were both grown under varying nutrient stoichiometry. Finally, the tuned mixotroph model was run to simulate (predict) growth of K. veneficum under variable N:P conditions and temperature (Fig. 5.1)

Data sources, experimental conditions and model parameters

The model builds on experimental data previously described as well as new experimental data. Experimental data based on both autotrophic growth of *K.*

veneficum and *R. salina* under varied nitrogen (N):phosphorus (P) stoichiometry (molar N:P of 4, 16 and 32) in exponential growth phase, were first applied to the model (Lin et al., 2017, Fig. 5.1). The constants that describe the autotrophic physiology of prey (e.g., half saturation constants for nitrogen (N) and phosphorus (P) uptake, aK_{Ni}, aK_P and of growth, $a\mu max^{phot}$) and predator (e.g., mK_{Ni}, and mK_P) were obtained from model tunings based on the change in residual NO_3^- and PO_4^{3-} concentrations (nutrient kinetics), and chlorophyll (Chl) and C biomass (see below) during culture growth data of monocultures for predator and prey, and based on the aforementioned data sources (Table 5.1). From a second set of experiments, based on monocultures of *K. veneficum* and *R. salina,* growing autotrophically, initial slopes of photosynthesis-irradiance (PI) curves were calculated, based on measurements of Phyto-PAM fluorometry (Lin and Glibert, submitted). Additional physiological data (Table AII.1) for parameterizing the autotrophic component of the model were obtained from Flynn and Mitra (2009).

New experimental data were also obtained on temperature responses of the mixotroph *K. veneficum* and *R. salina* (Fig. 5.1). The same strains of *K. veneficum* and *R. salina* used in Lin et al. (2017) were inoculated separately into *f*/2 media (Guillard, 1975) and maintained at 12, 17, 20, 25, 28 °C under irradiance of 430 μmol photons m^{-2} s^{-1} in a 12 h light:12 h dark cycle in batch cultures. The strains were acclimated for 2 weeks to the experimental conditions, after which growth was monitored over 96 h. To do so, aliquots (2 mL) were collected for cell enumeration at 0, 24, 48, 72 and 96 h from each flask and were preserved in paraformaldehyde (final concentrations of 1% v/v) at 4°C for subsequent cell enumeration. The cells were then

identified and gated based on size, shapes, and auto-fluorescence using a BD Accurri C6 flow cytometry. Cell-specific growth rates of predator and prey were determined separately based on the rates of changes in the slopes of the regression of natural log-transformed cell-densities change over 96 h.

The mixotrophic model structure (Flynn and Mitra, 2009), which is C-based, contains 8 state variables and parameters for phototrophic and heterotrophic physiology, interlinked through cell quota processes (Fig. 5.2, Appendix II). The constants for heterotrophic functions, the parameters controlling ingestion, digestion, and assimilation of prey C (e.g., *mKas*, *mKIng*, and *mAEmin*) were tuned with previously available experimental data in which predator, *K. veneficum,* and prey, *R. salina*, were combined in 9 different nutrient stoichiometric combinations (3 x 3 factorial of N:P conditions of predator and prey; Lin et al., 2017; Fig. 5.1, Table 5.2). The C biomass of *K. veneficum* was estimated based on a cellular C-volume relationship for dinoflagellates (Menden-Deuer and Lessard, 2000) and a conversion factor of 0.2 pg C μm^{-1} from volume to C for *R. salina* was applied (Jakobsen and Hansen, 1997). As cell size of predator and prey were recorded in parallel with the cell densities in the study of Lin et al. (2017), cellular volume (CV) was estimated using the following equation:

$$CV = 0.1875WL^2$$

where W and L are the width and length of cells.

Simulation with variable stoichiometry and temperature

After the mixotroph model was calibrated, and after autotrophic temperature responses of predator and prey were experimentally determined, the model was

applied to simulate growth of the mixotroph and its prey under 3 of the 9 experimental nutrient conditions (N:P = 4, N:P = 16, and N:P= 32 for both predator and prey) under varying temperatures (Fig. 5.1). Temperature-dependent rates of maximum phototrophic growth for both species were applied to predict 10-day growth responses. The assumption as made that the temperature responses of mixotroph and prey were independent of the inorganic stoichiometry of nutrients in the growth media. Specific growth rates (μ; d^{-1}) were determined based on the slopes of the regression of natural log-transformed C biomass change over the simulated periods.

Statistical analyses

All statistical analyses were performed with R. The Shapiro-Wilk test was used to verify normality of the experimental data while the Levenes' test was used to assess the homogeneity of variance. Cell-specific growth rates of *K. veneficum* and *R. salina* were compared for statistical differences in slopes of regression of natural log-transformed data under each temperature conditions (ANCOVA test). Two-way analysis of variance was applied to test for the interactive effects between temperature and species. Regressions were considered significant at $p < 0.05$ with the adjusted r^2 value.

Results

Temperature responses of phototrophic parameters

Simulating mixotrophy under variable nutrient and temperature conditions required that all parameters constraining for autotrophic growth in the model were first established, then the mixotrophy model was tuned and applied in the variable temperature scenarios (Fig. 5.1). Autotrophic growth parameters were all previously available (Table 5.1, 2) except for those of growth as a function of temperature.

The response to temperature of the tested mixotroph and its prey differed. Autotrophic growth rates of *K. veneficum* ranged between 0.06 and 0.29 d^{-1} and increased with increasing temperature up to 20 ºC above which growth rates fell sharply (Fig. 5.3). The growth rates of *R. salina* had a similar range as those in the predator, from 0.06 to 0.26 d^{-1}, but the prey grew significantly faster than its predator at temperatures >20ºC (ANCOVA, $p < 0.001$; Fig. 5.3). Variations between temperature responses of the maximal growth rates of *K. veneficum* and its prey were statistically significant (two-way ANOVA: F-value = 2.88, $p = 0.011$; Fig. 5.3).

Modeling tuning to experimental data sets

Model tuning was undertaken in 2 steps. Half saturation values (i.e., mK_{Ni}, mK_P, aK_{Ni} , and aK_P) were calculated based on nutrient depletion to determine transport of nutrients in relation to the cell quotas, and photosynthetic rates were used to determine cell C when cells were in autotrophic growth. Maximum and minimum ratios of N:C and P:C were calculated to determine the nutrient status of the cell (Table 5.1). These parameters were then applied to mixotrophic growth.

The mixotroph model was successfully calibrated against previously available data on the growth of the mixotroph and its prey as a function of variable nutrient stoichiometry (Fig. 5.4). Between 62 % and 97 % of the variations in the 9 experimental data sets could be explained by the simulations for biomass of the mixotroph, with no significant difference between the observed and predicted data ($p < 0.05$).

The parameters that control mixotrophic growth showed variability with the nutritional status (C:N:P) of *K. veneficum* and its prey (Table 5.2). The most sensitive parameters were assimilation efficiency (*mAEmin*) and half saturation constant for ingestion (*mKIng*) and maximum growth rate of heterotrophic growth ($m\mu max^{het}$; Table 5.2). For example, the minimum assimilation efficiency (*mAEmin*) of C in the mixotroph from the ingested prey ranged from 0.370 under conditions in which both the mixotroph and prey were grown with nutrients supplied in Redfield N:P conditions (N:P = 16), to 0.840 when the prey was under Redfield growth conditions but *K. veneficum* was grown under low N:P conditions. Thus, there was significantly higher *mAEmin* when the mixotroph was initially under low N:P conditions than when it was under Redfield N:P conditions and given the same quality prey. In addition, the half saturation for ingestion (*mKIng*) for *K. veneficum* grown under low N:P conditions was significantly lower when they were mixed with the high N:P prey, than when *K. veneficum* in the same nutrient state was given prey grown under Redfield N:P and low N:P conditions (0.204 vs. 0.295 and 0.490, respectively). For those *K. veneficum* grown under high N:P conditions, their *mKIng* ranged from 0.010 to 0.309 with the lowest value corresponding to prey grown under low N:P.

Maximum growth rate of *K. veneficum* as a heterotroph ($m\mu max^{het}$) was consistently higher than maximum growth rate of *K. veneficum* as an autotroph ($m\mu max^{phot}$) by factors of 1.19 (low N:P *K. veneficum* with Redfield N:P prey) to 2.72 (high N:P *K. veneficum* with low N:P prey; Table 5.2).

Simulating growth under variable stoichiometry and temperature

Using the tuned mixotroph-prey models, and having established individual temperature responses of *K. veneficum* and *R. salina*, scenarios were developed to estimate growth of both species under variable stoichiometry and temperature conditions (Fig. 5.1). For *K. veneficum*, growth as an autotroph and as a mixotroph were also compared, and for *R. salina*, growth with and without the predator were considered. Three stoichiometric conditions were simulated, holding both species in the same N:P condition for each scenario (N:P = 4, 16, 32).

In the low N:P scenario, significantly higher C biomass of *K. veneficum* in mixotrophic growth was attained with increased temperature (≥ 25 ºC) compared with its modeled biomass under comparable autotrophic conditions (ANCOVA, $p = 0.003$; Fig. 5.5A,D). The highest growth rate of 0.26 d^{-1} was attained at 25ºC, which was 2-fold higher than the simulation without prey. In the Redfield N:P scenarios, there were no significant differences between autotrophic and mixotrophic growth rates of *K. veneficum* (ANCOVA, $p = 0.107$) and relatively low overall C biomass of the mixotroph was attained in the 10-day simulation (Fig. 5.5B,E). Differences between mixotrophic and autotrophic growth of *K. veneficum* under high N:P conditions were at the edge of statistical significance (ANCOVA, $p = 0.052$). The growth patterns of *K. veneficum* in the two nutritional modes were very similar, showing increases in

biomass reaching the maximum value of ~1300 μgC L^{-1} at 20ºC under mixotrophic conditions, but a lower growth rate and corresponding C biomass accumulation at higher temperature (Fig. 5.5C,F).

The accumulation of C biomass and growth rates of *R. salina* in the presence and absence of the mixotroph were also estimated under variable nutrient and temperature conditions (Fig. 5.6). In the presence of the mixotroph, prey biomass in all N:P conditions declined, but the patterns of decline varied with varying nutrient conditions (Fig. 5.6A-C). Under low N:P conditions, prey biomass gradually declined to zero within the 10-day simulation. Under Redfield conditions, prey remained detectable, but low, throughout the 10-day growth simulation. In the highest N:P simulation, prey biomass declined most quickly, to a near-zero biomass within 4 days. The patterns of the changes in prey biomass without predator were comparable among the 3 nutrient conditions, but higher biomass values were usually attained in the N-rich conditions at the near-highest temperatures (Fig. 5.6F).

Change in cellular N:P of *K. veneficum* with time was also explored in the model output in autotrophic and mixotrophic growth to determine the extent to which the mixotroph was using inorganic nutrients under the different stoichiometric and temperature conditions. The cellular nutrient ratios of *K. veneficum* under low N:P and Redfield N:P growth conditions varied considerably in first 2 days of simulated growth, then converged a value of ~ 10, but those of *K. veneficum* grown in high N:P conditions converged on a value of ~ 6 within 2 days under all temperatures conditions (Fig. 5.7). Thus, in the modeled scenarios, under the condition of excess N (high N:P), *K. veneficum* appeared to become increasingly enriched with internal P.

Discussion

This study has successfully tuned an existing multi-nutrient mechanistic model of mixotrophy to experimental data sets of the harmful dinoflagellate, *K. veneficum* and its prey, *Rhodomonas* sp., under varying nutrient conditions. The mixotroph model, the "perfect beast" of Flynn and Mitra (2009), is a construct that can be configured to represent different types of constitutive and non-constitutive mixotrophs, as consistent with our understanding of the different physiologies (Mitra et al., 2016). Although the model has been configured to represent different generic mixotroph types and used to explore the implications of different types of mixotrophy in oligotrophic through to eutrophic conditions (Flynn and Mitra, 2009; Mitra and Flynn, 2010; Flynn and Hansen, 2013; Mitra et al., 2014), this is the first time that this, or indeed any, multi-stoichiometric model of protist mixotrophy has been specifically tuned to simulate experimental data. In large measure, this reflects the paucity of such data not only for mixotroph activity but also for the prey. Indeed, very few empirical or modeling studies of phytoplankton describe multiple stoichiometries (i.e., C:N:P), despite increasing evidence that in nature such multiple nutrient states are important features structuring ecology.

Despite the increasing recognition of the importance of mixotrophy in planktonic communities, especially HABs (Jeong et al., 2005a,b; Burkholder et al., 2008; Flynn et al., 2013; Stoecker et al., 2017), modeling of plankton dynamics that incorporates mixotrophy is in its infancy (but see Thingstad et al., 1996; Stickney et al., 2000; Ward et al., 2011; Våge et al., 2013; Mitra et al., 2014; Berge et al., 2017;

Ghyoot et al., 2017). Most model approaches assume independence between phototrophic and phagotrophic regulations for simplicity purposes (e.g., Thingstad et al., 1996; Baretta-Bekker et al., 1998; Jost et al., 2004; Våge et al., 2013; Ward and Follows, 2016). The use of "perfect beast" model structure (Flynn and Mitra, 2009) integrates phototrophy vs. phagotrophy with feedback functions to better represent a nearly true of mixotrophic behaviors, especially for predicting rates of ingestion (Mitra and Flynn, 2010). Indeed, it has been increasingly recognized that the benefits of mixotrophy to cells are synergistic, not additive (e.g., Mitra and Flynn, 2010).

The temperature growth responses had added to the original "perfect beast" construct and thus allowed to explore scenarios of mixotrophic growth under varying nutrient and temperature conditions. The modeled scenarios highlighted several distinct differences in responses of *K. veneficum* as an autotroph and as a mixotroph in different nutrient and temperature conditions. Both autotrophic and mixotrophic *K. veneficum* attained much higher biomass in non-Redfieldian conditions compared to balanced nutrient growth. While the highest mixotrophic growth constant ($m\mu max^{het}$) for *K. veneficum* was attained for growth under Redfield conditions based on tuning from the experimental data (Table 5.2), this growth potential was unrealized in the subsequent model. Under both low N:P and high N:P *in silico* conditions, *K. veneficum* appeared to be more mixotrophic and attain higher biomass with increasing temperature, compared with growth under Redfield conditions or growth as an autotroph (Fig. 5.5). Under low N:P condition, temperature effects on mixotrophic growth rates of *K. veneficum* were also significant, with mixotrophic growth rates increasing faster than autotrophic growth rates at the highest temperature (i.e., 25 ^{o}C;

Fig. 5.5A). This growth stimulation may imply a higher demand for C from prey. These growth patterns support the notion that mixotrophy is likely to be greater under nutrient imbalanced conditions, that is, mixotrophy is not just a mechanism to acquire C, but also a mechanism by which nutrients are acquired (e.g., Glibert and Burkholder, 2011). For example, the assimilation efficiency (*mAEmin*) in the mixotrophs was the highest for those *K. veneficum* grown under low N:P conditions and mixed with prey in Redfield N:P conditions, indicating nutrient sources from ingested prey were required (Table 5.2). On the other hand, the cellular N:P of *K. veneficum* in high N:P conditions is low compared to the other nutrient conditions for this mixotroph (Fig. 5.7C). It is likely that feeding increased under P deficiency (high N:P conditions), and provided more P than was needed to maintain growth rates.

These results herein also suggest that under the warmest temperatures simulated, increased growth rates of prey could contribute to an increased growth of the mixotroph (Fig. 5.6). The growth rates of *R. salina* were higher than those of *K. veneficum* >20ºC, and thus prey availability increases faster at these temperatures. This situation may be enhanced in the environments that deviate from balanced nutrient proportions. For example, rates of ingestion are higher in conditions of high N:P *in silico* conditions (e.g., Mitra et al., 2014).

Outputs from these modeled scenarios have implications for growth of this HAB in eutrophic conditions in warming environments. In eutrophic estuaries such as Chesapeake Bay, there are large seasonal variations in nutrient loads and in their stoichiometry (e.g., Kemp et al., 2005; Li et al., 2015). A conceptual model was previously developed of summer blooms of *K. veneficum* in Chesapeake Bay that

incorporates the role of prey with a high N:P ratio originating from river inputs and a source inocula of *K. veneficum* from southern Bay waters with a lower N:P content (Lin et al., 2018). Nutrient inputs through tributaries are greatest during the high-flow period, typically starting through March to May. During this period, prey species can accumulate in the tributaries and are typically characterized by high N:P ratios due to disproportionate high N loading (Fisher, 1992; Kemp et al., 2005). The peak in summer *K. veneficum* blooms generally occurs 1–3 months later relative to these freshet inputs, in June through September (Li et al., 2015). Enhanced growth of *K. veneficum* derived from the oceanic end member of the Bay may be enhanced if it encounters prey originating from the tributaries with different patterns of nutrient loading.

With accelerating climate change in the future mean temperatures may rise by 2-6 ^{o}C by the end of the century in all seasons for Chesapeake Bay (Muhling et al., 2018). This may expand the growth windows for *K. veneficum* bloom in several ways. Prey availability may increase due to growth stimulation at higher temperatures. Also, recent Mid-Atlantic climate projections show that warming will likely increase current interannual variability, and that winter/spring increases in precipitation are likely (e.g., Najjar et al., 2010), bringing increased N and high N:P conditions with these flows. These wetter spring conditions, with more nutrients may lead to more N-rich prey that may further support the development of these HABs. As mixotrophs may be more temperature sensitive than their autotrophic prey, the increased temperatures could enhance their ingestion capabilities and effectively control the growth of autotrophic prey (e.g., Yang et al., 2016). The modeled biomass of *K.*

veneficum as a mixotroph was found to achieve the highest biomass when they consumed prey under high N:P conditions (Fig 5.5). Interestingly, the model suggests that while the highest biomass for *K. veneficum* is attained at 20^{o}C under high N:P, and falls off rapidly above 20^{o}C, under low N:P conditions, highest biomass is attained at 25^{o}C. These differing temperature responses raise important questions that warrant further exploration experimentally

Using models of mixotrophy, based on food uptake and photosynthesis measurements of *K. veneficum* and its congener, *K. arminger*, and assuming constant Redfield ratios, Berge et al. (2017) predicted succession of these species and their relative investments in autotrophy and phagotrophy. Their model suggested that nutrient uptake and high investments in photosynthesis would yield high autotrophic growth rates in spring, but increased phagotrophy in summer. In another recent model, Ghyoot et al. (2017) developed a flexible model in which a distinction was made between constitutive mixotrophs, those that synthesize and maintain their chloroplasts, and nonconstitutive mixtrophs, those that acquire chloroplasts. In eutrophic systems, such as Chesapeake Bay, where nutrients may be unbalanced, and where light may be limiting, constitutive mixotrophs, which includes *K. veneficum*, appear to be dominant in the warmer months. The next important step in mixotroph modeling will be to incorporate variable nutrient stoichiometry in a model of seasonal succession of both constitutive and nonconstitutive mixotrophs.

In conclusion, the current study expanded modeling of mixotrophic growth to conditions of variable stoichiometry and temperature. These simulations have highlighted the consideration of particulate prey in modeling HAB dynamics under

future warming; it is insufficient to only consider dissolved nutrients. A challenge for the application of this model will be many uncharacterized relationships between the growth of HAB species and their prey in response to multiple stressors that better represent future climate conditions in eutrophic waters. Although the current models are based only on bottom-up, nutrient conditions, and are focused on only one typical prey species without modeling the role of the toxic contents of *K. veneficum* in predation purpose (Sheng et al., 2010), they have provided some insight into the potential trend in HABs under future eutrophication and warming conditions.

References

Adolf, J.E., Bachvaroff, T., Place, A.R., 2008. Can cryptophyte abundance trigger toxic *Karlodinium veneficum* blooms in eutrophic estuaries? Harmful Algae 8(1), 119-128.

Adolf, J.E., Bachvaroff, T.R., Deeds, J.R., Place, A.R., 2015. Ichthyotoxic *Karlodinium veneficum* (Ballantine) J Larsen in the Upper Swan River Estuary (Western Australia): Ecological conditions leading to a fish kill. Harmful Algae 48, 83-93.

Anderson, D.M., Glibert, P.M., Burkholder, J.M., 2002. Harmful algal blooms and eutrophication: nutrient sources, composition, and consequences. Estuaries 25(4), 704-726.

Baretta-Bekker, J.G., Baretta, J.W., Hansen, A.S., Riemann, B., 1998. An improved model of carbon and nutrient dynamics in the microbial food web in marine enclosures. Aquat. Microb. Ecol. 14(1), 91-108.

Berge, T., Chakraborty, S., Hansen, P.J., Andersen, K.H., 2017. Modeling succession of key resource-harvesting traits of mixotrophic plankton. ISME J. 11(1), 212.

Braarud, T., 1957. A red water organism from Walvis Bay (*Gymnodinium galatheanum* n. sp.). Galathea Deep Sea Exped. 1, 137-138.

Burkholder, J.M., Glibert, P.M., Skelton, H.M., 2008. Mixotrophy, a major mode of nutrition for harmful algal species in eutrophic waters. Harmful Algae 8(1), 77-93.

Dai, X., Lu, D., Guan, W., Wang, H., He, P., Xia, P., Yang, H., 2013. Newly recorded *Karlodinium veneficum* dinoflagellate blooms in stratified water of the East China Sea. Deep Sea Res. II 101, 237-243.

Deeds, J.R., Terlizzi, D.E., Adolf, J.E., Stoecker, D.K., Place, A.R., 2002. Toxic activity from cultures of *Karlodinium micrum* (= *Gyrodinium galatheanum*)(Dinophyceae)—a dinoflagellate associated with fish mortalities in an estuarine aquaculture facility. Harmful Algae 1(2), 169-189.

Fisher, T.R., 1992. Nutrient limitation of phytoplankton in Chesapeake Bay. Mar. Ecol. Prog. Ser. 82, 51-63.

Flynn, K., Mitra, A., Glibert, P.M., Burkholder, J.M., 2018. Mixotrophy in HABs: by whom, on whom, when, why and what next, In: Glibert, P.M., Berdalet, E., Burford, M.A., Pitcher, G.C., Zhou, M. (Eds.), Global Ecology and Oceanography of Harmful Algal Blooms. Springer, In press, USA.

Flynn, K.J., 2005. Castles built on sand: dysfunctionality in plankton models and the inadequacy of dialogue between biologists and modellers. J. Plankt. Res. 27(12), 1205-1210.

Flynn, K.J., 2010. Do external resource ratios matter?: Implications for modelling eutrophication events and controlling harmful algal blooms. J. Mar. Syst. 83(3), 170-180.

Flynn, K.J., 2009. Going for the slow burn: why should possession of a low maximum growth rate be advantageous for microalgae? Plant Ecol. Divers. 2(2), 179-189.

Flynn, K.J., 2001. A mechanistic model for describing dynamic multi-nutrient, light, temperature interactions in phytoplankton. J. Plankt. Res. 23(9), 977-997.

Flynn, K.J., Hansen, P.J., 2013. Cutting the canopy to defeat the "selfish gene"; conflicting selection pressures for the integration of phototrophy in mixotrophic protists. Protist 164(6), 811-823.

Flynn, K.J., Mitra, A., 2009. Building the "perfect beast": modelling mixotrophic plankton. J. Plankt. Res. 31(9), 965-992.

Flynn, K.J., Stoecker, D.K., Mitra, A., Raven, J.A., Glibert, P.M., Hansen, P.J., Granéli, E., Burkholder, J.M., 2013. Misuse of the phytoplankton–zooplankton dichotomy: the need to assign organisms as mixotrophs within plankton functional types. J. Plankt. Res. 35(1), 3-11.

Fu, F.X., Tatters, A.O., Hutchins, D.A., 2012. Global change and the future of harmful algal blooms in the ocean. Mar. Ecol. Prog. Ser. 470, 207-233.

Ghyoot, C., Flynn, K.J., Mitra, A., Lancelot, C., Gypens, N., 2017. Modeling Plankton Mixotrophy: A Mechanistic Model Consistent with the Shuter-Type Biochemical Approach. Front. Ecol. Evol. 5, 78.

Glibert, P.M., Allen, J.I., Bouwman, A.F., Brown, C.W., Flynn, K.J., Lewitus, A.J., Madden, C.J., 2010. Modeling of HABs and eutrophication: status, advances, challenges. J. Mar. Syst. 83(3), 262-275.

Glibert, P.M., Burford, M.A., 2017. Globally changing nutrient loads and harmful algal blooms: Recent advances, new paradigms, and continuing challenges. Oceanogr. 30(1), 58-69.

Glibert, P.M., Burkholder, J.M., 2011. Harmful algal blooms and eutrophication:"strategies" for nutrient uptake and growth outside the Redfield comfort zone. Chin. J. Oceanol. Limnol. 29(4), 724-738.

Glibert, P.M., Burkholder, J.M., 2018. Causes of harmful algal blooms, In: Shumway, S., Burkholder, J.M., Morton, S.L. (Eds.), Harmful Algal Blooms: A Compendium Desk Reference. Wiley. In press, USA.

Glibert, P.M., Heil, C.A., F., W., C, D.R., 2018. Nutrient and HABs: dynamics kinetics and flexible nutrition, In: Glibert, P.M., Berdalet, E., Burford, M.A., Pitcher, G.C., Zhou, M. (Eds.), Global Ecology and Oceanography of Harmful Algal Blooms. Springer, In press, USA.

Glibert, P.M., Seitzinger, S., Heil, C.A., Burkholder, J.M., Parrow, M.W., Codispoti, L.A., Kelly, V., 2005. The role of eutrophication in the global proliferation of harmful algal blooms. Oceanogr. 18(2), 198-209.

Glibert, P.M., Terlizzi, D.E., 1999. Cooccurrence of elevated urea levels and dinoflagellate blooms in temperate estuarine aquaculture ponds. Appl. Environ. Microbiol. 65(12), 5594-5596.

Guillard, R.R., 1975. Culture of phytoplankton for feeding marine invertebrates, In: Smith, W.L., Chanley, M.H. (Eds.), Culture of Marine Invertebrate Animals. Plenum Press, New York, pp. 29-60.

Haefner, J.W., 2005. Modeling Biological Systems: Principles and Applications. Springer Science & Business Media.

Hallegraeff, G.M., 2010. Ocean climate change, phytoplankton community responses, and harmful algal blooms: a formidable predictive challenge[1]. J. Phycol. 46(2), 220-235.

Heisler, J., Glibert, P.M., Burkholder, J.M., Anderson, D.M., Cochlan, W., Dennison, W.C., Dortch, Q., Gobler, C.J., Heil, C.A., Humphries, E., 2008. Eutrophication and harmful algal blooms: a scientific consensus. Harmful algae 8(1), 3-13.

Jakobsen, H.H., Hansen, P.J., 1997. Prey size selection, grazing and growth response of the small heterotrophic dinoflagellate *Gymnodinium* sp. and the ciliate *Balanion comatum*—a comparative study. Mar. Ecol. Prog. Ser., 75-86.

Jeong, H.J., Park, J.Y., Nho, J.H., Park, M.O., Ha, J.H., Seong, K.A., Jeng, C., Seong, C.N., Lee, K.Y., Yih, W.H., 2005a. Feeding by red-tide dinoflagellates on the cyanobacterium *Synechococcus*. Aquat. Microb. Ecol. 41(2), 131-143.

Jeong, H.J., Yoo, Y.D., Park, J.Y., Song, J.Y., Kim, S.T., Lee, S.H., Kim, K.Y., Yih, W.H., 2005b. Feeding by phototrophic red-tide dinoflagellates: five species newly revealed and six species previously known to be mixotrophic. Aquat. Microb. Ecol. 40(2), 133-150.

John, E.H., Flynn, K.J., 2002. Modelling changes in paralytic shellfish toxin content of dinoflagellates in response to nitrogen and phosphorus supply. Mar. Ecol. Prog. Ser. 225, 147-160.

Jost, C., Lawrence, C.A., Campolongo, F., Van de Bund, W., Hill, S., DeAngelis, D.L., 2004. The effects of mixotrophy on the stability and dynamics of a simple planktonic food web model. Theor. Popul. Biol. 66(1), 37-51.

Kemp, W., Boynton, W., Adolf, J., Boesch, D., Boicourt, W., Brush, G., Cornwell, J., Fisher, T., Glibert, P., Hagy, J., 2005. Eutrophication of Chesapeake Bay: historical trends and ecological interactions. Mar. Ecol. Prog. Ser. 303(21), 1-29.

Kempton, J.W., Lewitus, A.J., Deeds, J.R., Law, J.M., Place, A.R., 2002. Toxicity of *Karlodinium micrum* (Dinophyceae) associated with a fish kill in a South Carolina brackish retention pond. Harmful Algae 1(2), 233-241.

Kimmance, S.A., Atkinson, D., Montagnes, D.J.S., 2006. Do temperature–food interactions matter? Responses of production and its components in the model heterotrophic flagellate *Oxyrrhis marina*. Aquat. Microb. Ecol. 42(1), 63-73.

Li, J., Glibert, P.M., Gao, Y., 2015. Temporal and spatial changes in Chesapeake Bay water quality and relationships to *Prorocentrum minimum*, *Karlodinium veneficum*, and CyanoHAB events, 1991–2008. Harmful Algae 42, 1-14.

Lin, C.-H., Accoroni, S., Glibert, P.M., 2017. *Karlodinium veneficum* feeding responses and effects on larvae of the eastern oyster *Crassostrea virginica* under variable nitrogen: phosphorus stoichiometry. Aquat. Microb. Ecol. 79(2), 101-114.

Lin, C.-H., Glibert, P.M., Mixotrophy with multiple prey species measured with a multiwavelength-excitation PAM fluorometer: case study of *Karlodinium veneficum* J. Plankt. Res., submitted.

Lin, C.-H., Lyubchich, V., Glibert, P.M., 2018. Time series models of decadal trends in the harmful algal species *Karlodinium veneficum* in Chesapeake Bay Harmful Algae 73(C), 110-118.

Lundgren, V.M., Glibert, P.M., Granéli, E., Vidyarathna, N.K., Fiori, E., Ou, L., Flynn, K.J., Mitra, A., Stoecker, D.K., Hansen, P.J., 2016. Metabolic and physiological changes in *Prymnesium parvum* when grown under, and grazing on prey of, variable nitrogen: phosphorus stoichiometry. Harmful Algae 55, 1-12.

Menden-Deuer, S., Lessard, E.J., 2000. Carbon to volume relationships for dinoflagellates, diatoms, and other protist plankton. Limnol. Oceanogr. 45(3), 569-579.

Mitra, A., 2006. A multi-nutrient model for the description of stoichiometric modulation of predation in micro-and mesozooplankton. J. Plankt. Res. 28(6), 597-611.

Mitra, A., Flynn, K.J., 2005. Predator–prey interactions: is 'ecological stoichiometry'sufficient when good food goes bad? J. Plankt. Res. 27(5), 393-399.

Mitra, A., Flynn, K.J., 2010. Modelling mixotrophy in harmful algal blooms: More or less the sum of the parts? J. Mar. Syst. 83(3), 158-169.

Mitra, A., Flynn, K.J., 2006. Accounting for variation in prey selectivity by zooplankton. Ecol. Modell. 199(1), 82-92.

Mitra, A., Flynn, K.J., Burkholder, J., Berge, T., Calbet, A., Raven, J.A., Granéli, E., Glibert, P.M., Hansen, P.J., Stoecker, D.K., 2014. The role of mixotrophic protists in the biological carbon pump. Biogeosciences 10(8), 13535-13562.

Mitra, A., Flynn, K.J., Tillmann, U., Raven, J.A., Caron, D., Stoecker, D.K., Not, F., Hansen, P.J., Hallegraeff, G., Sanders, R., 2016. Defining planktonic protist functional groups on mechanisms for energy and nutrient acquisition: incorporation of diverse mixotrophic strategies. Protist 167(2), 106-120.

Montagnes, D.J.S., Kimmance, S.A., Atkinson, D., 2003. Using Q10: Can growth rates increase linearly with temperature? Aquat. Microb. Ecol. 32(3), 307-313.

Moore, S.K., Johnstone, J.A., Banas, N.S., Salathe Jr, E.P., 2015. Present-day and future climate pathways affecting *Alexandrium* blooms in Puget Sound, WA, USA. Harmful Algae 48, 1-11.

Muhling, B.A., Gaitán, C.F., Stock, C.A., Saba, V.S., Tommasi, D., Dixon, K.W., 2018. Potential salinity and temperature futures for the Chesapeake Bay using a statistical downscaling spatial disaggregation framework. Estuar. Coast. 41(2), 349-372.

Najjar, R.G., Pyke, C.R., Adams, M.B., Breitburg, D., Hershner, C., Kemp, M., Howarth, R., Mulholland, M.R., Paolisso, M., Secor, D., 2010. Potential climate-change impacts on the Chesapeake Bay. Estuar. Coast. Shelf. Sci. 86(1), 1-20.

Nielsen, M.V., 1993. Toxic effect of the marine dinoflagellate *Gymnodinium galatheanum* on juvenile cod Gadus morhua. Mar. Ecol. Prog. Ser., 273-277.

Place, A.R., Bowers, H.A., Bachvaroff, T.R., Adolf, J.E., Deeds, J.R., Sheng, J., 2012. *Karlodinium veneficum* —The little dinoflagellate with a big bite. Harmful Algae 14, 179-195.

Sheng, J., Malkiel, E., Katz, J., Adolf, J.E., Place, A.R., 2010. A dinoflagellate exploits toxins to immobilize prey prior to ingestion. Proc. Natl. Acad. Sci. 107(5), 2082-2087.

Stickney, H.L., Hood, R.R., Stoecker, D.K., 2000. The impact of mixotrophy on planktonic marine ecosystems. Ecol. Modell. 125(2-3), 203-230.

Stoecker, D.K., Adolf, J.E., Place, A.R., Glibert, P.M., Meritt, D.W., 2008. Effects of the dinoflagellates *Karlodinium veneficum* and *Prorocentrum minimum* on early life history stages of the eastern oyster (*Crassostrea virginica*). Mar. Biol. 154(1), 81-90.

Stoecker, D.K., Hansen, P.J., Caron, D.A., Mitra, A., 2017. Mixotrophy in the marine plankton. Annu. Rev. Mar. Sci. 9, 311-335.

Thingstad, T.F., Havskum, H., Garde, K., Riemann, B., 1996. On the strategy of" eating your competitor": A mathematical analysis of algal mixotrophy. Ecology 77(7), 2108-2118.

Våge, S., Castellani, M., Giske, J., Thingstad, T.F., 2013. Successful strategies in size structured mixotrophic food webs. Aquat. Ecol. 47(3), 329-347.

Van Dolah, F.M., 2000. Marine algal toxins: origins, health effects, and their increased occurrence. Environ. Health Perspect. 108, 133.

Ward, B.A., Dutkiewicz, S., Barton, A.D., Follows, M.J., 2011. Biophysical aspects of resource acquisition and competition in algal mixotrophs. Am. Nat. 178(1), 98-112.

Ward, B.A., Follows, M.J., 2016. Marine mixotrophy increases trophic transfer efficiency, mean organism size, and vertical carbon flux. Proc. Natl. Acad. Sci. 113(11), 2958-2963.

Wells, M.L., Trainer, V.L., Smayda, T.J., Karlson, B.S.O., Trick, C.G., Kudela, R.M., Ishikawa, A., Bernard, S., Wulff, A., Anderson, D.M., 2015. Harmful algal blooms and climate change: Learning from the past and present to forecast the future. Harmful Algae 49, 68-93.

Wilken, S., Huisman, J., Naus-Wiezer, S., Donk, E., 2013. Mixotrophic organisms become more heterotrophic with rising temperature. Ecol. Lett. 16(2), 225-233.

Yang, Z., Zhang, L., Zhu, X., Wang, J., Montagnes, D.J.S., 2016. An evidence-based framework for predicting the impact of differing autotroph-heterotroph thermal sensitivities on consumer–prey dynamics. ISME J. 10, 1767-1778.

Zhou, C., Fernández, N., Chen, H., You, Y., Yan, X., 2011. Toxicological studies of *Karlodinium micrum* (Dinophyceae) isolated from East China Sea. Toxicon 57(1), 9-18.

Tables

Table 5. 1. Autotrophic state constants that were calculated and gained from tuning against changes in experimental monoculture cultures of *Rhodomonas salina* and *Karlodinium veneficum*. Autotrophic growth rate of *K. veneficum* was not tuned here (ND; but see also Table 5.2).

Parameters	Units	*Rhodomonas salina*		*Karlodinium veneficun*		Sources
		Abbr.	Values	Abbr.	Values	
Half saturation for NO_3^- transport	μg N l^{-1}	aK_{Ni}	57.437	mK_{Ni}	14.628	Tuned herein
Half saturation for PO_4^{3-} transport	μg P l^{-1}	aK_P	1.550	mK_P	118.490	Tuned herein
Chl-specific initial slope to PI curve (α)	($m^2 g^{-1}$ chl *a*)(mgC μmol photon^{-1})	$a\alpha^{Chl}$	0.192	$m\alpha^{Chl}$	0.011	Lin and Glibert submitted
Maximum N:C	gN gC^{-1}	*aNCmax*	0.180	*mNCmax*	0.300	Calculated herein
Minimum N:C	gN gC^{-1}	*aNCmin*	0.010	*mNCmin*	0.005	Calculated herein
Maximum P:C	gP gC^{-1}	*aPCmax*	0.020	*mPCmax*	0.020	Calculated herein
Minimum P:C	gP gC^{-1}	*aPCmin*	0.005	*mPCmin*	0.001	Calculated herein
Maximum rate of phototrophic growth	d^{-1}	$a\mu max^{phot}$	1.280	$m\mu max^{pho}$	ND	Tuned herein

Table 5. 2. Heterotrophic state constants obtained from tuning the "perfect beast" model of Flynn and Mitra (2009) against experimentally derived changes in carbon biomass in mixed cultures of *Karlodinium veneficum* (mixotroph) with *Rhodomonas salina* (prey) when each was grown in different N:P condition (low NP= 4, Redfield = 16, and high N:P= 32 on a molar basis) and combined in 9 combinations.

Parameters	Models of mixotroph		
	Low-NP prey	Redfield-NP prey	High-NP prey
Low-NP *K. veneficum*			
mAEmin	0.658	0.840	0.814
mcap_a	0.050	0.050	0.050
mKas	0.999	0.835	0.647
mKIng	0.490	0.295	0.204
$m\mu max^{phot}$	0.200	0.400	0.400
$m\mu max^{het}$	0.450	0.477	0.504
Redfield-NP *K. veneficum*			
mAEmin	0.743	0.370	0.736
mcap_a	0.050	0.050	0.050
mKas	0.010	0.840	0.997
mKIng	0.086	0.551	0.464
$m\mu max^{phot}$	0.200	0.400	0.400
$m\mu max^{het}$	0.451	0.887	0.842
High-NP *K. veneficum*			
mAEmin	0.537	0.821	0.832
mcap_a	0.163	0.050	0.050
mKas	0.363	0.450	0.720
mKIng	0.010	0.296	0.309
$m\mu max^{phot}$	0.200	0.400	0.400
$m\mu max^{het}$	0.545	0.501	0.759

mAEmin: minimum assimilation efficiency; *mcap_a*: the likelihood of ingestion following encounter; *mKas*: mixotroph half saturation for digestion rate; *mKIng*: mixotroph half saturation for ingestion; $m\mu max^{phot}$: mixotroph maximum rate of phototrophic growth; $m\mu max^{het}$: mixotroph maximum rate of heterotrophic growth.

Figures

Fig. 5. 1. Schematic diagram to illustrate the steps taken to determine the constants required for development of the "perfect beast" model of mixotrophy of *Karlodinium veneficum* and its application under varying nutrient conditions and increasing temperature.

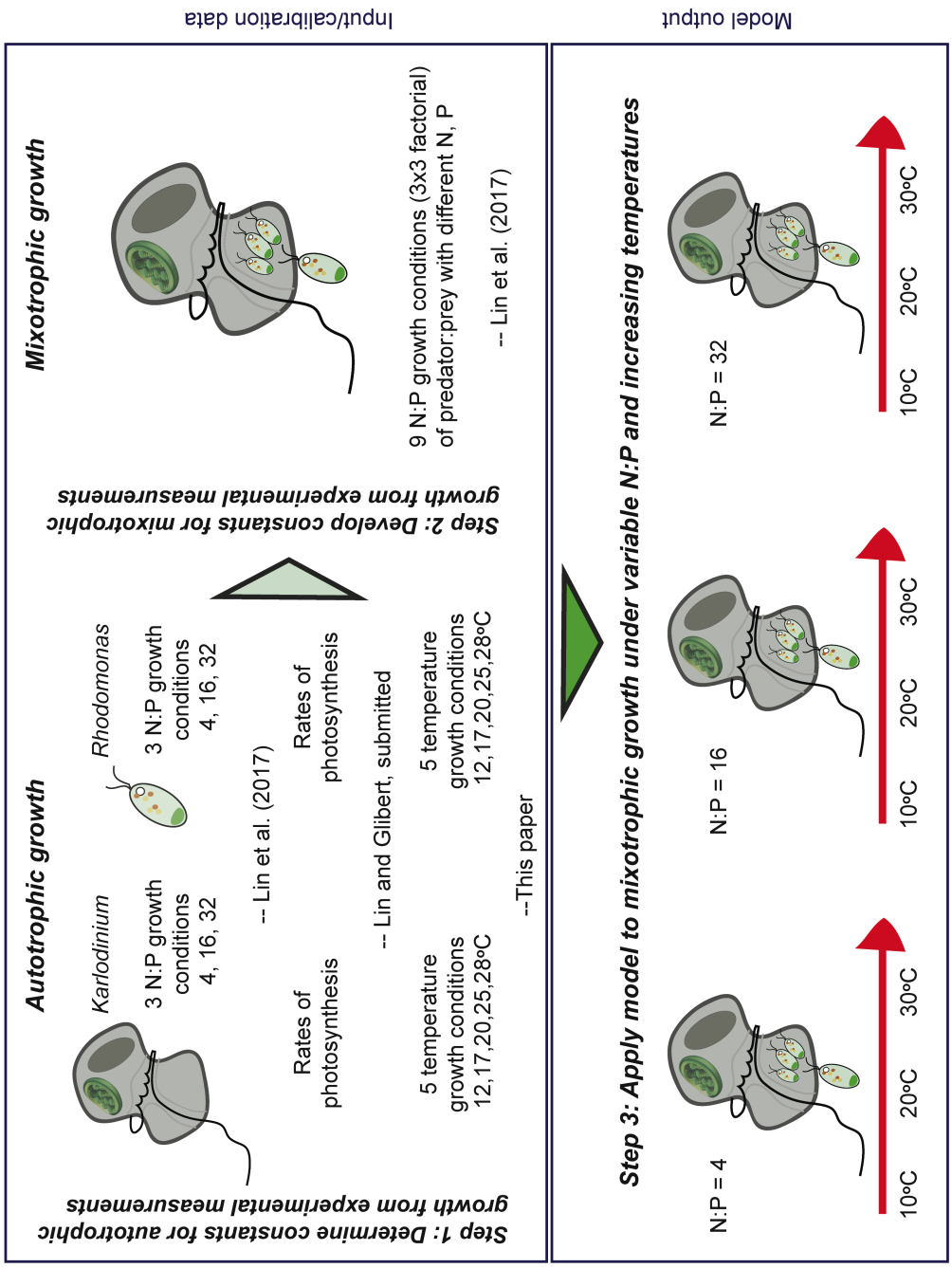

Fig. 5. 2. Schematic of the structure of the "perfect beast" model, showing major flows in and out of state variables (solid arrows and boxes) from the external parameters (NO_3^-, PO_4^{3-} and Light), and the major feedback processes (dashed arrows). Autotrophic growth uses inorganic nutrients and light via the photosystems of the mixotroph (phototrophy; white part). A proportion of activity leading to growth is required to support synthesis of those photosystems. Predation brings algal prey into the food vacuole within the confines of the mixotroph cell (heterotrophy; gray part). Interactions between phototrophic and heterotrophic nutrition (Int1) influence the growth of the mixotrophy (Flynn and Mitra 2009). The state variables (yellow boxes) that describe carbon (C), nitrogen (N), phosphorus (P) and chlorophyll (Chl) associated with core mixotroph biomass are mC (C-biomass of the mixotroph), ChlC (chlorophyll C quota), NC (cellular NC quota) and PC (cellular PC quota), while the same constituents (green boxes) associated with the content of food vacuole are FC (food vacuole C content relative to mC), FChlC (food vacuole Chl content relative to mC), FNC (food vacuole N content relative to mC) and FPC (food vacuole P content relative to mC).

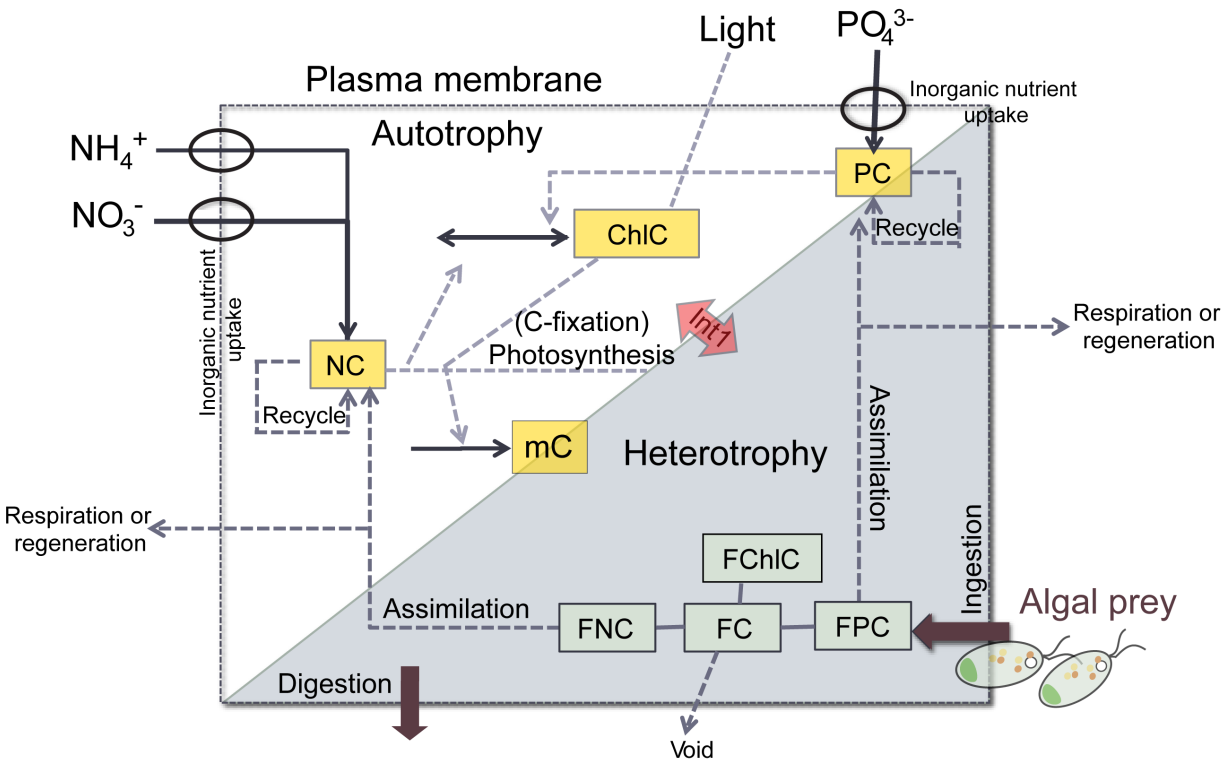
Light
PO_4^{3-}
Plasma membrane
Inorganic nutrient uptake
Autotrophy
NH_4^+
NO_3^-
PC
ChlC
Recycle
Inorganic nutrient uptake
(C-fixation)
Photosynthesis
Int1
Respiration or regeneration
NC
Recycle
mC
Heterotrophy
Assimilation
Respiration or regeneration
FChlC
Ingestion
Algal prey
Assimilation
FNC
FC
FPC
Digestion
Void

Fig. 5. 3. Effect of temperature on cell-specific, autotrophic growth rates (μ_{max}^{phot}; d^{-1}) of *Karlodinium veneficum* and *Rhodomonas salina*.

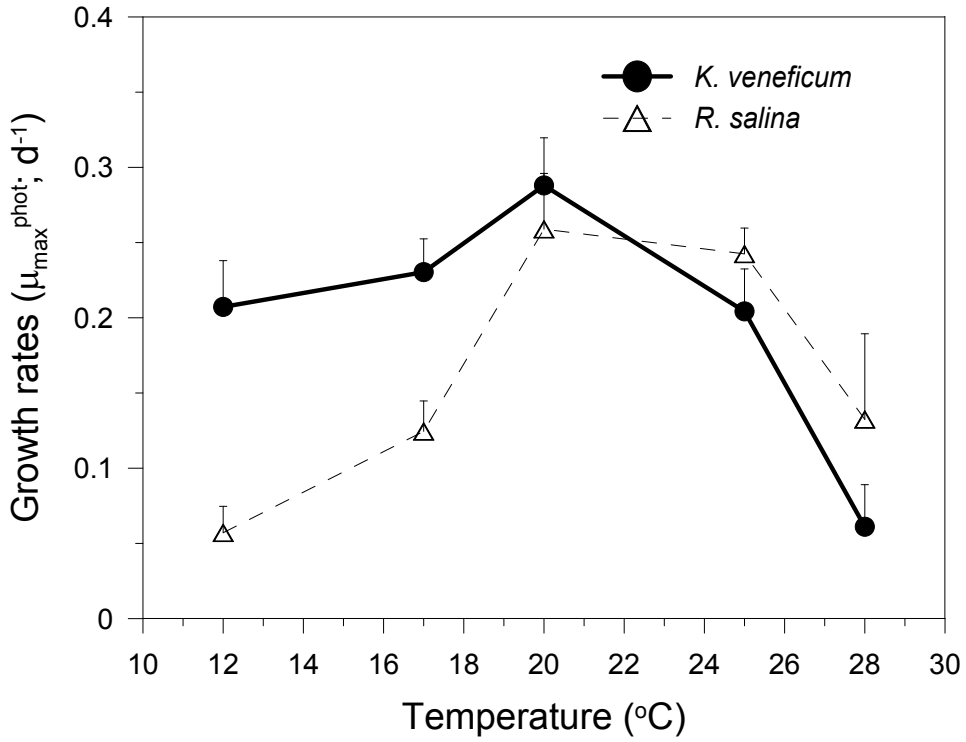

Fig. 5. 4. Fits of the "perfect beast" model (lines) to experimental data (symbols) for carbon biomass from 9 mixed-culture systems. The low-NP *Karlodinium veneficum* (A,B,C), Redfield-NP *K. veneficum* (D,E,F) and high-NP *K. veneficum* (G,H,I) provided with low-NP, Redfield-NP and high-NP prey *Rhodomonas salina* during mixed-culture experiments, respectively. N: nitrogen; P: phosphorus. R^2 coefficients are determined for the predator and prey under varying nutrient conditions.

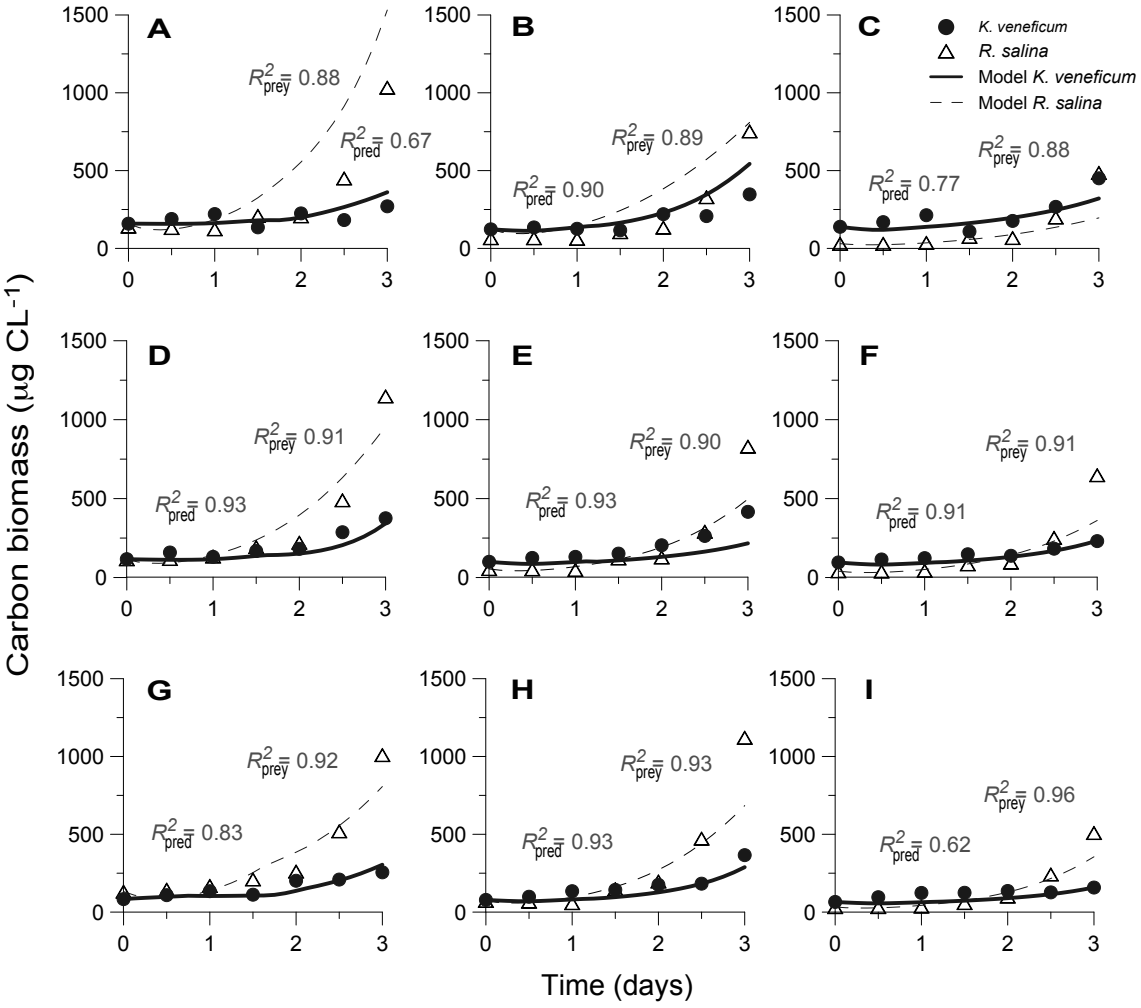

Fig. 5. 5. Modeled changes in carbon biomass of *Karlodinium veneficum* in mixotrophic (A,B,C) and autotrophic (D,E,F) growth under low N:P (=4), Redfield N:P (=16) and high N:P (=32) conditions, and variable temperature conditions over 10-day simulations.

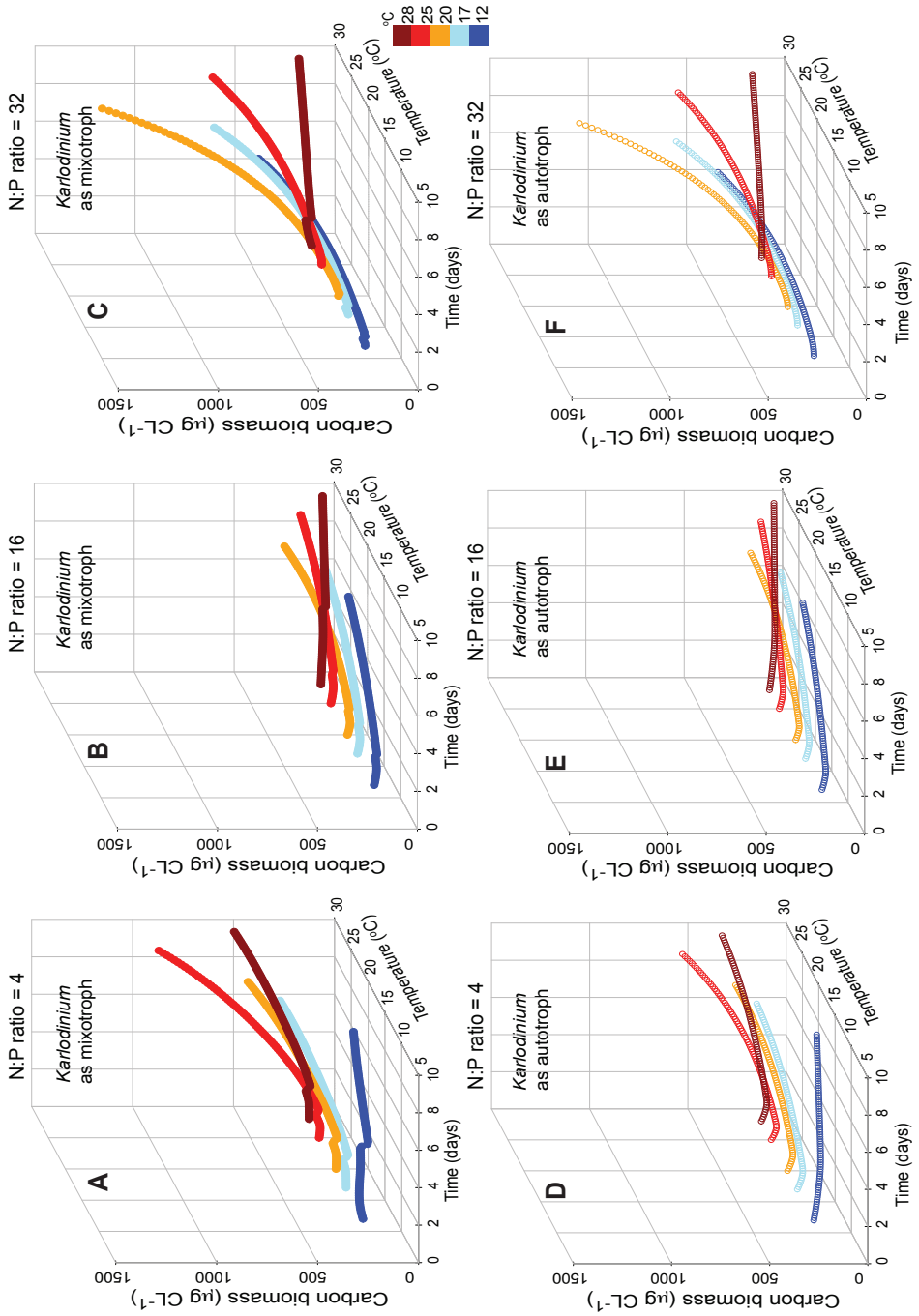

Fig. 5. 6. Modeled changes in carbon biomass of prey *Rhodomonas salina* with *Karlodinium veneficum* as predator (A,B,C) and without predator (D,E,F) under low N:P (=4), Redfield N:P (=16) and high N:P (=32) conditions, and variable temperature conditions over 10-day simulations.

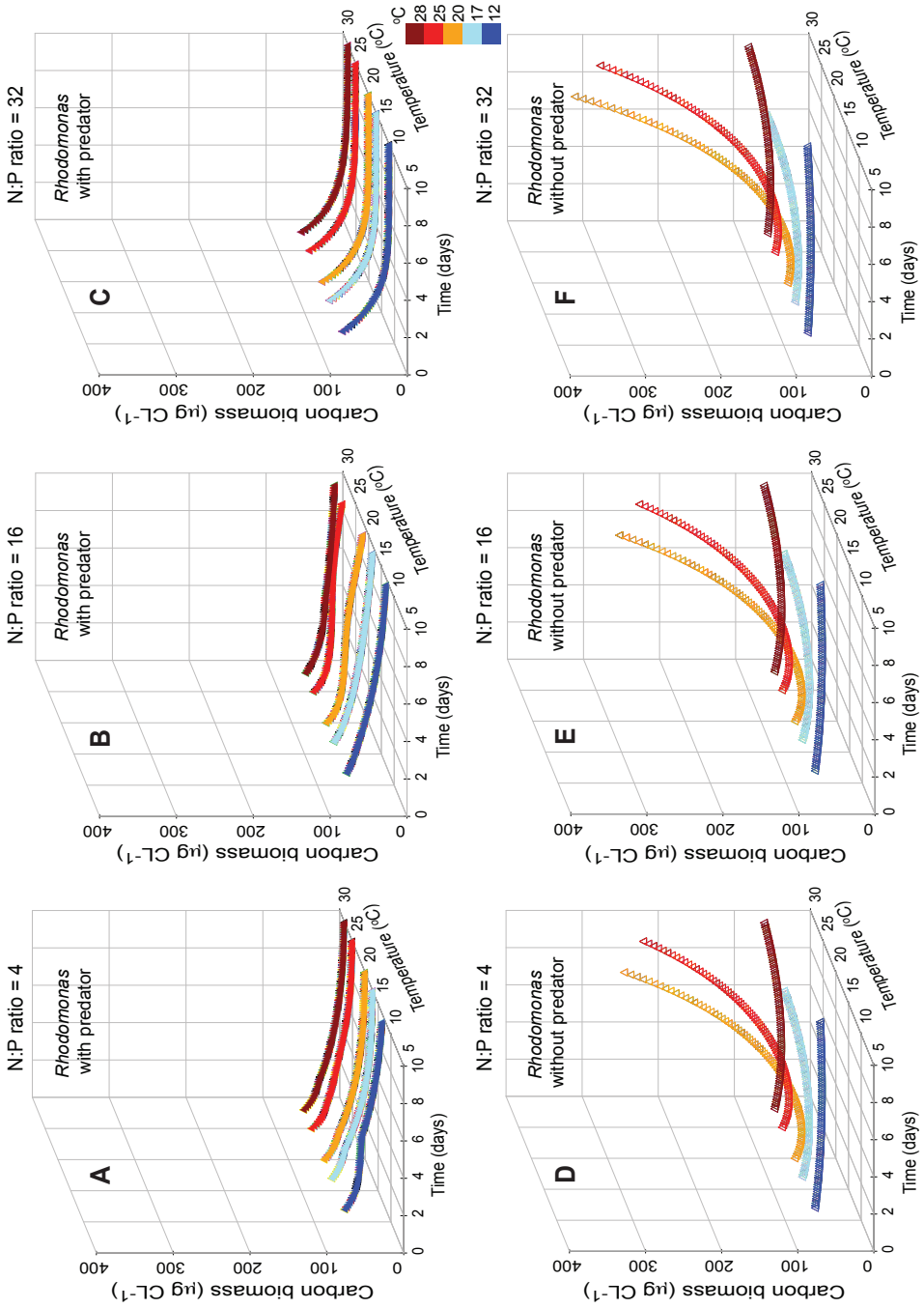

Fig. 5. 7. Modeled changes in cellular N:P ratio of *Karlodinium veneficum* in mixotrophic (A,B,C) and autotrophic (D,E,F) growth under low N:P (=4), Redfield N:P (=16) and high N:P (=32) conditions, and variable temperature conditions over 10-day simulations.

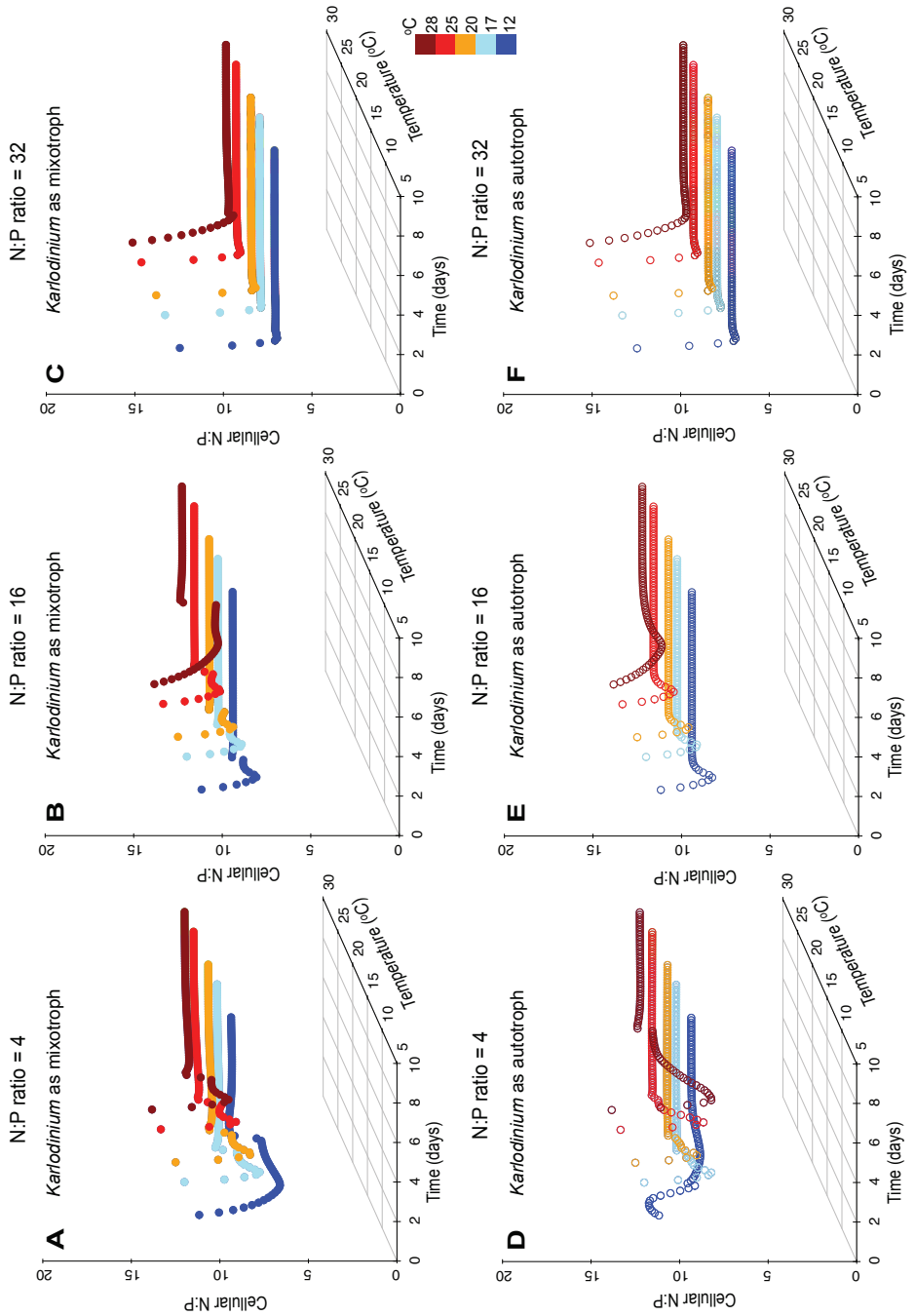

Appendix II: Supplemental Material Chapter 5

Model description

The model is derived from the 'perfect beast' model of Flynn and Mitra (2009), which describes carbon-nitrogen-phosphorus(C-N-P) -based interactions within a mixotroph cell, and which builds upon the variable stoichiometric zooplankton model of Mitra (2006) and the photosynthesis model of Flynn (2001). The explanation and documentation herein is based largely on that provided by Flynn and Mitra (2009). The construct has eight state variables (Fig. 5.2) describing C, N and P and chlorophyll (Chl) associated with the core mixotroph (m) biomass (mC, NC, PC, ChlC) and also the same constituents associated with the contents of the food (F) vacuole (namely, FC, FNC, FPC and FChlC) after the mixotroph have fed on algal prey. The amount of material associated with the food vacuole is relative to the core mC biomass. Thus, the total C associated with the mixotroph is mC·(1+FC) with the unit of gC L^{-1}. Equations related to the output of these state variables are described as follows:

$$\frac{dmC}{dt} = C\ fixation + C\ assimilation - C\ respiration - C\ void \quad (1)$$

$$\frac{dXC}{dt} = Inorganic\ X\ uptake + X\ assimilation - X\ regeneration - X\ void \quad (2)$$

$$\frac{dChlC}{dt} = f\{C\ demand\} - f\{C\ excess\} \quad (3)$$

$$\frac{dFW}{dt} = W\ ingestion - W\ digestion \tag{4}$$

In equation (2), X is either N or P; in equation (4), W is C, N, P or Chl in the food vacuole as a ratio to mC-biomass (Fig. 5.2); f is the function term.

As rectangular hyperbolic and normalized sigmoidal functions are frequently used to provide feedback response curves, such a function here, in the form of equation (5), allows different responses factors by simply changing K and H. This allows for the use of integration steps and feedback functions without changing entire model code. S is a quotient that modifies the function process, K is a half-saturation constant, H is the Hill number (which controls the shape of the sigmoidal curve; for example, a value of $H = 1$ returning a rectangular hyperbolic form) and RF is the response factor quotient.

$$RF = \frac{\left((1+K^H)\cdot S^H\right)}{S^H+K^H} \tag{5}$$

The quotients *mXCu* and *aXCu* are used to describe the nutrient status of the mixotroph and prey, respectively (equations 6a,b). The minimum and maximum quota values (*mXCmin, mXCmax*) or (*aXCmin, aXCmax*) control the growth rate. Constant *mKQx* (either mKQ_N or mKQ_P) or *aKQx* (either aKQ_N or aKQ_P) affect the shape of the relationship between *mXC* or *aXC* and the resultant quotient *mXCu* or *aXCu*. mKQ_N and aKQ_N is given a value of 10, giving a near-linear response curve, while mKQ_P and aKQ_P is 1, returning a sharp rectangular hyperbola (Table AII.1).

$$mXCu = \frac{(1+mKQx)\cdot(mXC-mXCmin)}{(mXC-mXCmin) + mKQx\cdot(mXCmax-mXCmin)} \tag{6a}$$

$$aXCu = \frac{(1+aKQx)\cdot(aXC-aXCmin)}{(aXC-aXCmin) + aKQx \cdot (aXCmax-aXCmin)} \quad (6b)$$

For controlling the interaction between N and P stress, the normalized quotas are combined to give the quotient *mNPCu* or *aNPCu*, which represents the nutrient status for the mixotroph [equation 7(a)] and prey [equation 7(b)], respectively.

$$mNPCu = MIN(mNCu, mPCu) \quad (7a)$$

$$aNPCu = MIN(aNCu, aPCu) \quad (7b)$$

Photosynthesis

The maximum rate of C-fixation [*mPqmax*, equation (8) for the mixotroph and *aPqmax*, equation (8b) for the prey] is a function of their individual nutrient status [*mNPCu*; equation (7a) for the mixotroph and *aNPCu*; equation (7b) for the prey]. The basis of this equation is the rate of C fixation needed to cover the costs of basal respiration (*mBR* or *aBR*) and of respiration associated with growth at the maximum N:C (*mNCmax* or *aNCmax*), the reduction of NO_3^- to NH_4^+ (*redco*) and the subsequent amino acid synthesis (*mAAsyn* or *aAAsyn*), to support a maximum phototrophic growth ($m\mu max^{phot}$ or $a\mu max^{phot}$).

$$mPqmax = \Big(m\mu max^{phot} + mBR + mNCmax \cdot m\mu max^{phot}(redco + mAAsyn)\Big) \cdot mNPCu \quad (8a)$$

$$aPqmax = \Big(a\mu max^{phot} + aBR + aNCmax \cdot a\mu max^{phot}(redco + aAAsyn)\Big) \cdot aNPCu \quad (8b)$$

The rate of photosynthesis rate within the mixotroph is the sum of its own photosynthesis (*PS*) and that potentially performed by ingested photosystems (*FPS*). The calculations are given in equation (9a,b) and computed separately by using their photosystem sizes relatively to core mixotroph (i.e., *ChlC* and *FChlC)*, initial PE-curves slopes of predator and prey ($m\alpha^{Chl}$ and $a\alpha^{Chl}$), maximal rate of C-fixation (*mPqmax* and *aPqmax*) and photon flux density (*PFD*; μmol photon $m^{-2}s^{-1}$).

$$PS = mPqmax \cdot TanH \cdot \left(m\alpha^{Chl} \cdot PFD \cdot \frac{ChlC}{mPqmax}\right) \quad (9a)$$

$$FPS = aPqmax \cdot TanH \cdot \left(a\alpha^{Chl} \cdot PFD \cdot \frac{FChlC}{aPqmax}\right) \quad (9b)$$

Total photosynthesis rate, PS_{Tot}, the sum of *PS* and *FPS*, is therefore:

$$PS_{Tot} = PS + FPS \quad (10)$$

The photosystems within captured prey are assumed not to be able to photoacclimate. The maximal value of Chl:C for photosystems associated with ingested prey is held fixed at the values of the ingested material. Photoacclimation is regulated by the mixotroph's photosystems, and modeled as its C input rate (equation 11). There is an additive interaction (*Smix* = 1) between phototrophy and heterotrophy in the model, but C entering from heterotrophy [C assimilation; *mCas* in equation (27)] has no effect on the operation of the core photosynthetic activity. The synthesis of *ChlC* is related to the rate of total C input, as defined by equation (12). Without considering sharing the cell volume between photosystems and food vacuole (*Svol* = 0), the model then sets *ChlCmax* = *ChlCabs*.

$$mC_{in} = PS_{Tot} + mC_{as} \cdot \ (Smix = 1) \qquad (11)$$

$$\frac{dChlC}{dt} =$$

$$ChlCmax \cdot mNPCu \ \cdot M \ \cdot \ m\mu max^{phot} \cdot \left(1 - MIN\left(1, \frac{mC_{in}}{mPqmax}\right)\right)^{0.5} \cdot$$

$$\frac{(1+0.05)\times\left(1-\frac{ChlC}{ChlCmax}\right)}{\left(1-\frac{ChlC}{ChlCmax}\right)+0.05} - ChlC \ \cdot (\mu + (1 - mNCu) \cdot \ m\mu max^{phot})$$

(12)

Ingestion and digestion of prey C

The ingestion and digestion of prey are controlled by the demand for heterotrophic nutrition relative to the maximum rate of growth ($m\mu max^{het}$). If $m\mu max^{het}$ is in excess of $m\mu max^{phot}$, then demand exists. In the model, the demand for heterotrophy affects the current maximum size of the food vacuole, *FCmax*, which is a value between the minimum (*FCmin*) and absolute maximum values (*FCabs*). While the model considers an additive interaction between phototrophic and heterotrophic nutrition (*Smix* =1), the setting of *FCmax* is equal to *FCabs*.

Prey capture (*Cpi*) is a function of prey availability (*aC*; prey carbon biomass) through equation (13). The constant *surge* (= 3) is used to enable ingestion to be greater than that required for the simulations. This is restricted in the model to a rate equal to three times the maximum growth rate ($m\mu max^{het}$).

$$Cpi = MIN\ (aC \cdot Cri, surge \cdot m\mu max^{het}) \qquad (13)$$

The rate of ingestion is down-regulated by the level of food vacuole satiation, FC_{relV}, given by equation (14). Ingestion [*IgC*; equation (15)] into the food vacuole (*FC*) is then controlled through a normalized sigmoidal feedback function from the level of FC_{relV}.

$$FC_{relV} = \frac{FC}{FCmax} \qquad (14)$$

$$IgC = Cpi \cdot \frac{\left((1+mK_{Ing}{}^{mHIng}) \cdot (1-FC_{relV})^{mHIng}\right)}{(1-FC_{relV})^{mHIng} + mK_{Ing}{}^{mHIng}} \qquad (15)$$

The rate of digestion is a function of C-demand through the control of $mPbal_{Con}$ [equation (18)]. The quotient $mPbal_{Con}$ is used to ensure that a critical proportion of total C entering the system is derived from photosynthesis. *mPbal* in equation (16) determines the contribution of total photosynthesis (PS_{Tot}) relative to the 24 h averaged growth rate (μ_{avg}), reflecting the expected development lag. The value of $mPbal_{Con}$ is set by the normalized sigmoidal function of *Bal*; this rapidly enables digestion of material from the food vacuole once $mPbal > mPbal_{crit}$.

$$mPbal = MIN\left(1, \frac{PS_{Tot}}{\mu_{avg}}\right) \cdot \left(\mu_{\text{avg}} > 0\right) \qquad (16)$$

$$Bal = (mPbal > mPbacl_{crit}) \cdot \frac{(mPbal - mPbal_{crit})}{(1 - mPbal_{crit})} \qquad (17)$$

$$mPbal_{Con} = (mPbacl_{crit} = 0) + (mPbacl_{crit} > 0)$$

$$\cdot \frac{\left((1+mK_{pbal}{}^{mHpbal})\cdot Bal^{mHpbal}\right)}{(Bal^{mHpbal}+mK_{pbal}{}^{mHpbal})} \quad (18)$$

The maximum digestion rates, *Dmax* [equation (19)], is set to enable the maximum growth rate to be attained when operating with an assimilation efficiency of *mAE*, a metabolic cost of *mMR*, and a basal respiration rate of *mBR*.

$$Dmax = \frac{(\mu_{max} + mBR)}{mAE \cdot (1 - mMR)} \quad (19)$$

The maximal digestion of material and the rate of removal of C from the food vacuole are then set by *DgC* [equation (20)]. This is determined by $mPbal_{Con}$ [equation (18)], *Dmax* [equation (19)] and a normalized sigmoidal function of the concentration of material in the food vacuole ($FC_{relA} = FC/FCabs$).

$$DgC = mPbal_{Con} \cdot Dmax \cdot \frac{\left((1+mK_{as}{}^{mHas})\cdot FC_{relA}{}^{mHas}\right)}{FC_{relA}{}^{mHas}+mK_{as}{}^{mHas}} \quad (20)$$

Changes in the size of the food vacuole are given by equation (21). The digestion of kleptochloroplastic material (*FChlC*) is assumed to occur with the digestion of other prey C so that the value of captured prey Chl:C remains the same during digestion. Equation (22a) describes the rate of change of kleptochloroplastic Chl.

$$\frac{dFC}{dt} = IgC - DgC \quad (21)$$

$$\frac{dFChlC}{dt} = aChlC \cdot lgC - FChlC \cdot \frac{DgC}{FC} \quad (22a)$$

The definition of changes in the X:C (i.e., N:C and P:C) of material in the food vacuole given in equation (22b) is similar to equation (22a); prey N:C (*aNC*) or P:C (*aPC*) for *aChlC*, and *FNC* or *FPC* for *FChlC* are substituted in equation (22a).

$$\frac{dFXC}{dt} = aXC \cdot lgC - FXC \cdot \frac{\mathrm{DgC}}{\mathrm{FC}} \quad (22b)$$

Assimilation of ingested C

Prey assimilation is based on the stoichiometric value of the prey, through the description of food quality within *FC* relative to the optimal core mixotroph values [equation (23)]; the assimilation efficiency (*mAE*) declines as food N:C and P:C declines. The description operates through two ways. First, a simple linear relationship with stoichiometric food quality is set via equation (23). Second, an additional relationship is used to reflect the fact that decreased food quality is often related to other chemical changes, such as the presence of toxins and other second metabolites. This latter relationship is governed by the value of mK_{ec} (= 10) in equation (24). In addition, *mAE* may decline if there is an excess of food; this condition is described by equation (25) using a normalized sigmoidal function, which is disabled by setting $mK_{eq} = 10^{-6}$.

$$MINup = MIN\left(\frac{FNC}{mNCmax}, \frac{FPC}{mPCmax}, 1\right) \quad (23)$$

$$mAE_{qual} = mAE_{min} + (mAE_{max} - mAE_{min}) \cdot \frac{(1+mK_{ec}) \cdot MINup}{MINup + mK_{ec}} \quad (24)$$

$$mAE_{quan} = (mK_{eq} > 10^{-6}) \cdot \left(mAE_{min} + (mAE_{max} - mAE_{min}) \times \frac{(1 + mK_{ec}) \cdot MINup}{MINup + mK_{ec}} \right) + (mK_{eq} = 10^{-6}) \cdot mAE_{max} \quad (25)$$

The operational value of *mAE* is set by equation (26) and the net result is that the available proportion of material within the feeding vacuole is ultimately assimilated into the core mixotroph biomass [*mCas*, equation (27)].

$$mAE = MINup \cdot MIN(mAE_{qual}, mAE_{quan}) \quad (26)$$

$$mCas = mAE \cdot DgC \quad (27)$$

Assimilation of N and P

Inorganic N gets into the mixotroph as NO_3^- and/or NH_4^+. The interaction of these assimilations is computed by reference to their potential transport rates, based on *f*-ratio (*frat* = ratio of NO_3^- assimilation: total inorganic N assimilation). Equation (28) demonstrates the maximum required N uptake rate to support growth at a maximum rate of $m\mu max^{phot}$, at which *NC* = *mNCmax* is required. Equations (29) and (30) give the potential transport rates of NH_4^+ and NO_3^-, respectively, without any interaction. That is, there is no term for repression of NO_3^- by NH_4^+. The value of $Pref_X$ in equation (29) and (30) is similar to a measure of *surge* uptake, that defines transport capability to be greater than that required to meet maximal steady-state demand. The rates considering the interaction are given by equation (31) and (32); the

uptake of NO_3^- occurs only if NH_4^+ transport is insufficient to meet demands.

The definition of inorganic N into the prey is similar to the description above for the mixotroph in equation (28-34) but prey values are substituted, such that $a\mu max^{phot}$ is substituted for $m\mu max^{phot}$, *aNCmax* for *mNCmax*, aK_{Ni} for mK_{Ni}, aK_A for mK_A and aK_p for mK_p (Table 5.1).

$$\mu N = m\mu max^{phot} \cdot mNCmax \tag{28}$$

$$PV_A = \mu_N \cdot Pref_A \cdot \frac{A}{A+mK_A} \tag{29}$$

$$PV_{Ni} = \mu_N \cdot Pref_{Ni} \cdot \frac{Ni}{Ni+mK_{Ni}} \tag{30}$$

$$\mathrm{V_A} = (\mu_\mathrm{N} \leq \mathrm{PV_A}) \cdot \mu_\mathrm{N} + (\mu_\mathrm{N} \leq \mathrm{PV_A}) \cdot \mathrm{PV_A} \tag{31}$$

$$\mathrm{V_{Ni}} = (\mathrm{PV_A} < \mu_\mathrm{N}) \cdot \left((\mathrm{PV_A} + \mathrm{PV_{Ni}} < \mu_\mathrm{N}) \cdot PV_{Ni} + (\mathrm{PV_A} + \mathrm{PV_{Ni}} \geq \mu_\mathrm{N}) \cdot (\mu_\mathrm{N} - \mathrm{PV_A})\right) \tag{32}$$

Total inorganic N uptake is described by equation (33), which is based on a normalized sigmoidal function as *mNC* (or *aNC*) approaches the absolute maximum allowed (*mNCabs or aNCabs*). Inorganic P uptake in equation (34) is similar to that of N uptake; except there is only one source of P. The constant *surge* enables nutrient transport to be greater than that required to meet steady-state demand. When X is unbalanced (i.e., *mXC* has deviated from *mXCabs*), *surge* was set to 5 in equation (34) to enable an enhanced transport capacity to support maximum steady-state growth.

$$up_N = (V_A + V_{Ni}) \cdot \Big((mNCu > mPCu) \cdot (mNC < mNCabs) \cdot mNPCu^{\beta} + (mNCu = mNPCu)\Big) \cdot \frac{\left((1+mK_q{}^{mHq}) \cdot \left(1-\frac{NC}{mNC_{abs}}\right)^{mHq}\right)}{\left(1-\frac{NC}{mNC_{abs}}\right)^{mHq} + mK_q{}^{mHq}} \tag{33}$$

$$up_P = (mPC < mPCabs) \cdot\ m\mu max^{phot} \cdot mNCmax\ \cdot surge\ \cdot \Big((mPCu > mNPCu) \cdot mNPCu^{\beta} +\ (mPCu = mNPCu)\Big) \cdot \frac{P}{P+mK_P} \cdot \frac{\left((1+mK_q{}^{mHq}) \times \left(1-\frac{mPC}{mPC_{abs}}\right)^{mHq}\right)}{\left(1-\frac{mPC}{mPC_{abs}}\right)^{mHq} + mK_q{}^{mHq}} \tag{34}$$

The assimilation rates of N and P (*NC* or *PC*) entering the mixotroph, in conjunction with C through prey assimilation, are maintained at a ratio consistent with core cellular structure that enables maximal growth to be attained (namely, *mNCmax* and *mPCmax*). Thus, the input of X (N or P) from the ingested material into mixotroph biomass is given by equation (35). The sufficiency of X associated with the assimilated material is ensured by *MINup* [equation (23)].

$$Inc_X = mCas \cdot mXCmax \tag{35}$$

Respiration and regeneration

The processes of phototrophic-associated respiration [R_{phot}, equation 36], which includes the cost of reducing NO_3^- [as $\{redco \cdot up_N \cdot frat\}$] and re-assimilating NH_4^+ that would be regenerated through heterotrophic metabolism [$N_{reas} = R_{het} \cdot mNCmax \cdot (1\text{-}Reg_N)$], are given in equation (36). Heterotrophic-associated respiration [R_{het}, equation (37)] includes basal and metabolic components. Total respiration is described as the sum of R_{phot} and R_{het} (equation 38).

$$R_{phot} = \{redco \cdot up_N \cdot frat\} + (up_N + N_{reas}) \cdot mAAsyn \quad (36)$$

$$R_{het} = mBR \cdot mCas \cdot mMR \quad (37)$$

$$R_{Tot} = R_{phot} + R_{het} \quad (38)$$

The control of nutrient regeneration within the mixotroph is parameterized differently in this model compared to that of typical heterotrophic grazers. The capability of assimilating inorganic nutrient enables a re-assimilation of nutrients that may be lost during normal biochemical cycling (such as protein turnover). If this re-assimilation is not simulated, the release of inorganic N and P from the mixotroph is allowed. Thus, C respiration is not associated with a regeneration of N and/or P unless N:C and/or P:C in the mixotroph is maintained at a high level. As the C-quota (X:C) approaches an absolute maximum value (*mXCabs*), the likelihood of regeneration rather than retention increases. This is controlled by Reg_X [equation (39)] within the range of *mXCmax* and *mXCabs* defined by Rep_X in equation (40).

$$Reg_X = \frac{\left((1+mK_{reg}{}^{mHreg}) \cdot Reg_X{}^{mHreg}\right)}{Reg_X{}^{mHreg} + mK_{reg}{}^{mHreg}} \quad (39)$$

$$Rep_X = (mXC > mXCmax) \cdot \left(1 - \frac{mXCabs - mXC}{mXCabs - mXCmax}\right) \quad (40)$$

The actual regeneration of X is given by equation (41), which is downregulated by Reg_x until *XC* is close to *mXCabs*. The overall changes in *mXC* are given by equation (42).

$$Res_X = R_{het} \cdot mXCmax \cdot Reg_X \quad (41)$$

$$\frac{dmXC}{dt} = up_X + Inc_X - Reg_X \quad (42)$$

Table AII.1. Summary of constants for the mixotroph model. Data sources from Flynn and Mitra (2009).

Parameters	Description	Units	Value
mAAsyn or aAAsyn	Cost for amino acid synthesis	gC gN^{-1}	1.5
mAEmax	Maximum assimiliation efficiency (AE)	-	0.75
mBR or aBR	Basal respiration rate	gC gC^{-1} d^{-1}	0.05
Cri	Slope of grazing rate	$d^{-1}/(\mu gC\ L)^{-1}$	0.01
ChlCmax	Absoluate maximum Chl:C	gChl gC^{-1}	0.06
FCabs	Maximum feeding vacuole size	gC gC^{-1}	0.4
FCmin	Minimum feeding vacuole size	gC gC^{-1}	0
mHas	Hill number for digestion rate	-	1
mHeq	Hill number for quantity-linked AE	-	4
mHhet	Hill number for derepression of FCmax	-	10
mHIng	Hill number for ingestion control	-	4
mHpbal	Hill number for digestion link to critical C-fixation	-	4
mHpd	Hill number for digestion control by photosynthesis	-	10
mHq	Hill number for uptake control	-	4
mHreg	Hill number fro regeneration	-	4
mK_A *or* aK_A	Half saturation for NH_4^+ transport for predator and prey	$\mu g\ N\ L^{-1}$	28 (mK_A), 14 (aK_A)
mKeq	Response control to ingestion quantity	-	10
mKhet	Half saturation for FCmax	-	1
mKQx or aKQx	Half saturation for cell quota curve	-	10 (N), 0.1(P)
mKreg	Half saturation for regeneration	-	1
mKq	Half saturation for nutrient uptake	-	0.1
M	The scalar for controlling photoacclimation	-	3
mMR	Metabolic respiration functions	gC gC^{-1}	0.2
mNCabs or aNCabs	Absoluate maximum N:C for predator and prey	gN gC^{-1}	0.35
mPbalcrit	Minimum critical proportion of growth supported by photosynthesis	-	0.25
$Pref_A$	Relative preference of NH_4^+	-	2
$Pref_{Ni}$	Relative preference of NO_3^-	-	1
mPCabs or aPCabs	Absoluate maximum P:C for predator and prey	gP gC^{-1}	0.04
redco	Cost of NO_3^- reduction to NH_4^+	gC gN^{-1}	1.71
β	Control constant for nutrient uptake	-	0.05

Table AII.2. External variables used for the model.

Parameters	Description	Units
A	NH_4^+	gN L^{-1}
Ni	NO_3^-	gN L^{-1}
P	PO_4^{3-}	gP L^{-1}
PFD	Photon flux density; light	μmol photon m^{-2} s^{-1}
aC	Initial prey carbon biomass	gC L^{-1}
aChlC	Initial Chl:C for prey	gChl gC^{-1}
aNC	Initial prey N:C	gN gC^{-1}
aPC	Initial pre	gP gC^{-1}

Chapter 6: Summary and Synthesis

Outbreaks of HABs are escalating in frequency and extent worldwide and have been increasing linked to increasing nutrient runoff and rising temperature due to global climate change (Anderson et al., 2002; Glibert et al., 2005; Hallegraeff, 2010; Wells et al., 2015; Glibert and Burford, 2017). Appropriate data on HAB physiology and new quantitative approaches that can incorporate multifactorial factors are needed to model the responses of HAB species under dynamic environmental conditions in climate change scenarios. Of the many HAB species, toxigenic *K. veneficum* (formerly *Gyrodinium galatheanum*, *Gymnodinium galatheanum* and *K. micrum*) is a particular concern due to its ichthyotoxic properties and global distribution in diverse estuarine systems (Adolf et al., 2009; Place et al., 2012, , and reference therein). In Chesapeake Bay, toxin produced by *K. veneficum* has lethal effects on fish (Kempton et al., 2002; Deeds et al., 2006) and has been implicated in the failure of oyster spawning and the growth of early life stage of oysters (Glibert et al., 2007; Stoecker et al., 2008).

In this dissertation, the role of mixotrophy in the dinoflagellate *Karlodinium veneficum* was addressed through statistical modeling of long-term time series data from Chesapeake Bay, in conjunction with a series of laboratory experiments, and multi-nutrient quota models to understand bloom formation and to predict growth under variable nutrient and temperature conditions. The following overarching hypothesis was addressed: phagotrophy is an adaptive strategy that may aid dinoflagellates in compensating for nutritional imbalances. As a result, increasing nutrient and prey availability associated with nutrient-enriched conditions will favor

HABs that are comprised of mixotrophic species. More specifically, the dinoflagellate *K. veneficum* is prevalent in varying environmental conditions because it can use mixotrophy to adjust to the variations in nutrient availability. When nutrient supply ratio is imbalanced, the cellular nutrient stoichiometry of this dinoflagellate will change accordingly. The specific questions that were addressed included:

- What combinations of environmental factors including climate-related variables (e.g., temperature, salinity, and flow), nutrient and prey concentrations best predict the occurrence of *K. veneficum* in different regions of Chesapeake Bay?
- How does the nutrient condition of the mixotroph and/or the prey affect the rates of feeding and putative toxicity of *K. veneficum*?
- How does feeding and growth by *K. veneficum* change in response to multiple prey species and their concentrations?
- How does prey availability under different temperature regimes influence the growth response of *K. veneficum* in modeled simulations?

Applying time series analysis, the temporal and spatial variability of *K. veneficum* in Chesapeake Bay over a 10-year (2002–2011) period was predicted based on multiple interactive factors, including climate-related physical factors, flow-regulated nutrient concentrations and prey. Trends in in *K. veneficum* showed irregular patterns in Chesapeake Bay, increasing in the mesohaline stations of the Bay, but not in oligohaline tributary stations. Relationships between nutrients and *K. veneficum* varied among the different salinity zones of the Bay. For the mesohaline

regions, riverine sources of nutrients with seasonal lags, together with particulate prey with zero lag, explained 15%–46% of the variation in the *K. veneficum* time series. For the oligohaline regions, nutrients and particulate prey generally showed significant decreasing trends with time, likely a reflection of nutrient reduction efforts. A conceptual model of mid-Bay blooms is presented, in which *K. veneficum*, derived from the oceanic end member of the Bay, may experience enhanced growth if it encounters prey originating from the tributaries with different nutrient patterns, which are enriched with N.

Laboratory experiments were conducted to measure growth and feeding rates of *K. veneficum* with addition of *Rhodomonas salina* as prey under varied N:P stoichiometry (molar N:P of 4, 16 and 32) of both predator and prey initially in different growth phases (exponential and stationary). Highest feeding rates were found for *K. veneficum* initially grown under low N:P conditions and given N-rich prey. The nutritionally different *K. veneficum* were tested with larvae of the eastern oyster *Crassostrea virginica* to compare putative toxicity. Larval mortality was significantly increased in 2 d exposures to high-NP *K. veneficum* monocultures in both growth phases. When mixed with N-rich prey, the presence of *K. veneficum* resulted in significantly enhanced larval mortality. Mixotrophic feeding for *K. veneficum* may not only provide nutritional needs, but also appears to increase negative effects of *K. veneficum* on larval survival when mixed with prey with higher N:P content.

In a second set of laboratory experiments, a multiwavelength PAM fluorometer was used to detect changes in photophysiology, rates of growth and

grazing of *K. veneficum* with single or multiple prey. Growth and physiological states of *K. veneficum* have fundamentally different responses to individual prey species. An increased rate of growth of *K. veneficum* was achieved with increasing prey concentrations of the cryptophyte *Rhodomonas salina*; its photosynthetic status remained unchanged by feeding. There was little grazing on *Synechococcus* as the prey by the mixotroph, and in its presence growth rates and photosynthetic status of the mixotroph declined.

A dynamic mathematical model was then developed to simulate the growth of *K. veneficum* and its algal prey, *R. salina,* based on these laboratory data sets. A multi-nutrient, C-N-P-based model was developed that interlinks autotrophy and mixotrophy at the cellular level. The model was run for 10-day growth periods under varying N:P stoichiometry (molar N:P of 4, 16 and 32). Across all simulations, *K. veneficum* became more heterotrophic and attained higher biomass with increasing temperature under both low N:P and high N:P conditions compared to balanced nutrient conditions (Redfield stoichiometry). When nutrients were in balanced proportions, lower biomass of the mixotroph was attained at all temperatures in the model, suggesting that natural systems might be more resilient for development of this HAB in warming temperatures if nutrients were available in balanced proportions.

Although multi-faceted, the research herein also exposed gaps in data obtained that are necessary to fully characterize the physiology of this HAB species and that are necessary to fully parameterize models. Both conceptual and mechanistic models highlighted the importance of considering particulate prey for predicting

HABs. Some of the gaps that are important to address in future studies of mixotrophs and HABs in Chesapeake Bay include:

1) There are many other HAB taxa in Chesapeake Bay for which much less has been studied. Grazing experiments with different Chesapeake Bay dominant HABs should be conducted under varying nutrient stoichiometry in order to contrast the differences in these HABs. For example, Chesapeake Bay has recurrent blooms of peridinin-type dinoflagellates (*Prorocentrum* spp.) and their physiology should be contrasted with gymnodinium-type dinoflagellates (*Karlodinium* spp.) under various scenarios of changes in nutrient and temperature;

2) Mixotrophy models should be coupled with existing hydrodynamics and water quality models to simulate cell transport and dynamics of *K. veneficum* and other HAB taxa in Chesapeake Bay. With the development of various scenarios that better represent the interactions with the HABs species, such simulation could help to project how HAB taxa respond to nutrient eutrophication and future climate changes, based on existing climate projections and nutrient reduction strategies.

3) Modeling toxin contents of *K. veneficum* should be developed with additional modules of toxin synthesis in current mathematical structures. As it has been shown that toxicity of *K. veneficum* is associated with predation (Sheng et al., 2010), integrating the intrinsic aspects for toxin production into ecosystem models could help to better predict or prevent both natural and aquaculture mortalities of fish and/or shellfish in Chesapeake Bay.

4) Additional studies on trophic interactions are needed. Jeong et al. (2010) has suggested that as mixotrophs, many HABs serve as hubs of microbial food webs,

by serving as both consumers of multiple prey and as food for other consumers. Studies on selective feeding by *K. veneficum* and other mixtrophs are needed. For example, *in situ* dilution experiments for *Karlodinium* blooms events are proposed to estimate grazing rates on different prey types in natural communities in the field. This application could provide a basis understanding the interaction between *K. veneficum* and co-occurring phytoplankton community to better understanding on planktonic food webs and nutrient cycling in eutrophic coastal waters.

5) Additional studies on physiological mechanisms related to nutritional preferences of *K. veneficum* and other mixotrophs should be undertaken. The physiological adaptive strategies that make them favored under elevated N:P conditions and increased supply of chemically reduced N (e.g., dissolved organic nitrogen) are not yet fully understood at the physiological level. New molecular approaches, and studies that couple metabolomics with classic physiology will advance this understanding.

This dissertation has thus demonstrated the importance of various nutrient sources and particulate prey in predicting HABs. This study has shown that prey quality, not just prey quantity is important, and that these modes of nutrition are highly variable with growth condition. The integration of HAB physiology (e.g., nutrient status, photosynthesis and feeding) with a cell quota mechanistic model has advanced the understanding of mixotroph physiology. The modeling approaches used here have potential for nutrient management decisions in the context of warming conditions. The challenges, however, continue to be large for predicting HABs with multiple nutritional strategies and multiple prey items.

References

Adolf, J.E., Bachvaroff, T.R., Place, A.R., 2009. Environmental modulation of karlotoxin levels in strains of the cosmopolitan dinoflagellate, *Karlodinium veneficum*. J. Phycol. 45(1), 176-192.

Anderson, D.M., Glibert, P.M., Burkholder, J.M., 2002. Harmful algal blooms and eutrophication: nutrient sources, composition, and consequences. Estuaries 25(4), 704-726.

Deeds, J.R., Reimschuessel, R., Place, A.R., 2006. Histopathological effects in fish exposed to the toxins from *Karlodinium micrum*. J. aquat. anim. health 18(2), 136-148.

Glibert, P.M., Alexander, J., Meritt, D.W., North, E.W., Stoecker, D.K., 2007. Harmful algae pose additional challenges for oyster restoration: Impacts of the harmful algae *Karlodinium veneficum* and *Prorocentrum minimum* on early life stages of the oysters *Crassostrea virginica* and *Crassostrea ariakensis*. J. Shellfish Res. 26(4), 919-925.

Glibert, P.M., Burford, M.A., 2017. Globally changing nutrient loads and harmful algal blooms: Recent advances, new paradigms, and continuing challenges. Oceanogr. 30(1), 58-69.

Glibert, P.M., Seitzinger, S., Heil, C.A., Burkholder, J.M., Parrow, M.W., Codispoti, L.A., Kelly, V., 2005. The role of eutrophication in the global proliferation of harmful algal blooms. Oceanogr. 18(2), 198-209.

Hallegraeff, G.M., 2010. Ocean climate change, phytoplankton community responses, and harmful algal blooms: a formidable predictive challenge[1]. J. Phycol. 46(2), 220-235.

Jeong, H.J., Du Yoo, Y., Kim, J.S., Seong, K.A., Kang, N.S., Kim, T.H., 2010. Growth, feeding and ecological roles of the mixotrophic and heterotrophic dinoflagellates in marine planktonic food webs. Ocean. Sci. J. 45(2), 65-91.

Kempton, J.W., Lewitus, A.J., Deeds, J.R., Law, J.M., Place, A.R., 2002. Toxicity of *Karlodinium micrum* (Dinophyceae) associated with a fish kill in a South Carolina brackish retention pond. Harmful Algae 1(2), 233-241.

Place, A.R., Bowers, H.A., Bachvaroff, T.R., Adolf, J.E., Deeds, J.R., Sheng, J., 2012. *Karlodinium veneficum* —The little dinoflagellate with a big bite. Harmful Algae 14, 179-195.

Sheng, J., Malkiel, E., Katz, J., Adolf, J.E., Place, A.R., 2010. A dinoflagellate exploits toxins to immobilize prey prior to ingestion. Proc. Natl. Acad. Sci. 107(5), 2082-2087.

Stoecker, D.K., Adolf, J.E., Place, A.R., Glibert, P.M., Meritt, D.W., 2008. Effects of the dinoflagellates *Karlodinium veneficum* and *Prorocentrum minimum* on early life history stages of the eastern oyster (*Crassostrea virginica*). Mar. Biol. 154(1), 81-90.

Wells, M.L., Trainer, V.L., Smayda, T.J., Karlson, B.S.O., Trick, C.G., Kudela, R.M., Ishikawa, A., Bernard, S., Wulff, A., Anderson, D.M., 2015. Harmful algal blooms and climate change: Learning from the past and present to forecast the future. Harmful Algae 49, 68-93.

Complete References Cited

Accoroni, S., Glibert, P.M., Pichierri, S., Romagnoli, T., Marini, M., Totti, C., 2015. A conceptual model of annual *Ostreopsis* cf. *ovata* blooms in the northern Adriatic Sea based on the synergic effects of hydrodynamics, temperature, and the N: P ratio of water column nutrients. Harmful Algae 45, 14-25.

Adolf, J.E., Bachvaroff, T., Place, A.R., 2008. Can cryptophyte abundance trigger toxic *Karlodinium veneficum* blooms in eutrophic estuaries? Harmful Algae 8(1), 119-128.

Adolf, J.E., Bachvaroff, T.R., Deeds, J.R., Place, A.R., 2015. Ichthyotoxic *Karlodinium veneficum* (Ballantine) J Larsen in the Upper Swan River Estuary (Western Australia): Ecological conditions leading to a fish kill. Harmful Algae 48, 83-93.

Adolf, J.E., Bachvaroff, T.R., Place, A.R., 2009. Environmental modulation of karlotoxin levels in strains of the cosmopolitan dinoflagellate, *Karlodinium veneficum*. J. Phycol. 45(1), 176-192.

Adolf, J.E., Krupatkina, D., Bachvaroff, T., Place, A.R., 2007. Karlotoxin mediates grazing by *Oxyrrhis marina* on strains of *Karlodinium veneficum*. Harmful Algae 6(3), 400-412.

Adolf, J.E., Stoecker, D.K., Harding, L.W., 2006. The balance of autotrophy and heterotrophy during mixotrophic growth of *Karlodinium micrum* (Dinophyceae). J. Plankt. Res. 28(8), 737-751.

Affronti, L.F., Marshall, H.G., 1994. Using frequency of dividing cells in estimating autotrophic picoplankton growth and productivity in the Chesapeake Bay. Hydrobiologia 284(3), 193-203.

Ajani, P., Hallegraeff, G., Pritchard, T., 2001. Historic overview of algal blooms in marine and estuarine waters of New South Wales, Australia. Proc. Linn. Soc. N. S. W. 123, 1-22.

Anderson, D.M., Burkholder, J.M., Cochlan, W.P., Glibert, P.M., Gobler, C.J., Heil, C.A., Kudela, R.M., Parsons, M.L., Rensel, J.E.J., Townsend, D.W., 2008. Harmful algal blooms and eutrophication: examining linkages from selected coastal regions of the United States. Harmful Algae 8(1), 39-53.

Anderson, D.M., Glibert, P.M., Burkholder, J.M., 2002. Harmful algal blooms and eutrophication: nutrient sources, composition, and consequences. Estuaries 25(4), 704-726.

Arar, E.J., Collins, G.B., 1997. *In vitro* determination of chlorophyll a and pheophytin a in marine and freshwater algae by fluorescence. Method 445.0, National Exposure Research Laboratory, EPA, Cincinnati, OH.

Baretta-Bekker, J.G., Baretta, J.W., Hansen, A.S., Riemann, B., 1998. An improved model of carbon and nutrient dynamics in the microbial food web in marine enclosures. Aquat. Microb. Ecol. 14(1), 91-108.

Berge, T., Chakraborty, S., Hansen, P.J., Andersen, K.H., 2017. Modeling succession of key resource-harvesting traits of mixotrophic plankton. ISME J. 11(1), 212.

Berge, T., Hansen, P.J., Moestrup, O., 2008a. Prey size spectrum and bioenergetics of the mixotrophic dinoflagellate *Karlodinium armiger*. Aquat. Microb. Ecol. 50(3), 289.

Berge, T., Hansen, P.J., Moestrup, Ø., 2008b. Feeding mechanism, prey specificity and growth in light and dark of the plastidic dinoflagellate *Karlodinium armiger*. Aquat. Microb. Ecol. 50(3), 279-288.

Bergholtz, T., Daugbjerg, N., Moestrup, Ø., Fernández-Tejedor, M., 2006. On the identity of *Karlodinium veneficum* and description of *Karlodinium armiger* sp. *nov.* (Dinophyceae), based on light and electron microscopy, nuclear-encoded LSU rDNA, and pigment composition. J. Phycol. 42(1), 170-193.

Bjornland, T., Tangen, K., 1979. Pigmentation and morphology of a marine *Gyrodinium* (Dinophyceae) with a major carotenoid different from peridinin and fucoxanthin. J. Phycol. 15, 457-463.

Boesch, D.F., Brinsfield, R.B., Magnien, R.E., 2001. Chesapeake Bay eutrophication. J. Environ. Qual. 30(2), 303-320.

Boynton, W.R., Garber, J.H., Summers, R., Kemp, W.M., 1995. Inputs, transformations, and transport of nitrogen and phosphorus in Chesapeake Bay and selected tributaries. Estuar. Coast. 18(1), 285-314.

Braarud, T., 1957. A red water organism from Walvis Bay (*Gymnodinium galatheanum* n. sp.). Galathea Deep Sea Exped. 1, 137-138.

Burkholder, J.M., Dickey, D.A., Kinder, C.A., Reed, R.E., Mallin, M.A., McIver, M.R., Cahoon, L.B., Melia, G., Brownie, C., Smith, J., 2006. Comprehensive trend analysis of nutrients and related variables in a large eutrophic estuary: a

decadal study of anthropogenic and climatic influences. Limnol. Oceanogr. 51(1part2), 463-487.

Burkholder, J.M., Glibert, P.M., Skelton, H.M., 2008. Mixotrophy, a major mode of nutrition for harmful algal species in eutrophic waters. Harmful Algae 8(1), 77-93.

Calbet, A., Bertos, M., Fuentes-Grünewald, C., Alacid, E., Figueroa, R., Renom, B., Garcés, E., 2011. Intraspecific variability in *Karlodinium veneficum*: Growth rates, mixotrophy, and lipid composition. Harmful Algae 10(6), 654-667.

Carvalho, W.F., Granéli, E., 2006. Acidotropic probes and flow cytometry: a powerful combination for detecting phagotrophy in mixotrophic and heterotrophic protists. Aquat. Microb. Ecol. 44(1), 85-96.

Carvalho, W.F., Granéli, E., 2010. Contribution of phagotrophy versus autotrophy to *Prymnesium parvum* growth under nitrogen and phosphorus sufficiency and deficiency. Harmful Algae 9(1), 105-115.

Cloern, J.E., 2001. Our evolving conceptual model of the coastal eutrophication problem. Mar. Ecol. Prog. Ser. 210(2001), 223-253.

Cloern, J.E., Jassby, A.D., 2010. Patterns and scales of phytoplankton variability in estuarine–coastal ecosystems. Estuar. Coast. 33(2), 230-241.

Cooper, S.R., Brush, G.S., 1991. Long-term history of Chespeake Bay anoxia. Science 254(5034), 992.

Dai, X., Lu, D., Guan, W., Wang, H., He, P., Xia, P., Yang, H., 2013. Newly recorded *Karlodinium veneficum* dinoflagellate blooms in stratified water of the East China Sea. Deep Sea Res. II 101, 237-243.

Deeds, J., 2009. The evolving story of *Gymnodinium galatheanum= Karlodinium micrum= Karlodinium veneficum*. A ten year perspective. J. Phycol. 45, 1-2.

Deeds, J.R., Reimschuessel, R., Place, A.R., 2006. Histopathological effects in fish exposed to the toxins from *Karlodinium micrum*. J. aquat. anim. health 18(2), 136-148.

Deeds, J.R., Terlizzi, D.E., Adolf, J.E., Stoecker, D.K., Place, A.R., 2002. Toxic activity from cultures of *Karlodinium micrum* (= *Gyrodinium galatheanum*)(Dinophyceae)—a dinoflagellate associated with fish mortalities in an estuarine aquaculture facility. Harmful Algae 1(2), 169-189.

Doane, T.A., Horwáth, W.R., 2003. Spectrophotometric determination of nitrate with a single reagent. Anal. Lett. 36(12), 2713-2722.

Edler, L., Elbrächter, M., 2010. The Utermöhl method for quantitative phytoplankton analysis, In: Karlson, B., Cusack, C., Bresnan, E. (Eds.), Microscopic and Molecular Methods for Quantitative Phytoplankton Analysis. IOC UNESCO, Paris, pp. 13-20.

Fisher, T.R., 1992. Nutrient limitation of phytoplankton in Chesapeake Bay. Mar. Ecol. Prog. Ser. 82, 51-63.

Flynn, K., Mitra, A., Glibert, P.M., Burkholder, J.M., 2018. Mixotrophy in HABs: by whom, on whom, when, why and what next, In: Glibert, P.M., Berdalet, E., Burford, M.A., Pitcher, G.C., Zhou, M. (Eds.), Global Ecology and Oceanography of Harmful Algal Blooms. Springer, In press, USA.

Flynn, K.J., 2005. Castles built on sand: dysfunctionality in plankton models and the inadequacy of dialogue between biologists and modellers. J. Plankt. Res. 27(12), 1205-1210.

Flynn, K.J., 2010. Do external resource ratios matter?: Implications for modelling eutrophication events and controlling harmful algal blooms. J. Mar. Syst. 83(3), 170-180.

Flynn, K.J., 2009. Going for the slow burn: why should possession of a low maximum growth rate be advantageous for microalgae? Plant Ecol. Divers. 2(2), 179-189.

Flynn, K.J., 2001. A mechanistic model for describing dynamic multi-nutrient, light, temperature interactions in phytoplankton. J. Plankt. Res. 23(9), 977-997.

Flynn, K.J., Hansen, P.J., 2013. Cutting the canopy to defeat the "selfish gene"; conflicting selection pressures for the integration of phototrophy in mixotrophic protists. Protist 164(6), 811-823.

Flynn, K.J., Mitra, A., 2009. Building the "perfect beast": modelling mixotrophic plankton. J. Plankt. Res. 31(9), 965-992.

Flynn, K.J., Stoecker, D.K., Mitra, A., Raven, J.A., Glibert, P.M., Hansen, P.J., Granéli, E., Burkholder, J.M., 2013. Misuse of the phytoplankton–zooplankton dichotomy: the need to assign organisms as mixotrophs within plankton functional types. J. Plankt. Res. 35(1), 3-11.

Frost, B.W., 1972. Effects of size and concentration of food particles on the feeding behavior of the marine planktonic copepod *Calanus Pacificus*. Limnol. Oceanogr. 17, 805-815.

Fu, F.X., Tatters, A.O., Hutchins, D.A., 2012. Global change and the future of harmful algal blooms in the ocean. Mar. Ecol. Prog. Ser. 470, 207-233.

Fuentes-Grünewald, C., Garcés, E., Rossi, S., Camp, J., 2009. Use of the dinoflagellate *Karlodinium veneficum* as a sustainable source of biodiesel production. J. Ind. Microbiol. Biotechnol. 36(9), 1215-1224.

Geider, R.J., Roche, J., Greene, R.M., Olaizola, M., 1993. Response of the photosynthetic apparatus of *Phaeodactylum tricornutum* (Bacillariophyceae) to nitrate, phosphate, or iron starvation. J. Phycol. 29(6), 755-766.

Ghyoot, C., Flynn, K.J., Mitra, A., Lancelot, C., Gypens, N., 2017. Modeling Plankton Mixotrophy: A Mechanistic Model Consistent with the Shuter-Type Biochemical Approach. Front. Ecol. Evol. 5, 78.

Glibert, P.M., 2017. Eutrophication, harmful algae and biodiversity—Challenging paradigms in a world of complex nutrient changes. Marine Poll. Bull. 124(2), 591-606.

Glibert, P.M., Alexander, J., Meritt, D.W., North, E.W., Stoecker, D.K., 2007. Harmful algae pose additional challenges for oyster restoration: Impacts of the harmful algae *Karlodinium veneficum* and *Prorocentrum minimum* on early life stages of the oysters *Crassostrea virginica* and *Crassostrea ariakensis*. J. Shellfish Res. 26(4), 919-925.

Glibert, P.M., Allen, J.I., Bouwman, A.F., Brown, C.W., Flynn, K.J., Lewitus, A.J., Madden, C.J., 2010. Modeling of HABs and eutrophication: status, advances, challenges. J. Mar. Syst. 83(3), 262-275.

Glibert, P.M., Burford, M.A., 2017. Globally changing nutrient loads and harmful algal blooms: Recent advances, new paradigms, and continuing challenges. Oceanogr. 30(1), 58-69.

Glibert, P.M., Burkholder, J.M., 2011. Harmful algal blooms and eutrophication:"strategies" for nutrient uptake and growth outside the Redfield comfort zone. Chin. J. Oceanol. Limnol. 29(4), 724-738.

Glibert, P.M., Burkholder, J.M., 2018. Causes of harmful algal blooms, In: Shumway, S., Burkholder, J.M., Morton, S.L. (Eds.), Harmful Algal Blooms: A Compendium Desk Reference. Wiley. In press, USA.

Glibert, P.M., Burkholder, J.M., Kana, T.M., 2012. Recent insights about relationships between nutrient availability, forms, and stoichiometry, and the distribution, ecophysiology, and food web effects of pelagic and benthic *Prorocentrum* species. Harmful Algae 14, 231-259.

Glibert, P.M., Burkholder, J.M., Kana, T.M., Alexander, J., Skelton, H., Shilling, C., 2009. Grazing by *Karenia brevis* on *Synechococcus* enhances its growth rate and may help to sustain blooms. Aquat. Microb. Ecol. 55(1), 17-30.

Glibert, P.M., Heil, C.A., F., W., C, D.R., 2018. Nutrient and HABs: dynamics kinetics and flexible nutrition, In: Glibert, P.M., Berdalet, E., Burford, M.A., Pitcher, G.C., Zhou, M. (Eds.), Global Ecology and Oceanography of Harmful Algal Blooms. Springer, In press, USA.

Glibert, P.M., Hinkle, D.C., Sturgis, B., Jesien, R.V., 2014. Eutrophication of a Maryland/Virginia coastal lagoon: a tipping point, ecosystem changes, and potential causes. Estuar. Coast. 37(1), 128-146.

Glibert, P.M., Kana, T.M., Brown, K., 2013. From limitation to excess: the consequences of substrate excess and stoichiometry for phytoplankton physiology, trophodynamics and biogeochemistry, and the implications for modeling. J. Mar. Syst. 125, 14-28

Glibert, P.M., Legrand, C., 2006. The diverse nutrient strategies of harmful algae: focus on osmotrophy, In: Granéli, E., Turner, J.T. (Eds.), Ecology of Harmful Algae, 1st ed., Ecological Studies. Springer Berlin/Heidelberg, pp.163-175.

Glibert, P.M., Magnien, R., Lomas, M.W., Alexander, J., Tan, C., Haramoto, E., Trice, M., Kana, T.M., 2001. Harmful algal blooms in the Chesapeake and coastal bays of Maryland, USA: Comparison of 1997, 1998, and 1999 events. Estuaries 24(6), 875-883.

Glibert, P.M., Magnien, R.E., Hall, S., Anderson, D., Kleindinst, J., Zhu, M., Zou, Y., 2004. Harmful algal blooms in the Chesapeake Bay, USA: common species, relationships to nutrient loading, management approaches, successes, and challenges. Harmful algae management and mitigation. Asia-Pacific Economic Cooperation Publications (204-MR-04.2), Singapore, pp. 48-55.

Glibert, P.M., Seitzinger, S., Heil, C.A., Burkholder, J.M., Parrow, M.W., Codispoti, L.A., Kelly, V., 2005. The role of eutrophication in the global proliferation of harmful algal blooms. Oceanogr. 18(2), 198-209.

Glibert, P.M., Terlizzi, D.E., 1999. Cooccurrence of elevated urea levels and dinoflagellate blooms in temperate estuarine aquaculture ponds. Appl. Environ. Microbiol. 65(12), 5594-5596.

Goto, N., Kihira, M., Ishida, N., 2008. Seasonal distribution of photosynthetically active phytoplankton using pulse amplitude modulated fluorometry in the large monomictic Lake Biwa, Japan. J. Plankt. Res. 30(10), 1169-1177.

Graneli, E., Carlsson, P., 1998. The ecological significance of phagotrophy in photosynthetic flagellates, In: Anderson, D., Cambella, A., Hallegraeff, G. (Eds.), Physiological Ecology of Harmful Algal Blooms, NATO ASI Series., 539-557 ed. Springer, Berlin/Heidelberg, pp. 539-557.

Granéli, E., Edvardsen, B., Roelke, D.L., Hagström, J.A., 2012. The ecophysiology and bloom dynamics of *Prymnesium* spp. Harmful Algae 14, 260-270.

Granéli, E., Flynn, K., 2006. Chemical and physical factors influencing toxin content, In: Granéli, E., Turner, J.T. (Eds.), Ecology of Harmful Algae, 1st ed., Ecological Studies. Springer, Berlin/Heidelberg, pp. 229-241.

Granéli, E., Johansson, N., 2003. Increase in the production of allelopathic substances by *Prymnesium parvum* cells grown under N-or P-deficient conditions. Harmful Algae 2(2), 135-145.

Guillard, R.R., 1975. Culture of phytoplankton for feeding marine invertebrates, In: Smith, W.L., Chanley, M.H. (Eds.), Culture of Marine Invertebrate Animals. Plenum Press, New York, pp. 29-60.

Guillard, R.R., 1978. Counting slides, In: Sournia, A. (Ed.), Phytoplankton manual Monographs on Oceanographic Methodology. UNESCO, Paris, pp. 182-189.

Gurbisz, C., Kemp, W.M., 2014. Unexpected resurgence of a large submersed plant bed in Chesapeake Bay: Analysis of time series data. Limnol. Oceanogr. 59(2), 482-494.

Haefner, J.W., 2005. Modeling Biological Systems: Principles and Applications. Springer Science & Business Media.

Hagy, J.D., Boynton, W.R., Keefe, C.W., Wood, K.V., 2004. Hypoxia in Chesapeake Bay, 1950–2001: long-term change in relation to nutrient loading and river flow. Estuaries 27(4), 634-658.

Hall, J.A., Barrett, D.P., James, M.R., 1993. The importance of phytoflagellate, heterotrophic flagellate and ciliate grazing on bacteria and picophytoplankton sized prey in a coastal marine environment. J. Plankt. Res. 15(9), 1075-1086.

Hall, N.S., Litaker, R.W., Fensin, E., Adolf, J.E., Bowers, H.A., Place, A.R., Paerl, H.W., 2008. Environmental factors contributing to the development and demise of a toxic dinoflagellate (*Karlodinium veneficum*) bloom in a shallow, eutrophic, lagoonal estuary. Estuar. Coast. 31(2), 402-418.

Hallegraeff, G.M., 2010. Ocean climate change, phytoplankton community responses, and harmful algal blooms: a formidable predictive challenge[1]. J. Phycol. 46(2), 220-235.

Hansen, P.J., 2011. The role of photosynthesis and food uptake for the growth of marine mixotrophic dinoflagellates. J. Eukaryot. Microbiol. 58(3), 203-214.

Hansen, P.J., Skovgaard, A., Glud, R.N., Stoecker, D.K., 2000. Physiology of the mixotrophic dinoflagellate *Fragilidium subglobosum*. II. Effects of time scale and prey concentration on photosynthetic performance. Mar. Ecol. Prog. Ser. 201, 137-146.

Harding, L.W., Gallegos, C.L., Perry, E.S., Miller, W.D., Adolf, J.E., Mallonee, M.E., Paerl, H.W., 2016. Long-term trends of nutrients and phytoplankton in Chesapeake Bay. Estuar. Coast. 39(3), 664-681.

Harding, L.W., Perry, E.S., 1997. Long-term increase of phytoplankton biomass in Chesapeake Bay, 1950–1994. Mar. Ecol. Prog. Ser., 39-52.

Hardison, D.R., Sunda, W.G., Wayne Litaker, R., Shea, D., Tester, P.A., 2012. Nitrogen limitation increases brevetoxins in *Karenia brevis* (Dinophyceae): implications for bloom toxicity[1]. J. Phycol. 48(4), 844-858.

Heinbokel, J.F., 1978. Studies on the functional role of tintinnids in the Southern California Bight. I. Grazing and growth rates in laboratory cultures. Mar. Biol. 47(2), 177-189.

Heisler, J., Glibert, P.M., Burkholder, J.M., Anderson, D.M., Cochlan, W., Dennison, W.C., Dortch, Q., Gobler, C.J., Heil, C.A., Humphries, E., 2008. Eutrophication and harmful algal blooms: a scientific consensus. Harmful algae 8(1), 3-13.

Hung, S.-H., Chung, C.-C., Liao, C.-W., Gong, G.-C., Chang, J., 2013. Sequence diversity and expression levels of *Synechococcus* phosphate transporter gene in the East China Sea. J. Exp. Mar. Biol. Ecol. 440, 90-99.

Izaguirre, I., Sinistro, R., Schiaffino, M.R., Sánchez, M.L., Unrein, F., Massana, R., 2012. Grazing rates of protists in wetlands under contrasting light conditions due to floating plants. Aquat. Microb. Ecol. 65(3), 221-232.

Jakobsen, H.H., Hansen, P.J., 1997. Prey size selection, grazing and growth response of the small heterotrophic dinoflagellate *Gymnodinium* sp. and the ciliate *Balanion comatum*—a comparative study. Mar. Ecol. Prog. Ser., 75-86.

Jeong, H.J., Du Yoo, Y., Kim, J.S., Seong, K.A., Kang, N.S., Kim, T.H., 2010. Growth, feeding and ecological roles of the mixotrophic and heterotrophic dinoflagellates in marine planktonic food webs. Ocean. Sci. J. 45(2), 65-91.

Jeong, H.J., Park, J.Y., Nho, J.H., Park, M.O., Ha, J.H., Seong, K.A., Jeng, C., Seong, C.N., Lee, K.Y., Yih, W.H., 2005a. Feeding by red-tide dinoflagellates on the cyanobacterium *Synechococcus*. Aquat. Microb. Ecol. 41(2), 131-143.

Jeong, H.J., Yoo, Y.D., Park, J.Y., Song, J.Y., Kim, S.T., Lee, S.H., Kim, K.Y., Yih, W.H., 2005b. Feeding by phototrophic red-tide dinoflagellates: five species newly revealed and six species previously known to be mixotrophic. Aquat. Microb. Ecol. 40(2), 133-150.

John, E.H., Flynn, K.J., 2002. Modelling changes in paralytic shellfish toxin content of dinoflagellates in response to nitrogen and phosphorus supply. Mar. Ecol. Prog. Ser. 225, 147-160.

Jones, R.I., 1994. Mixotrophy in planktonic protists as a spectrum of nutritional strategies. Mar. Microb. Food Webs 8, 87-96.

Jost, C., Lawrence, C.A., Campolongo, F., Van de Bund, W., Hill, S., DeAngelis, D.L., 2004. The effects of mixotrophy on the stability and dynamics of a simple planktonic food web model. Theor. Popul. Biol. 66(1), 37-51.

Kana, T.M., Glibert, P.M., 2017. On saturating response curves from the dual

perspectives of photosynthesis and nitrogen metabolism, In: Glibert, P.M., Kana, T.M. (Eds.), Aquatic Microbiology and Biogeochemistry – A Dual Perspective. Springer Internatioanl Pub., Switzerland, pp. 93-102.

Kemp, W., Boynton, W., Adolf, J., Boesch, D., Boicourt, W., Brush, G., Cornwell, J., Fisher, T., Glibert, P., Hagy, J., 2005. Eutrophication of Chesapeake Bay: historical trends and ecological interactions. Mar. Ecol. Prog. Ser. 303(21), 1-29.

Kempton, J.W., Lewitus, A.J., Deeds, J.R., Law, J.M., Place, A.R., 2002. Toxicity of *Karlodinium micrum* (Dinophyceae) associated with a fish kill in a South Carolina brackish retention pond. Harmful Algae 1(2), 233-241.

Kendall, M.G., Ord, J.K., 1990. Time-series. Edward Arnold London.

Kimmance, S.A., Atkinson, D., Montagnes, D.J.S., 2006. Do temperature–food interactions matter? Responses of production and its components in the model heterotrophic flagellate *Oxyrrhis marina*. Aquat. Microb. Ecol. 42(1), 63-73.

Kolber, Z., Zehr, J., Falkowski, P., 1988. Effects of growth irradiance and nitrogen limitation on photosynthetic energy conversion in photosystem II. Plant Physiol. 88(3), 923-929.

Legrand, C., 2001. Phagotrophy and toxicity variation in the mixotrophic *Prymnesium patelliferum* (Haptophyceae). Limnol. Oceanogr. 46(5), 1208-1214.

Li, A., 1998. The feeding physiology and ecology of the mixotrophic dinoflagellate *Gyrodinium galatheanum*, Marine, Estuarine, Environmental Sciences Graduate Program. University of Maryland, College Park, MD.

Li, A., 1996. Ingestion of fluorescently labeled and phycoerythrin-containing prey by mixotrophic dinoflagellates. Aquat. Microb. Ecol. 10, 139-147.

Li, A., Stoecker, D.K., Adolf, J.E., 1999. Feeding, pigmentation, photosynthesis and growth of the mixotrophic dinoflagellate *Gyrodinium galatheanum*. Aquat. Microb. Ecol. 19, 163-176.

Li, A., Stoecker, D.K., Coats, D.W., 2000a. Spatial and temporal aspects of *Gyrodinium galatheanum* in Chesapeake Bay: distribution and mixotrophy. J. Plankt. Res. 22(11), 2105-2124.

Li, A., Stoecker, D.K., Coats, D.W., 2000b. Mixotrophy in *Gyrodinium galatheanum* (Dinophyceae): grazing responses to light intensity and inorganic nutrients. J. Phycol. 36(1), 33-45.

Li, A., Stoecker, D.K., Coats, D.W., 2001. Use of the 'food vacuole content'method to estimate grazing by the mixotrophic dinoflagellate *Gyrodinium galatheanum* on cryptophytes. J. Plankt. Res. 23(3), 303-318.

Li, J., Glibert, P.M., Gao, Y., 2015. Temporal and spatial changes in Chesapeake Bay water quality and relationships to *Prorocentrum minimum*, *Karlodinium veneficum*, and CyanoHAB events, 1991–2008. Harmful Algae 42, 1-14.

Lin, C.-H., Accoroni, S., Glibert, P.M., 2017. *Karlodinium veneficum* feeding responses and effects on larvae of the eastern oyster *Crassostrea virginica* under variable nitrogen: phosphorus stoichiometry. Aquat. Microb. Ecol. 79(2), 101-114.

Lin, C.-H., Glibert, P.M., Mixotrophy with multiple prey species measured with a multiwavelength-excitation PAM fluorometer: case study of *Karlodinium veneficum*. J. Plankt. Res, submitted.

Lin, C.-H., Lyubchich, V., Glibert, P.M., 2018. Time series models of decadal trends in the harmful algal species *Karlodinium veneficum* in Chesapeake Bay Harmful Algae 73(C), 110-118.

Lindehoff, E., Granéli, E., Glibert, P.M., 2010. Influence of prey and nutritional status on the rate of nitrogen uptake by *Prymnesium parvum* (Haptophyte). J. Am. Water Resour. Assoc. 46(1), 121-132.

Lundgren, V.M., Glibert, P.M., Granéli, E., Vidyarathna, N.K., Fiori, E., Ou, L., Flynn, K.J., Mitra, A., Stoecker, D.K., Hansen, P.J., 2016. Metabolic and physiological changes in *Prymnesium parvum* when grown under, and grazing on prey of, variable nitrogen: phosphorus stoichiometry. Harmful Algae 55, 1-12.

Lyubchich, V., Gel, Y.R., El-Shaarawi, A., 2013. On detecting non-monotonic trends in environmental time series: a fusion of local regression and bootstrap. Environmetrics 24(4), 209-226.

Malone, T.C., Crocker, L.H., Pike, S.E., Wendler, B.W., 1988. Influences of river flow on the dynamics of phytoplankton production in a partially stratified estuary. Mar. Ecol. Prog. Ser. 48(3), 235-249.

Marshall, H.G., Burchardt, L., Lacouture, R., 2005. A review of phytoplankton composition within Chesapeake Bay and its tidal estuaries. J. Plankt. Res. 27(11), 1083-1102.

Menden-Deuer, S., Lessard, E.J., 2000. Carbon to volume relationships for dinoflagellates, diatoms, and other protist plankton. Limnol. Oceanogr. 45(3), 569-579.

Millette, N.C., Pierson, J.J., Aceves, A., Stoecker, D.K., 2017. Mixotrophy in *Heterocapsa rotundata*: A mechanism for dominating the winter phytoplankton. Limnol. Oceanogr. 62(2), 836-845.

Mitra, A., 2006. A multi-nutrient model for the description of stoichiometric modulation of predation in micro-and mesozooplankton. J. Plankt. Res. 28(6), 597-611.

Mitra, A., Flynn, K.J., 2005. Predator–prey interactions: is 'ecological stoichiometry'sufficient when good food goes bad? J. Plankt. Res. 27(5), 393-399.

Mitra, A., Flynn, K.J., 2006a. Promotion of harmful algal blooms by zooplankton predatory activity. Biol. Lett. 2(2), 194-197.

Mitra, A., Flynn, K.J., 2010. Modelling mixotrophy in harmful algal blooms: More or less the sum of the parts? J. Mar. Syst. 83(3), 158-169.

Mitra, A., Flynn, K.J., 2006b. Accounting for variation in prey selectivity by zooplankton. Ecol. Modell. 199(1), 82-92.

Mitra, A., Flynn, K.J., Burkholder, J., Berge, T., Calbet, A., Raven, J.A., Granéli, E., Glibert, P.M., Hansen, P.J., Stoecker, D.K., 2014. The role of mixotrophic protists in the biological carbon pump. Biogeosciences 10(8), 13535-13562.

Mitra, A., Flynn, K.J., Tillmann, U., Raven, J.A., Caron, D., Stoecker, D.K., Not, F., Hansen, P.J., Hallegraeff, G., Sanders, R., 2016. Defining planktonic protist

functional groups on mechanisms for energy and nutrient acquisition: incorporation of diverse mixotrophic strategies. Protist 167(2), 106-120.

Montagnes, D.J.S., Kimmance, S.A., Atkinson, D., 2003. Using Q10: Can growth rates increase linearly with temperature? Aquat. Microb. Ecol. 32(3), 307-313.

Moore, S.K., Johnstone, J.A., Banas, N.S., Salathe Jr, E.P., 2015. Present-day and future climate pathways affecting *Alexandrium* blooms in Puget Sound, WA, USA. Harmful Algae 48, 1-11.

Muhling, B.A., Gaitán, C.F., Stock, C.A., Saba, V.S., Tommasi, D., Dixon, K.W., 2018. Potential salinity and temperature futures for the Chesapeake Bay using a statistical downscaling spatial disaggregation framework. Estuar. Coast. 41(2), 349-372.

Najjar, R.G., Pyke, C.R., Adams, M.B., Breitburg, D., Hershner, C., Kemp, M., Howarth, R., Mulholland, M.R., Paolisso, M., Secor, D., 2010. Potential climate-change impacts on the Chesapeake Bay. Estuar. Coast. Shelf. Sci. 86(1), 1-20.

Nielsen, M.V., 1996. Growth and chemical composition of the toxic dinoflagellate *Gymnodinium galatheanum* in relation to irradiance, temperature and salinity. Mar. Ecol. Prog. Ser. 136, 205-211.

Nielsen, M.V., 1993. Toxic effect of the marine dinoflagellate *Gymnodinium galatheanum* on juvenile cod Gadus morhua. Mar. Ecol. Prog. Ser., 273-277.

Park, M.G., Kim, S., Kim, H.S., Myung, G., Kang, Y.G., Yih, W., 2006. First successful culture of the marine dinoflagellate *Dinophysis acuminata*. Aquat. Microb. Ecol. 45(2), 101-106.

Place, A.R., Bowers, H.A., Bachvaroff, T.R., Adolf, J.E., Deeds, J.R., Sheng, J., 2012. *Karlodinium veneficum* —The little dinoflagellate with a big bite. Harmful Algae 14, 179-195.

R Core Team, 2016. R: A Language and Environment for Statistical Computing. Vienna, Austria: R Foundation for Statistical Computing; 2014. R Foundation for Statistical Computing, http://www.R-project.org.

Raateoja, M., Seppälä, J., Ylöstalo, P., 2004. Fast repetition rate fluorometry is not applicable to studies of filamentous cyanobacteria from the Baltic Sea. Limnol. Oceanogr. 49(4), 1006-1012.

Raven, J.A., Beardall, J., Flynn, K.J., Maberly, S.C., 2009. Phagotrophy in the origins of photosynthesis in eukaryotes and as a complementary mode of nutrition in phototrophs: relation to Darwin's insectivorous plants. J. Exp. Bot. 60(14), 3975-3987.

Ray, R.T., Haas, L.W., Sieracki, M.E., 1989. Autotrophic picoplankton dynamics in a Chesapeake Bay sub-estuary. Mar. Ecol. Prog. Ser., 273-285.

Ringuet, S., Sassano, L., Johnson, Z.I., 2011. A suite of microplate reader-based colorimetric methods to quantify ammonium, nitrate, orthophosphate and silicate concentrations for aquatic nutrient monitoring. J. Environ. Monit. 13(2), 370-376.

Sanders, R.W., 1991. Mixotrophic protists in marine and freshwater ecosystems. J. Eukaryotic Microbiol. 38(1), 76-81.

Schnepf, E., Elbrächter, M., 1992. Nutritional strategies in dinoflagellates: a review with emphasis on cell biological aspects. Eur. J. Protistol. 28(1), 3-24.

Shapiro, S.S., Wilk, M.B., 1965. An analysis of variance test for normality (complete samples). Biometrika 52(3/4), 591-611.

Sheng, J., Malkiel, E., Katz, J., Adolf, J.E., Place, A.R., 2010. A dinoflagellate exploits toxins to immobilize prey prior to ingestion. Proc. Natl. Acad. Sci. 107(5), 2082-2087.

Smalley, G.W., Coats, D.W., 2002. Ecology of the red-tide dinoflagellate *Ceratium furca*: Distribution, mixotrophy, and grazing impact on ciliate populations of Chesapeake Bay. J. Eukaryot. Microbiol. 49(1), 63-73.

Smalley, G.W., Coats, D.W., Adam, E.J., 1999. A new method using fluorescent microspheres to determine grazing on ciliates by the mixotrophic dinoflagellate *Ceratium furca*. Aquat. Microb. Ecol. 17(2), 167-179.

Smalley, G.W., Coats, D.W., Stoecker, D.K., 2003. Feeding in the mixotrophic dinoflagellate *Ceratium furca* is influenced by intracellular nutrient concentrations. Mar. Ecol. Prog. Ser. 262, 137-151.

Smayda, T.J., 2008. Complexity in the eutrophication–harmful algal bloom relationship, with comment on the importance of grazing. Harmful Algae 8(1), 140-151.

Staunton, J., Weissman, K.J., 2001. Polyketide biosynthesis: a millennium review. Nat. Prod. Rep. 18(4), 380-416.

Stickney, H.L., Hood, R.R., Stoecker, D.K., 2000. The impact of mixotrophy on planktonic marine ecosystems. Ecol. Modell. 125(2-3), 203-230.

Stoecker, D., Li, A., Coats, D.W., Gustafson, D., Nannen, M., 1997. Mixotrophy in the dinoflagellate *Prorocentrum minimum*. Mar. Ecol. Prog. Ser. 152(1), 1-12.

Stoecker, D., Tillmann, U., Graneli, E., 2006. Phagotrophy in harmful algae, In: Graneli, E., Turner, J.T. (Eds.), Ecology of Harmful Algae, 1st ed., Ecological Studies. Springer, Verlag, Berlin/Heidelberg, pp. 177-187.

Stoecker, D.K., 1999. Mixotrophy among dinoflagellates[1]. J. Eukaryotic Microbiol. 46(4), 397-401.

Stoecker, D.K., Adolf, J.E., Place, A.R., Glibert, P.M., Meritt, D.W., 2008. Effects of the dinoflagellates *Karlodinium veneficum* and *Prorocentrum minimum* on early life history stages of the eastern oyster (*Crassostrea virginica*). Mar. Biol. 154(1), 81-90.

Stoecker, D.K., Hansen, P.J., Caron, D.A., Mitra, A., 2017. Mixotrophy in the marine plankton. Annu. Rev. Mar. Sci. 9, 311-335.

Stoecker, D.K., Johnson, M.D., de Vargas, C., Not, F., 2009. Acquired phototrophy in aquatic protists. Aquat. Microb. Ecol. 57, 279-310.

Thingstad, T.F., Havskum, H., Garde, K., Riemann, B., 1996. On the strategy of" eating your competitor": A mathematical analysis of algal mixotrophy. Ecology 77(7), 2108-2118.

Tittel, J., Bissinger, V., Zippel, B., Gaedke, U., Bell, E., Lorke, A., Kamjunke, N., 2003. Mixotrophs combine resource use to outcompete specialists: implications for aquatic food webs. Proc. Natl. Acad. Sci. 100(22), 12776-12781.

Urabe, J., Gurung, T.B., Yoshida, T., Sekino, T., Nakanishi, M., Maruo, M., Nakayama, E., 2000. Diel changes in phagotrophy by *Cryptomonas* in Lake Biwa. Limnol. Oceanogr. 45(7), 1558-1563.

Våge, S., Castellani, M., Giske, J., Thingstad, T.F., 2013. Successful strategies in size structured mixotrophic food webs. Aquat. Ecol. 47(3), 329-347.

Van Dolah, F.M., 2000. Marine algal toxins: origins, health effects, and their increased occurrence. Environ. Health Perspect. 108, 133.

Ward, B.A., Dutkiewicz, S., Barton, A.D., Follows, M.J., 2011. Biophysical aspects of resource acquisition and competition in algal mixotrophs. Am. Nat. 178(1), 98-112.

Ward, B.A., Follows, M.J., 2016. Marine mixotrophy increases trophic transfer efficiency, mean organism size, and vertical carbon flux. Proc. Natl. Acad. Sci. 113(11), 2958-2963.

Waterbury, J.B., Watson, S.W., Valois, F.W., Franks, D.G., 1986. Biological and ecological characterization of the marine unicellular cyanobacterium *Synechococcus*, In: Platt, T., Li, W.K.W. (Eds.), Photosynthetic Picoplankton. Can. Bull. Fish. Aquat. Sci., Toronto, pp. 71-120.

Wells, M.L., Trainer, V.L., Smayda, T.J., Karlson, B.S.O., Trick, C.G., Kudela, R.M., Ishikawa, A., Bernard, S., Wulff, A., Anderson, D.M., 2015. Harmful algal blooms and climate change: Learning from the past and present to forecast the future. Harmful Algae 49, 68-93.

Wilken, S., Huisman, J., Naus-Wiezer, S., Donk, E., 2013. Mixotrophic organisms become more heterotrophic with rising temperature. Ecol. Lett. 16(2), 225-233.

Yang, Z., Zhang, L., Zhu, X., Wang, J., Montagnes, D.J.S., 2016. An evidence-based framework for predicting the impact of differing autotroph-heterotroph thermal sensitivities on consumer–prey dynamics. ISME J. 10, 1767-1778.

Yoo, Y.D., Seong, K.A., Jeong, H.J., Yih, W., Rho, J.R., Nam, S.W., Kim, H.S., 2017. Mixotrophy in the marine red-tide cryptophyte *Teleaulax amphioxeia* and ingestion and grazing impact of cryptophytes on natural populations of bacteria in Korean coastal waters. Harmful algae 68, 105.

Zhou, C., Fernández, N., Chen, H., You, Y., Yan, X., 2011. Toxicological studies of *Karlodinium micrum* (Dinophyceae) isolated from East China Sea. Toxicon 57(1), 9-18.

Zubkov, M.V., Tarran, G.A., 2008. High bacterivory by the smallest phytoplankton in the North Atlantic Ocean. Nature 455(7210), 224-226.